

Porphyrinoids

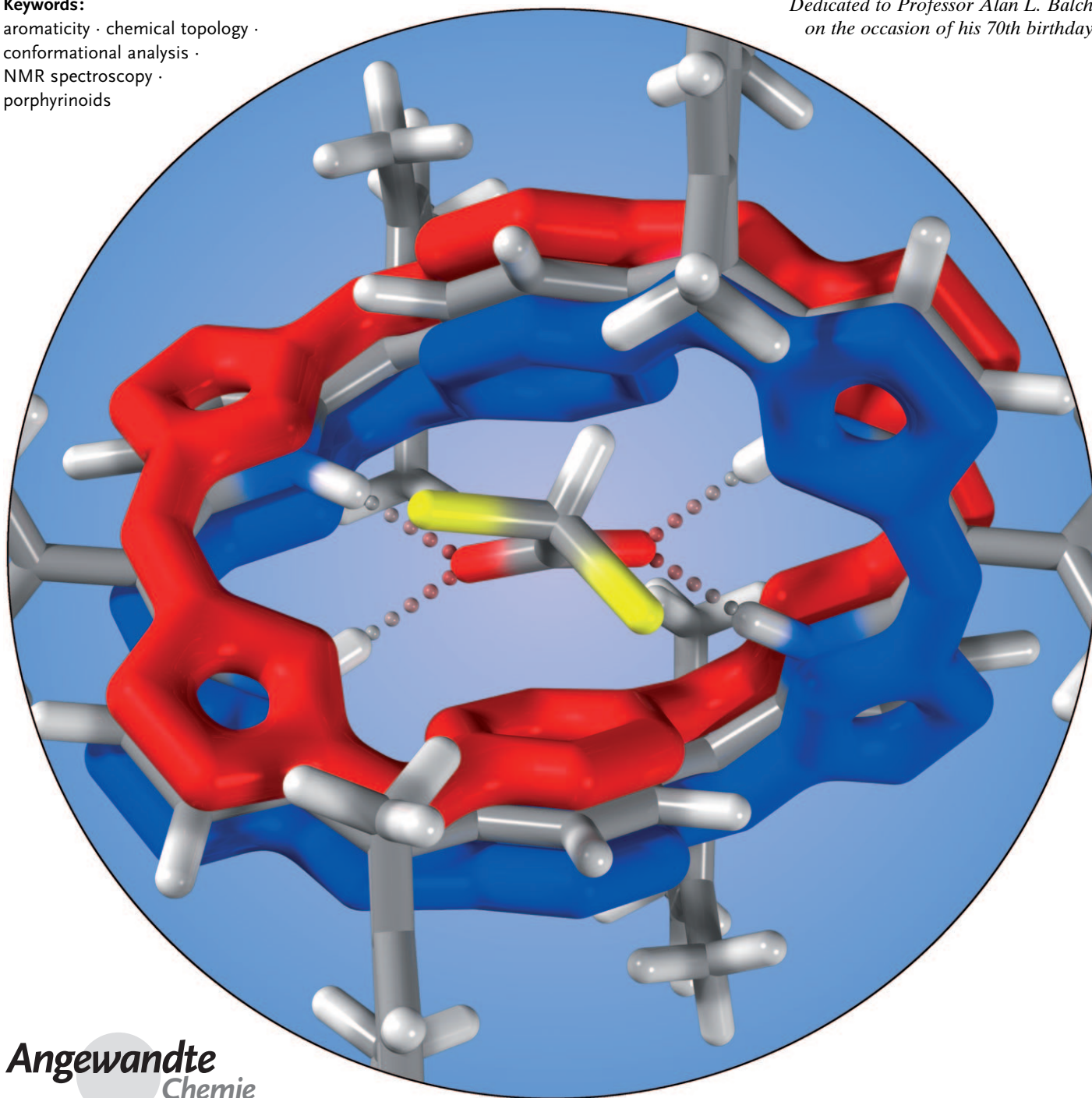
Figure Eights, Möbius Bands, and More: Conformation and Aromaticity of Porphyrinoids**

Marcin Stępień, Natasza Sprutta, and Lechosław Latos-Grażyński**

Keywords:

aromaticity · chemical topology ·
conformational analysis ·
NMR spectroscopy ·
porphyrinoids

*Dedicated to Professor Alan L. Balch
on the occasion of his 70th birthday*



The aromatic character of porphyrins, which has significant chemical and biological consequences, can be substantially altered by judicious modifications of the parent ring system. Expansion of the macrocycle, which is achieved by introducing additional subunits, usually increases the so-called free curvature of the ring, leading to larger angular strain. This strain is reduced by a variety of conformational changes, most notably by subunit inversion and π surface twisting. The latter effect creates a particularly convenient access to Möbius aromatic molecules, whose properties, predicted over 40 years ago, are of considerable theoretical importance. The conformational processes occurring in porphyrin analogues are often coupled to other chemical phenomena, and can thus be exploited as a means of constructing functional molecular devices. In this Review, the structural chemistry of porphyrinoids is discussed in the context of their conformational dynamics and π -electron conjugation

1. Introduction and Scope

The research on aromaticity, dating back to Faraday's landmark discovery of benzene,^[1] has seen a dramatic evolution in the course of the last two centuries.^[2–4] During that time, our understanding of π -conjugated molecules has been greatly expanded by complementary and mutually dependent efforts of experimental and theoretical chemists. In fact, the most significant advances in the field have been marked not only by synthetic victories but also by the proposal of successful theoretical models. The quest for nontrivial aromatic molecules had its beginnings in the early work on the annulene series,^[5,6] and has since continued to encompass a remarkable diversity of structures. One of the recurring topics in the research on aromaticity is that of making the π -conjugated system three-dimensional. Non-planar structures are implicated by many types of π -conjugation, including bowl-like,^[7] spherical,^[8,9] tubular or in-plane,^[9,10] and twisted.^[11] The occurrence and properties of three-dimensional π -aromatics are determined by the interplay between the conformational properties of a molecule and its π -conjugation.

The present Review discusses the influence of three-dimensional structure on the aromaticity of porphyrin analogues, a rich family of compounds structurally related to Nature's original tetrapyrrole.^[12–18] π -Conjugation in porphyrinoids is controlled by many factors, including prototropic tautomerism, acid–base equilibria, metal coordination, and redox chemistry, as discussed in our recent, complementary review.^[17] Among these effects, the role of conformational flexibility is especially important because of the diversity of observed structural effects and their apparent complexity. Even though porphyrinoids are formally derived from the planar porphyrin ring, systematic exploration of their chemistry, especially intense in the last two decades, unveiled a number of structural features quite different from those of the parent macrocycle (Scheme 1). Apparently, the first observation of an unusual conformation in a porphyrin

analogue was in the palladium(II) complex of [26]hexaphyrin(1.1.1.1.1.1) reported in 1993.^[19] In this species, two pyrrole rings were found to be inverted in such a way that the nitrogens were placed on the periphery of the macrocycle (Section 2.2). In the notable case of N-confused porphyrin^[20,21] implicit ring inversion was a prerequisite for the formation of so-called N-fused porphyrin.^[22] The synthesis of turcasarin, accomplished in 1994,^[23] demonstrated the structural viability of “giant” porphyrinoid macrocycles, and provided the first example of a figure-eight conformation, in which the π system is formally twisted by 360°. The gap between the untwisted and figure-eight structures was filled in 2007 when A,D-di-*p*-benziporphyrin was reported to adopt a Möbius-band conformation, containing a 180° twist.^[24,25] That latter discovery, and subsequent reports on other Möbius aromatic porphyrinoids,^[26] provided an incentive for summarizing the state of the field in the present Review.


The goal of this work is not so much to provide an exhaustive catalogue of existing porphyrinoids as to search for regularities in the unusually diverse body of structural and spectroscopic data. The scope will be limited to macrocyclic systems that are fully conjugated and show a distinct three-dimensional structure. Consequently, several important fam-

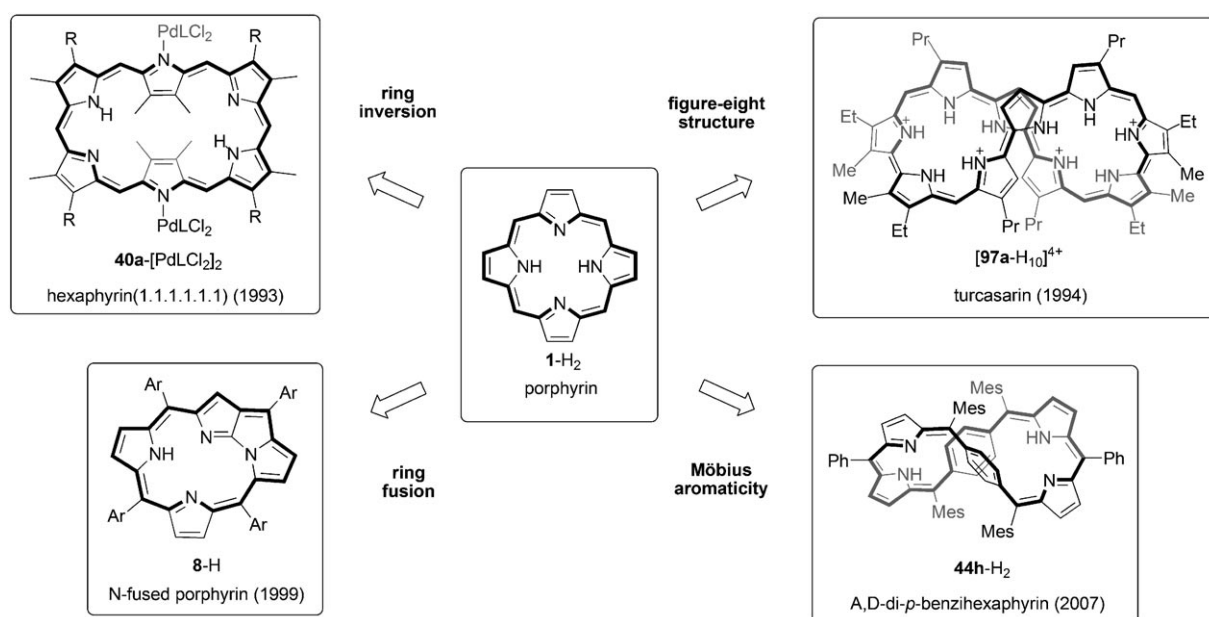
From the Contents

1. Introduction and Scope	4289
2. Conformation of Porphyrinoids	4293
3. Aromaticity of Porphyrinoids	4300
4. Triphyrins and Tetraphyrins	4303
5. Pentaphyrins	4309
6. Hexaphyrins	4312
7. Heptaphyrins	4320
8. Octaphyrins	4322
9. Giant Porphyrinoids	4327
10. Concluding Remarks	4334

[*] Dr. M. Stępień, Dr. N. Sprutta, Prof. L. Latos-Grażyński
Wydział Chemii, Uniwersytet Wrocławski
ul. F. Joliot-Curie 14, 50-383 Wrocław (Poland)
E-mail: ms@wchuwr.pl
llg@wchuwr.pl
Homepage: <http://www.mstepien.edu.pl>
<http://llg.chem.uni.wroc.pl>

[**] The frontispiece shows the host–guest interaction between the figure-eight dication of di-*p*-benzihexaphyrin and a dichloroacetate anion. For details see Section 6.5.

 Supporting information for this article is available on the WWW under <http://dx.doi.org/10.1002/anie.201003353>.



Scheme 1. Examples of expanded porphyrinoids with different structural features (L = NH₃ or pyridine). In this and all following schemes, parts of molecules lying below the viewing plane are shown in gray.

ilies of porphyrin analogues, such as calixpyrroles,^[27,28] calixpyrins,^[29] Schiff-base macrocycles,^[12,30] and vinylogous porphyrins^[30,31] will fall outside the scope of this Review. The relationship between conformation and aromaticity is particularly consequential in expanded porphyrins, which will be our primary area of interest. Several excellent reviews on expanded porphyrins have been published in recent years, emphasizing various facets of their chemistry.^[11,16,26,30,32–34] What is apparently lacking, however, is a general and up-to-

date discussion of the structural chemistry of porphyrinoids, examined in the context of π conjugation. We feel that such a discussion may be of interest not only to scientists directly involved in porphyrinoid research but also to those active in other areas, including heterocyclic chemistry, aromaticity theory and conformational analysis.

The present Review is organized as follows. We begin with a short introductory section containing basic definitions and delineating the nomenclature system. Section 2 provides a



Marcin Stępień was born in 1977 in Wrocław. He received his Ph.D. in 2003 from the University of Wrocław for his work on porphyrinoid chemistry carried out with Professor Lechosław Latos-Grażyński. In 2005, he joined the group of Professor Jonathan L. Sessler at the University of Texas to work on liquid-crystalline expanded porphyrins. In 2010, he completed his habilitation at the University of Wrocław. His research interests include macrocyclic chemistry, design of new aromatic molecules, and NMR spectroscopy.



Lechosław Latos-Grażyński was born in 1951 in Szczecin. He received his Ph.D. in 1974 from the University of Wrocław while working with Professor Bogusława Jeżowska-Trzebiatowska. After a period of postdoctoral research under the guidance of Professors Gerd N. La Mar and Alan L. Balch, he returned to Wrocław where he initiated research on the chemistry of porphyrins and their analogues. His current interests include the synthesis of new porphyrinoids, their coordination chemistry, and spectroscopy. In 1998, Professor Latos-Grażyński received the award of the Foundation for Polish Science. He has been corresponding member of the Polish Academy of Sciences since 2004.



Natasza Sprutta was born in 1972 in Wrocław. She earned her Ph.D. in 2001 from the University of Wrocław for her research on thiophene-containing porphyrinoids carried out with Professor Lechosław Latos-Grażyński. She did her postdoctoral research in the group of Professor Alan Balch at the University of California, Davis, working on heme degradation models. She is currently working at the University of Wrocław, where she is exploring the chemistry of azulene-containing macrocycles.

generalized treatment of porphyrinoid conformation, whereas porphyrinoid aromaticity is discussed in Section 3. These two sections introduce new concepts, such as the free curvature or torsional π -conjugation index, which require some technical explanation. However, the rest of the paper can be easily followed without going into the technical details given in Sections 2 and 3. Subsequent chapters contain a detailed review of π -conjugated porphyrinoids, organized according to the increasing macrocycle size. Systems containing more than eight cyclic subunits are covered in Section 9.

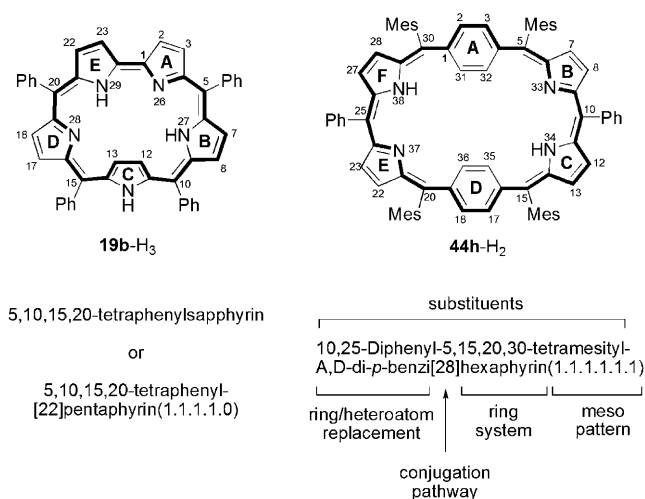
1.1. Definitions

The current usage of the term “porphyrinoid” covers a large number of systems, which occasionally bear little resemblance to the parent porphyrin macrocycle. For the sake of the present Review, we will adopt the following definition: A porphyrinoid is a molecule constructed of a number of smaller (typically five-membered) rings that are connected, either directly or by bridging atoms, into a macrocyclic structure, which usually exhibits a high degree of π -conjugation. The constituent rings are hetero- or carbocyclic, whereas the “meso” bridges, as they are denoted in the porphyrin nomenclature, are usually carbon atoms or linear chains thereof. Structures of porphyrinoids are typically further modified, for example, by peripheral or internal substitution, ring fusion, or metal coordination.

Macrocycle size appears to be the property most widely used to classify porphyrinoids. A porphyrin analogue may be viewed as a cyclic array of subunits, which may be cyclic (e.g. pyrrole rings) or linear (meso bridges). In the following discussion, each meso carbon atom will be treated as a separate subunit. Names such as triphyrin, tetraphyrin, pentaphyrin, etc. reflect the size of the macrocycle expressed as the number of cyclic subunits in the ring. Alternatively, the smallest macrocyclic circuit (SMC) can be considered, defined as the smallest circuit in the molecular graph passing through all subunits. The size S of this circuit provides a useful and unambiguous distinction between “contracted” ($S < 16$) and “expanded” porphyrinoids ($S > 16$).^[16] The borderline value of $S = 16$ corresponds to the parent porphyrin macrocycle and many tetraphyrins. Some tetraphyrins, however, are classified as contracted (e.g. corrole **2**-H₃, $S = 15$) or expanded (e.g. *p*-benzporphyrin **11**-H, $S = 17$).

1.2. Nomenclature and Numbering Convention

The naming system used in this Review reflects the current literature practice, which is largely based on the IUPAC-recommended tetrapyrrole nomenclature^[35] and its extensions.^[31] As shown in Scheme 2, the full name of a porphyrinoid will include several of the following: 1) substituent list; 2) designation of replaced heteroatoms or cyclic subunits; 3) length of the conjugation pathway $[N]$ (Section 3.1); 4) systematic name indicating the number of cyclic subunits; 5) designation of the meso pattern. The latter designator, which is of the general form (*a.b.c.d...*), shows



Scheme 2. Examples of porphyrinoid nomenclature.

how many carbon atoms separate consecutive pairs of adjacent cyclic subunits. The starting point of the labeling sequence and its direction are chosen so as to maximize the value of the meso designator (taken as a decimal number without periods). Cyclic subunits are labeled with capital letters, in such a way that subunit A lies between the first and last meso bridge. For instance, the preferred subunit labeling for the sapphyrin ring yields (1.1.1.1.0), with the rings of the bipyrrole subunit labeled as A and E (Scheme 2). If the meso pattern has cyclic symmetry the non-pyrrolic subunits are labeled as early as possible (e.g. A,D-di-*p*-benzihexaphyrin, Scheme 2). Finally, numbering of atoms begins with the atom of ring A that is directly bonded to the last labeled ring or to the meso bridge separating them. The numbering sequence then follows the convex sides of subunits (typically on the outside of the macrocycle, see Section 2.1) and the intervening meso bridges, as seen in Scheme 2. Positions on the concave sides of subunits are labeled at the end. In this Review, structures will be drawn in such a way that the numbering will increase clockwise. The present convention, used consistently, may occasionally lead to numbering schemes differing slightly from those reported in the literature (notable examples are corrole and vacataporphyrin, discussed in Section 4). In particular, it will be assumed that ring fusion does not affect the numbering sequence even though it obviously changes the size of the SMC. Replacements of heteroatoms are given relative to the corresponding all-pyrrolic structure. Consequently, a carbon replacing one of the pyrrolic nitrogens is denoted with the prefix “carba-”. When the non-pyrrolic subunit is not a five-membered ring, prefixes such as *m*-benzi-, *p*-benzi-, and pyri- are used to indicate the replacement.

The structures in this Review will be labeled with consecutive bold numbers, each number corresponding to a particular type of macrocycle (defined by its constitution, connectivity between subunits, and oxidation level). The relevant structures will be listed in tables separately for each section. The bold number will be suffixed with a letter

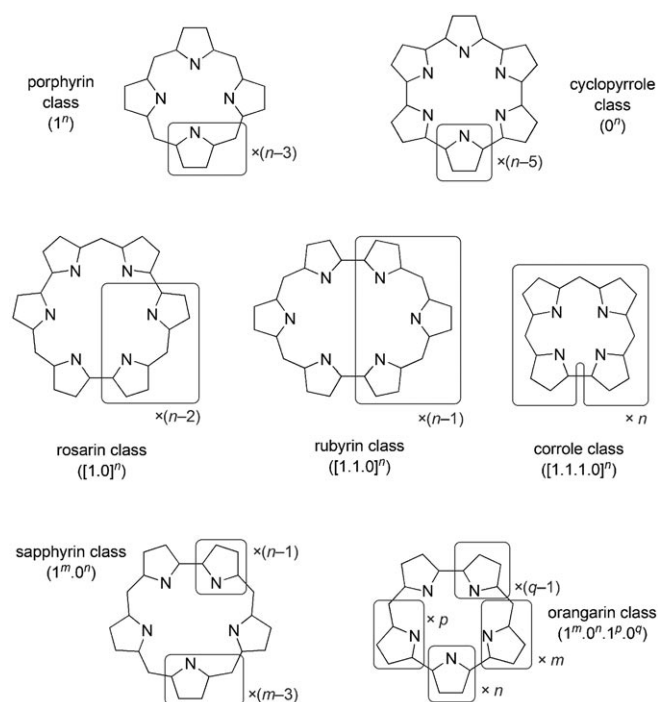
denoting the substitution pattern (defined in the footnote of the corresponding table). The protonation or complexation status of the system will be indicated after a hyphen and any further modifiers will be explained in the text. For example tetraphenylsapphyrin and di-*p*-benzihexaphyrin shown in Scheme 2 are labeled respectively **19b**-H₃ and **44h**-H₂ in the subsequent text. The number of hydrogens indicated for the free base is in most cases equal to the number of available NH and OH groups, even when the macrocycle is capable of forming M–C bonds. Metal complexes containing M–C bonds or other unusual structural features are given separate numbers in the text. An exception will be made for vacataporphyrin, which is conveniently treated as a tribasic molecule (one NH and two CH groups, Section 4.5).

1.3. Typology and Synthetic Considerations

By varying the number and identity of cyclic subunits and the length of meso bridges, it is possible to design countless porphyrinoid macrocycles. In reality, the chemist's invention is restrained not only by structural limits but also by the synthetic accessibility of particular motifs. In particular, as the majority of large ring porphyrinoids are constructed from short-chained oligopyrrolic precursors (typically up to three cyclic subunits), the resulting macrocyclic skeletons often exhibit cyclic or reflective permutational symmetry, which may occasionally lack its geometrical counterpart in an actual three-dimensional conformation. The classification introduced below will be helpful in subsequent discussion of larger macrocycles. It covers the majority of reported motifs containing single-carbon (C₁) bridges, including all systems bearing trivial names (Scheme 3, Table 1). For simplicity, the explanations given below refer to all-pyrrole macrocycles.

The “porphyrin class”, denoted (1ⁿ), includes systems containing only single-carbon meso bridges. Porphyrinoids without meso bridges, which can be denoted (0ⁿ) are known as cyclo[*n*]pyrroles. The rosarin, rubyrin, and corrole classes, named after their most characteristic representatives, are also characterized by *n*-fold cyclic symmetry, and are related by a common construction paradigm. Specifically, representatives of these classes can be viewed as cyclic oligomers of dipyrins, tripyrrins, and tetrapyrins, respectively. All of these structures formally contain bipyrrrole subunits, and some of them can indeed be synthesized from bipyrrrole derivatives. It can be noted that norcorrole (Section 4), not yet isolated in a metal-free form, is formally the smallest feasible member of the rosarin class (*n* = 2). The sapphyrin class includes systems of the general structure (1^m.0ⁿ), which corresponds to reflective rather than cyclic symmetry. The corrole skeleton could formally be included in the sapphyrin class. Among the systems that do not fit into any of the above categories, many contain two contiguous sequences of one-carbon bridges separated by two sequences of direct pyrrole-pyrrole linkages, and can be described with the general formula (1^m.0ⁿ.1^p.0^q). These systems will be considered to be homologues of orangarin.

The preparative aspects of porphyrinoid chemistry^[16] are beyond the scope of this Review, however, some highlights of



Scheme 3. Proposed classification of typical meso patterns observed in porphyrinoids. Patterns containing multi-atom meso bridges are not included.

synthetic work will be included, whenever they contribute to the discussion of conformational effects. Nevertheless, it is important to emphasize that the structural richness of the porphyrinoid world is largely due to very significant synthetic advances accomplished in the last decades. Macrocyclizations used in porphyrinoid synthesis are usually electrophilic aromatic substitutions, but their realization is dependent on the intended substitution pattern. Syntheses of *meso*-substituted systems are usually direct condensations of pyrroles, aldehydes, and possibly other building blocks, using the so-called Rothemund–Lindsey protocol (or its variants), involving oligopyrroles with saturated meso bridges (pyrranes, Table 2).^[62] The modern approach to β -substituted systems involves condensations of appropriate pyrranes, such as dipyrromethanes^[63] or tripyrranes.^[64] Tripyrranes proved particularly versatile as building blocks enabling the synthesis of numerous β -substituted macrocycles.^[14,16] Direct linkages between cyclic subunits (“0” bridges) are created oxidatively at the time of macrocyclization^[16,33] or are already present in the starting materials. Of particular importance are building blocks such as bipyrrrole,^[65] terpyrrrole,^[55] and higher oligopyrroles.^[66] Bridges containing more than one carbon are available using such procedures as McMurry coupling,^[65] or Wittig reaction.^[16,30] Apart from macrocyclizations, a number of reactions are available in which a structurally distinct porphyrinoid molecule is built starting from a preformed macrocycle. These reactions include macrocycle extrusion,^[67] fusion of cyclic subunits or peripheral substituents,^[22] and reductive removal of heteroatoms (“vacatization”).^[68]

Table 1: Representative meso patterns of porphyrinoids containing only single-carbon meso bridges.^[a]

<i>m</i>	<i>n</i>	<i>p</i>	<i>q</i>	Meso pattern	Trivial name
porphyrin class (1 ⁿ)					
3				(1.1.1)	subporphyrin ^[36]
4				(1.1.1.1)	porphyrin
5				(1.1.1.1.1)	[37]
cyclopyrrole class (0 ⁿ)					
6				(0.0.0.0.0.0)	[38]
7				(0.0.0.0.0.0.0)	[38]
8				(0.0.0.0.0.0.0.0)	[39]
rosarin class ([1.0] ⁿ)					
3				(1.0.1.0.1.0)	rosarin ^[40]
4				(1.0.1.0.1.0.1.0)	[41]
6				(1.0.1.0.1.0.1.0.1.0.1.0)	[42]
8				(1.0.1.0.1.0.1.0.1.0.1.0.1.0.1.0)	[42]
ruberin class ([1.1.0] ⁿ)					
2				(1.1.0.1.1.0)	ruberin ^[43]
3				(1.1.0.1.1.0.1.0)	[44]
4				(1.1.0.1.1.0.1.0.1.0.1.0)	[45]
5				(1.1.0.1.1.0.1.0.1.0.1.0.1.0.1.0)	[45]
corrole class ([1.1.1.0] ⁿ)					
1				(1.1.1.0)	corrole ^[46]
2				(1.1.1.0.1.1.1.0)	[47]
sapphyrin class (1 ^m .0 ⁿ)					
4	1			(1.1.1.1.0)	sapphyrin ^[48]
3	2			(1.1.1.0.0)	isosmaragdyrin ^[49]
4	2			(1.1.1.1.0.0)	[50]
4	3			(1.1.1.1.0.0.0)	[51]
5	2			(1.1.1.1.1.0.0)	[52, 53]
6	1			(1.1.1.1.1.1.0)	[51]
6	2			(1.1.1.1.1.1.0.0)	[54]
orangarin class (1 ^m .0 ⁿ .1 ^p .0 ^q)					
1	1	1	2	(1.0.1.0.0)	orangarin ^[55]
2	1	1	1	(1.1.0.1.0)	smaragdyrin ^[56]
1	2	1	2	(1.0.0.1.0.0)	amethyryn ^[55]
1	1	1	3	(1.0.1.0.0.0)	isoamethyryn ^[57]
1	2	1	3	(1.0.0.1.0.0.0)	[58]
3	1	1	1	(1.1.1.0.1.0) ^[a]	[59]
2	1	2	2	(1.1.0.1.1.0.0) ^[a]	[60]
2	1	2	3	(1.1.0.1.1.0.0.0) ^[a]	[61]
1	1	1	2	(1.0.1.0.0.1.0.1.0.0) ^[b]	turcasarin ^[23]

[a] Variables *m*, *n*, *p*, and *q* are defined in Scheme 3. [b] No all-aza analogue has been reported. [c] Orangarin dimer.

2. Conformation of Porphyrinoids

In his famous paper, published in 1885, Adolf von Baeyer argued that rings composed of tetrahedral carbon atoms are inherently strained if they are smaller or larger than five-membered.^[69] The resulting conviction that large rings are too unstable to exist was impeding the development of macrocyclic chemistry until the structural elucidation of muscone and civetone by Lavoslav Ružická^[70] and porphyrins by Hans Fischer.^[71] These macrocyclic structures, brought to light in the 1920s, demonstrated two points that Baeyer did not include in his strain theory: 1) that the rings need not be

Table 2: Strategies used for the synthesis of expanded porphyrinoids.^[13, 14, 16, 18, 33, 65]

Reaction	Scope
Macrocyclizations	
Rothmund–Lindsey	typically <i>meso</i> -substituted systems
condensation of pyrranes	<i>meso</i> - and β -substituted systems
McMurry coupling	porphycenes
DDQ oxidative coupling	rubyrins
Fe ^{III} , Cr ^{VI} oxidative coupling	oligobipyrrole macrocycles
Wittig reaction	vinyllogous porphyrins
Post-macrocyclization modifications	
macrocycle extrusion	tri- and tetrapyrins
ring fusion	ring-fused systems
peripheral fusion	peripherally fused systems
“vacatization”	vacataporphyrin

planar and 2) that even a planar ring does not need to be a convex polygon. Today, both of these notions are essential to understanding the observed structural diversity of porphyrinoids. It may be viewed as a singular twist of fate that a molecule Baeyer reported soon after publishing his strain theory actually contained a 16-membered ring.^[72] Octamethylcalix[4]pyrrole,^[73] as the compound is now known, could well be the first synthetic macrocycle isolated in pure form.

The observed conformation of a porphyrinoid is a complicated function of such structural features as the constitution of the macrocyclic ring, its size, peripheral substitution, and the formal oxidation state. Furthermore, the conformation is not an invariable attribute of a certain ring type and, especially in the case of larger macrocycles, it may be affected by metal coordination, anion binding, acid–base chemistry, solvation, and even temperature. Consequently, conformational preferences of porphyrinoids are difficult to predict even though certain trends can be observed among the systems reported to date. Below we introduce a quantity called free curvature (τ_F), which we have found helpful in rationalizing some of the empirical observations.

2.1. Free Curvature and the Turning Number

The turning number τ of a plane curve is defined as the number of rotations of the tangent line moving along that curve,^[74] and is equivalent to the total curvature^[75] expressed in the units of 2π . Thus in the following discussion, the turning number will often be called “curvature” for simplicity. For any closed curve, τ takes integer values, and in the specific case of the circle, $\tau = 1$. The lemniscate ∞ is characterized by $\tau = 0$, because the two cyclic loops have opposite circulations. Consider a macrocyclic skeleton with a given value of *S* (size of the SMC). If the macrocycle is dissected at any bond not contained in a cyclic subunit, one obtains a chain of subunits, which contains a path of *S* atoms originally belonging to the SMC (Figure 1). Now assume that the chain is fully coiled, that is, it maximizes its total curvature (see the porphyrin example in Figure 1), and all angles are relaxed to their estimated equilibrium values. Additionally, the coil is held completely planar and all possible steric interactions are

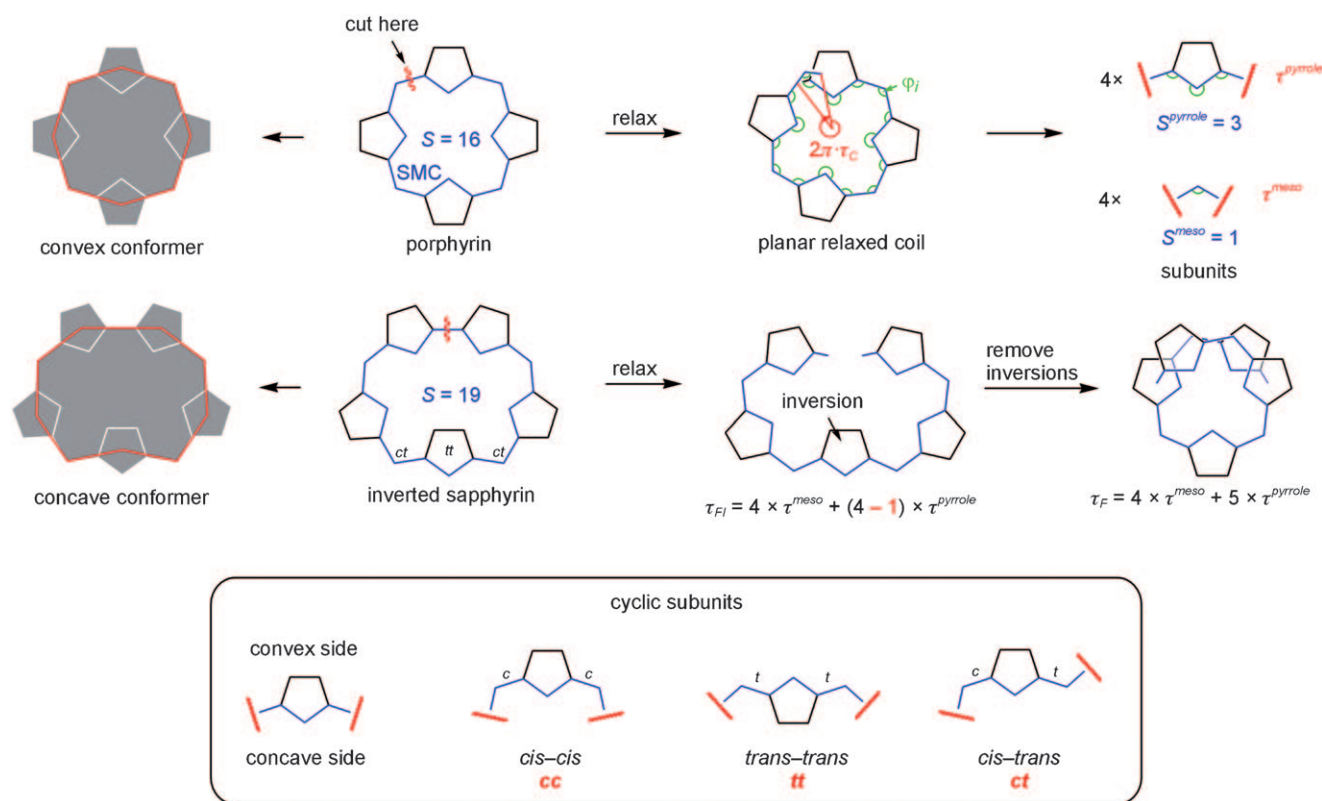


Figure 1. Definition of the free curvature (τ_F) and related concepts. The definitions given for cyclic subunits (in the box) are also applicable to meso bridges.

disregarded. The turning number of such a coil will be called “free curvature.” It is conveniently expressed as

$$\tau_F = \frac{1}{2\pi} \left(\pi S - \sum_i \varphi_i \right) \quad (1)$$

where S is the size of the smallest macrocyclic circuit as defined in Section 1.2, and the summation goes over all interior angles φ_i (“interior” is defined as the concave side of the coil). It should be noted that τ_F is not a conformational descriptor because it is associated with an idealized macrocyclic system and not with any particular three-dimensional structure. The value of τ_F can easily be converted into a sum of increments

$$\tau_F = \sum_{\text{subunit}} \tau^{\text{subunit}} \quad (2)$$

where τ^{subunit} is defined by the curvature introduced by the number S^{subunit} of angles pertaining to a given subunit

$$\tau^{\text{subunit}} = \frac{1}{2\pi} \left(\pi S^{\text{subunit}} - \sum_j \varphi_j \right) \quad (3)$$

The exact values of such increments would in general be specific to a particular macrocycle, and calculating them would be impractical. They can however be estimated on the basis of simple geometrical reasoning or from equilibrium geometries of corresponding unsubstituted heterocycles, with sufficient accuracy for a semi-quantitative discussion. Values

of τ^{subunit} increments for relevant subunits, given in Table 3, are mostly based on DFT-optimized geometries. It is apparent from the above analysis that each subunit with a nonzero τ^{subunit} value will have two geometrically nonequivalent sides, which can be labeled convex and concave, as shown in Figure 1. A subunit (either cyclic or linear) can be aligned with respect to the chain in three ways differing in the

Table 3: Subunits and the corresponding τ^{subunit} increments.

Subunit	Connectivity	τ^{subunit}
methine		0.167 ^[a]
pyrrole	2,5 (regular)	0.132 ^[b]
	2,4 (N-confused)	0.148 ^[b]
	2,3 (“protruding”)	0.286 ^[b]
furan	2,5	0.154 ^[b]
thiophene	2,5	0.087 ^[b]
selenophene	2,5	0.070 ^[c]
tellurophene	2,5	0.046 ^[c]
benzene	1,3 (<i>m</i> -phenylene)	0.167 ^[a]
	1,4 (<i>p</i> -phenylene)	0.000 ^[a]
pyridine	2,6	0.181 ^[b]
<i>H</i> -pyrrolo[3,2- <i>b</i>]pyrrolizine ^[d]	2,7	0.346 ^[b]
<i>H</i> -pyrrolo[2,3- <i>b</i>]pyrrolizine ^[e]	2,5	0.306 ^[b]
2-methylene-2H-telluropheno-[2,3- <i>b</i>]pyrrolizine ^[f]	2,5	0.377 ^[c]

[a] Idealized geometry. [b] B3LYP/6-31G** geometry. [c] B3LYP/LANL2DZ geometry. [d] The N-fused fragment with an N-confused pyrrole. For explanation, see Section 4.2. [e] The N-fused fragment in the absence of N-confusion. [f] The fused unit in N-fused 21-telluraporphyrin (see Section 4.2). The 2-methylene group provides the necessary exocyclic double bond.

geometry of the inter-subunit bonds of the SMC. These alignment types will be denoted *cis-cis* (*cc*), *trans-trans* (*tt*), and *cis-trans* (*ct*).

The preferred conformation of the tetrapyrrolic porphyrin ring (Figure 1) may be called a convex conformer. While the polygon closed by the SMC is actually concave, the polygon formed by meso positions and centroids of cyclic subunits is convex. In a convex conformer, all subunits have the *cc* alignment, and their concave sides point towards the center of the macrocycle. If some subunits are inverted, that is, they are incorporated into the macrocycle with their concave sides pointing outside we will call the corresponding conformation concave (or bi-, triconcave, etc. depending on the number of subunits). Typically, the inverted subunit has the *tt* alignment and it is accompanied by two adjoining *ct*-aligned subunits. The sapphyrin conformer shown in Figure 1 is an example of a concave conformation. We can dissect a concave conformer at any bond not contained in a cyclic subunit and allow the chain to relax while keeping the inverted subunits. It follows from a simple geometrical reasoning that the turning number corresponding to such an arrangement can be calculated by adding the increments of regular subunits and subtracting the increments of inverted subunits. We will call the resulting value “free curvature with inversions”, τ_{FI} . The τ_{FI} value, which is always smaller than the corresponding τ_F , is a useful characteristic of concave conformers. Further discussion of the free curvature and its properties is given in the following sections.

2.2. Types of Conformational Effects

Angular Distortion. In purely geometrical terms, a chain of subunits should provide for a strain-free macrocycle closure only if it is characterized by $\tau_F = 1$. However, fulfilling this requirement may increase other energetic contributions (notably the steric interactions between neighboring subunits), and consequently the overall strain in the macrocycle may not be minimized by $\tau_F = 1$. In particular, the porphyrin macrocycle, normally assumed to be relatively strain-free, is characterized by $\tau_F = 1.19$, which can be considered a convenient reference value for comparison with other systems. The analysis carried out in this Review shows that the actual range of τ_F values for experimentally verified convex structures extends from 0.79 (cyclo[6]pyrrole, **29-H₄**) to 1.49 (pentaphyrin(1.1.1.1.1) in the form of a uranyl complex **26a-UO₂**). Interestingly, even macrocycles with τ_F strongly deviating from unity are capable of sustaining relatively planar convex conformations (e.g. rubyrin **35a-H₄**). In general, the deviation of τ_F from unity may be considered a rough measure of angular strain that will be induced upon closing the macrocycle. It should be noted, however, that $\tau_F = 1$ does not implicate geometric closure of the chain but only that the tangents at its ends are parallel (an appropriately chosen section of a spiral may have $\tau = 1$). Nevertheless, in most cases of $\tau_F \approx 1$ discussed in this Review, the distance between the ends of the chain is relatively small.

Out-of-Plane Distortion. The angular distortion described above is usually accompanied by varying amounts of torsional

(out-of-plane) deformation, which is a complementary way of dealing with the excess free curvature. The importance of the out-of-plane distortion increases at larger τ_F values, for which further increasing of the bonding angles is no longer energetically preferred. However, out-of-plane distortion is also caused by a variety of other effects and can be observed even in systems with small τ_F values. This phenomenon has been amply demonstrated for regular porphyrins, which can become significantly non-planar as a consequence of heavy peripheral substitution, internal modifications, coordination of elements with small or large ionic radii, axial ligation, or anion binding.^[76,77]

Inversion of Subunits. When the value of τ_F is approximately 1.2 or larger, the excessive free curvature is frequently eliminated (completely or in part) in a process known as “ring inversion”^[19,78] (Figure 1). An inverted ring (cyclic subunit) is oriented with its convex side towards the macrocyclic core. Inversion of meso carbons is also observed and it becomes a nearly standard feature of vinylogous porphyrins, containing meso bridges of three or more carbons.^[31] As a consequence of inversion, the polygon defined by ring centroids and meso bridges is no longer convex. Obviously, ring inversion will not lead to a reduction of curvature if the subunit possesses rotational symmetry (and hence $\tau_{subunit} = 0$), as it is the case of *p*-phenylene. Ring inversion is a ubiquitous feature, and can be observed in systems of widely varying macrocycle sizes, starting with tetrapyrins. In smaller macrocycles, however, ring inversion increases steric crowding inside the macrocycle, and consequently, concave conformers of reported tetra- and pentaphyrins are never completely planar. Finally, it should be noted that the effectiveness of subunit inversion as a strain-reducing device is usually limited whenever the subunit to be inverted bears bulky substituents that would cause additional crowding in the macrocyclic core. Consequently, inversion of cyclic subunits is rare in β -substituted systems whereas inversion of meso bridges is seldom observed in *meso*-substituted macrocycles.

2.3. π -Surface Topology

In typical aromatic compounds the ring containing the delocalized π electrons is planar and indeed, for small-ring systems, planarization is one of the manifestations of an aromatic structure. Larger rings, such as porphyrinoid macrocycles, may show additional conformational features, namely out-of-plane distortion and subunit inversion, both of which preserve the topology of the π -system. In the present Review, the term “topology” will always refer to the properties of the p orbital basis (or its subset) in its actual three-dimensional realization. It should be noted that from the stereochemical point of view, different topologies of a π -electron system are geometrical rather than topological isomers. Additionally, they are also topologically equivalent in terms of their molecular graphs.^[79–81]

We can simplify the following discussion if we associate the π system with a ribbon (“SMC ribbon”) that passes through all atomic centers along the SMC and is tangential to the nodal planes of the respective p orbitals (Figure 2). In the

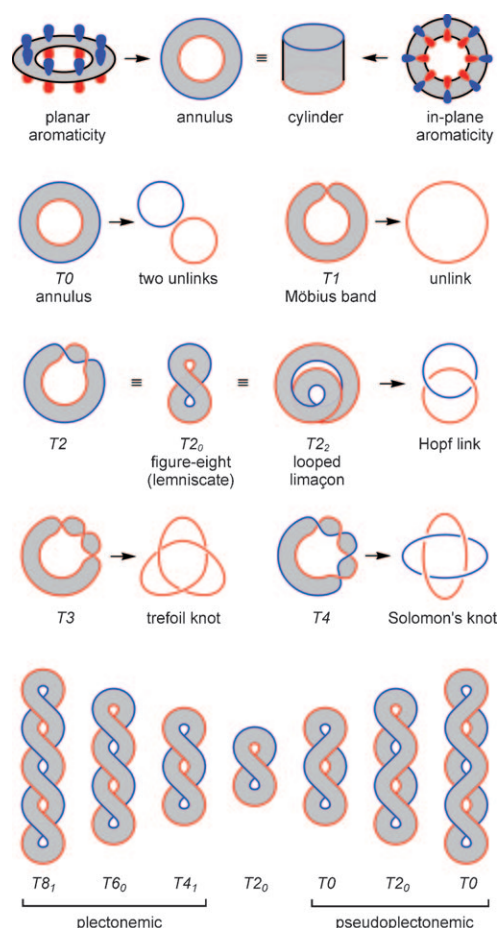


Figure 2. Topological representations of various π -conjugated surfaces.

case of a planar structure, the SMC ribbon adopts the shape of an annulus, that is, a punctured disk. A further simplifying observation is that a monocyclic π electron system can always be continuously deformed in such a way that the axes of p orbitals all lie on the surface of the ribbon (Figure 2). As a consequence, the topological properties of the π system are equivalent to those of the edges of the ribbon. For instance, the annulus, which represents a planar aromatic system, possesses two edges, which are not topologically linked (they can be separated without cutting). This is in agreement with the properties of the π -system, which consists of two lobes that are not interlocked in space. An additional consequence of the above analysis is the topological equivalence of planar and in-plane (tubular) π -conjugation.^[10] The latter can be identified with the π -conjugated surface in the form of a cylinder (Figure 2) which is another representation of the annulus.

Topological diversity is now introduced by cutting the annulus, applying one or more half-twists across the longitudinal axis of the ribbon, and joining the ends back. The resulting cyclic bands will be labeled T_n , where n is the number of half-twists (or, more precisely, the linking number, as discussed below). In particular, all untwisted rings will be denoted T_0 throughout this Review. With one half-twist (T_1 , Figure 2), one obtains the Möbius band, which is a one-sided surface possessing a single, unknotted edge. The band with

two half-twists (T_2) is two-sided and has two interlocked edges (forming the so-called Hopf link). An important representation of this topology, in which the twist is “flattened out”, is the figure eight (or lemniscate), which is frequently encountered among porphyrinoid conformers. As the lemniscate is characterized by $\tau = 0$, the figure-eight representation may be denoted T_{2_0} . In another flattened form, T_{2_2} , the band adopts a shape of the so-called looped limaçon,^[82] which has $\tau = 2$. In the case of higher twist levels, the T_n bands with n odd are always one-sided and possess a single edge, which is increasingly more knotted as n increases (for T_3 , one obtains the trefoil knot). Conversely, even n values generate two-sided bands with two interlocked edges (the link obtained for T_4 is known as Solomon's knot). To date, there are virtually no examples of porphyrinoids containing more than two formal half twists in their π -system and this limitation likely applies to other types of π -conjugated macrocycles as well. One interesting exception is the single unusual example of the T_4 topology, which will be discussed in Section 9.1. The problem of stabilizing higher twist levels stems in part from the difficult control over the conformation of very large rings.

In terms of the above “rubber band” description, a convex T_0 system is topologically equivalent to all derivative concave conformers (see however Section 2.5 for a more detailed analysis). In the following discussion, we will distinguish concave conformations by adding a list of inverted subunits in the superscript to the T_0 symbol. For instance, the concave conformer of sapphyrin (Scheme 2) will be labeled T_0^C . Meso bridges will be referred to with their locant numbers, as for instance in $T_0^{15,G}$ (cf. **62a-H₄** in Section 7).

It should be noted that the τ_{FI} value is a well-defined quantity only for T_n topologies with n even. This happens because in the calculation of τ_{FI} , the subunit is classified as inverted if its curvature is opposite to the local curvature of the coil. However, the sign of the local curvature is not well defined for odd-numbered T_n topologies, because the curvature vector becomes inverted during a second pass along the band. In the figure-eight conformations T_{2_0} , the two loops have opposite curvatures and, as long as they are symmetry-equivalent, τ_{FI} will always equal 0. Thus τ_{FI} is a useful parameter only in the case of T_0 conformers.

The principal representations of T_n conformers shown in Figure 2, contain half-twists compressed over a short section of the macrocycle, so as to facilitate their counting. In the theoretical description of π conjugation, the twist was originally assumed to be evenly distributed around the ring.^[83] However, it is evident from the structures T_{2_0} and T_{2_2} that the T_2 topology can in fact be achieved by only minimally twisting the band. This observation can be explained by using the more general concept of the linking number. Its initial application to chemistry was to describe folding of double-stranded DNA,^[84] whereas its utility for the description of π -conjugated molecules has only been appreciated recently.^[85] The linking number, Lk , is an integer value that corresponds to the number of half-twists formally applied to the ribbon, as discussed above, whereas its sign determines the direction of twisting (i.e. the sense of chirality of the ribbon). For a three-dimensional ribbon, the linking number satisfies the Călugăreanu theorem

$$Lk = Tw + Wr, \quad (4)$$

where Tw and Wr are respectively twist and writhe and are not, in general, integer quantities. Tw is the total rotation of the normal vector integrated along the length of the ribbon and expressed in units of π , whereas Wr measures the extent to which the coiling of the central line of the band has relieved the local twisting.^[84] While analytical expressions exist for the writhe, its value is more easily calculated as a difference between Lk and Tw . Tw and Wr are geometrical invariants of the ribbon, and as both of them are signed values, they also distinguish the sense of chirality. The linking number can be computed from the link diagram formed by the edges of the ribbon^[86] or through the so-called Gauss linking integral.^[85] In the simple topologies encountered among π aromatics, the value of Lk is conveniently verified by disentangling the edges of the ribbon and comparing the resulting knot or link with those given in Figure 2.

For a given topology of the π system, the maximum attainable value of $|Tw|$ equals $|Lk|$, corresponding to a circular ribbon with uniformly distributed twist. In contrast, the lemniscate ($T2_0$) and limaçon ($T2_2$) representations approaching complete planarity will be characterized by $Tw \rightarrow 0$, meaning that, in the limiting case, almost all of the twist can be projected into writhe. However, in a real aromatic system the crossing cannot be planar for steric reasons and the expected distance between the intersecting parts of the macrocycle will be normally larger than 3 Å. In the majority of actual $T2_0$ conformations discussed below, Tw lies in the range 0.5 to 1.3. In the Möbius topology $T1$, the lower bound of possible Tw is also 0, but this result is possibly less evident than in the case of $T2$. It can be explained by using the construction shown in Figure 3. The $T1$ π system may be viewed as a combination of two sections characterized respectively by planar and in-plane conjugation, a notion that proved instrumental in designing the first Möbius conjugated hydrocarbon.^[11,87] Such a union of two conjugation types introduces a phase change necessary for a Möbius system. However, if we want the connection points between the two parts not to coincide in space it is necessary to introduce a helical distortion to at least one section. If we now start to reduce the helical pitch we will approach a structure consisting of two planar parts: an annulus and a cylinder, each characterized by zero twist (the connections do not contribute to the twist).

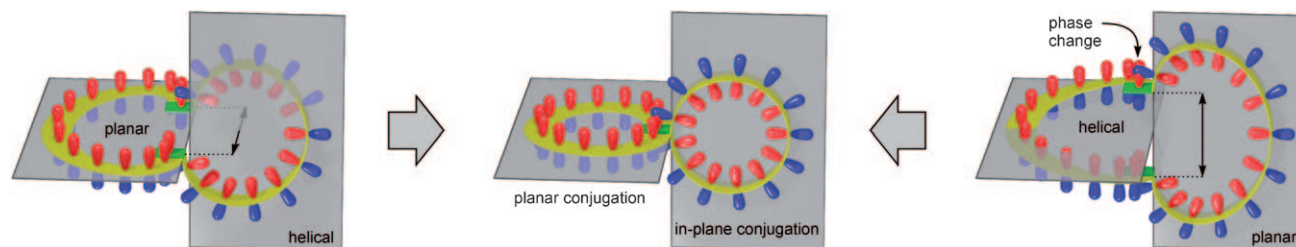


Figure 3. Möbius topology ($T1$) obtained by combining planar and in-plane π -conjugation. Connections between the two conjugated sections are shown in green. Left: structure with a helically distorted in-plane conjugated section. Right: structure with a helically distorted planar conjugated section. Center: the limiting case with no helical distortion and the connections overlapping in space.

An interesting series of figures can be obtained by combining several crossings of the kind present in the lemniscate $T2_0$ (Figure 2, bottom). If all the crossings have the same handedness we will call the resulting figures “plectonemes”, emphasizing their similarity to the plectonemic conformations of DNA.^[86] Consecutive plectonemes increase their linking number by two units at a time, whereas their turning numbers alternate between values 0 and 1 (Figure 2). If the consecutive crossings alternate their handedness we obtain a series of similar-looking figures that we will call pseudoplectonemes. Interestingly, the topology of a pseudoplectoneme is $T2_0$ for an odd number of crossings and $T0$ for an even number of crossings. The two series of lemniscate homologues will be important in the discussion of some of the giant porphyrinoids presented in Section 9.

Conformation and the Free Curvature. Figure 4 shows free curvature values observed for different porphyrinoid conformations. As discussed above, stable convex $T0$ structures reported to date have τ_F values in the range 0.79–1.49. Structures with significantly smaller τ_F values are expected to be destabilized because of the high level of angular strain necessary for macrocyclic closure. In the case of larger τ_F values, subunit inversion and π -surface twisting become viable routes to eliminating the excess curvature. The

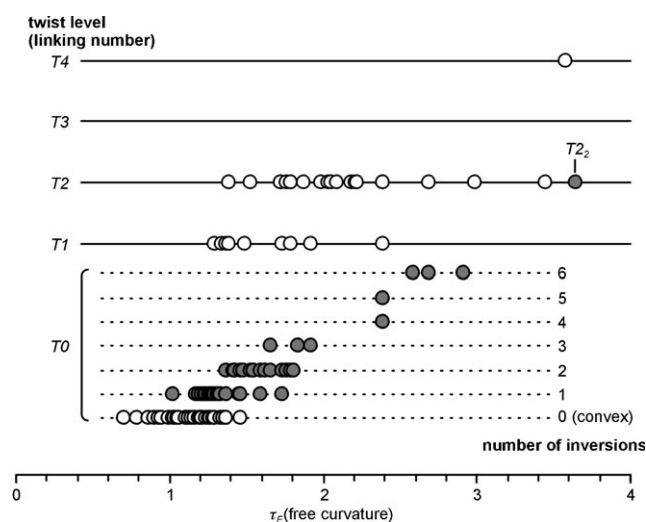


Figure 4. Free curvature ranges for different types of porphyrinoid conformers. Data points correspond to macrocycles discussed in this Review.

majority of concave T_0 structures contain either one or two inverted subunits, with the corresponding τ_F ranges of 1.02–1.73 and 1.37–1.81 (Figure 4). Systems with more than two inverted subunits (not including vinyllogous porphyrins) are observed less frequently. The highest τ_F value for which a stable T_0 conformation was reported is 2.92, corresponding to the sixuply inverted decaphyrin **112b**-H₈ (Section 9.2). The τ_F range for structurally characterized Möbius-like T_1 conformers is currently 1.29–2.39, whereas figure-eight T_2 structures cover a much larger range of 1.39–3.44 (the limaçon T_2 conformer, described in Section 9.2, has $\tau_F = 3.65$). Finally, the only known example of a higher twist level, the T_4 structure of dodecaphyrin **107c**-H₈ is characterized by $\tau_F = 3.58$ (Section 9.2).

It should be noted that stability ranges for different conformations are only approximately defined for large τ_F values, because of the scarcity of available data. Still, Figure 4 enables prediction of feasible conformers for structurally diverse macrocycles (including ones not yet synthesized), once the free curvature has been calculated. For instance, a macrocycle with $\tau_F = 1.3$ will likely adopt convex or singly inverted T_0 conformations. T_1 Möbius-like structures are also feasible, whereas multiply inverted or T_2 conformers are unlikely to be stable.

2.4. Conformational Descriptors

The symbols introduced above to describe conformers of porphyrinoids are of the general form $Tn_\tau^{[...]}$, where n equals the linking number Lk , τ is the turning number of the idealized planar projection of the conformer ($Tw \rightarrow 0$), and [...] is an optional list of inverted subunits used with concave T_0 conformers. The τ parameter, which should not be confused with the free curvature τ_F , can only be given for even values of Lk (it is not defined for odd Lk values) and it is always 1 for $Lk = 0$. However, as discussed above, ring inversion is not well defined in systems with $Lk > 0$ and cannot be used to differentiate twisted conformations. Usually this is not a problem, because in the majority of systems, only one conformation has been identified for each accessible Lk value. For some macrocycles, however, more than one T_1 or T_2 conformer has been observed (see for example compound **15**-H₃) and distinguishing between them would require a more general conformational descriptor. One such descriptor can easily be derived from the analysis of macrocyclic curvature given in Section 2.1. The method described below is directly related to the descriptors used in the chemistry of annulenes.^[88]

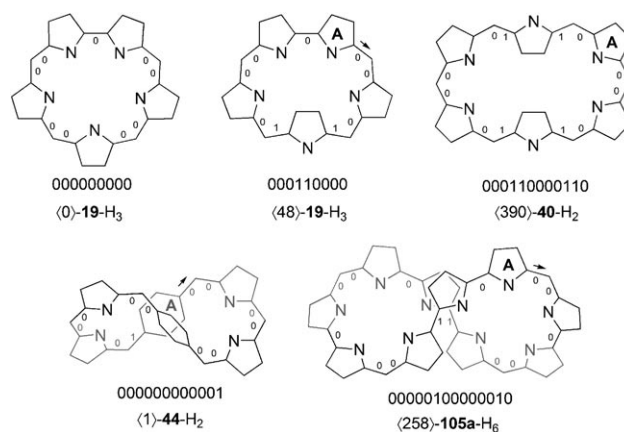
To construct the descriptor, the stereochemistry of the SMC is encoded in the following way:

1. *Cis* and *trans* bonds belonging to the SMC are labeled with binary digits 0 and 1, respectively. *Cis* and *trans* geometry around a bond in the SMC is defined by the absolute torsion angle $|\theta| < 90^\circ$ and $|\theta| > 90^\circ$, respectively.
2. Values corresponding to inter-subunit linkages (i.e. all bonds not contained in cyclic subunits) are then listed to form a binary number, starting with cyclic subunit A. The resulting number of digits is equal to the number of

subunits. In contrast to the convention used in annulene chemistry,^[88] the binary number is not rotated to minimize its value. This is because, in general, porphyrinoids do not possess complete cyclic symmetry of their skeletons. For the descriptor to be meaningful, the starting point has to be identical for all conformers.

3. The binary number thus obtained is converted to its decimal value, which is enclosed in angle brackets $\langle \rangle$ to distinguish it from the CP designator and meso pattern.

Examples of using the descriptor are given in Scheme 4. Subunit A and the direction of labeling are chosen according to the conventions described in Section 1.2. If the ring system



Scheme 4. Usage of the conformational descriptor proposed in Section 2.4.

has a cyclic symmetry that is absent in the actual conformer subunit A is chosen in such a way as to minimize the value of the descriptor (e.g. $\langle 390 \rangle$ -40-H₂). If a cyclic subunit with rotational symmetry (e.g. *p*-phenylene) is encountered, the SMC is chosen in such a way as to give the *cis* arrangement for the first analyzed bond (see **44**-H₂, Scheme 4). By default, the value of $\langle 0 \rangle$ corresponds to a convex T_0 conformer. In the form described above, the present conformational descriptor is suited for encoding different conformations of the same ring system. It will not, in general, yield identical values for structurally analogous conformers of different ring systems (e.g. different heteroanalogues) because the choice of subunit A may differ.

2.5. Topology Switching

In general, ribbons with different Lk values embedded in the three dimensional space cannot be elastically deformed into each other. It is therefore of interest that in the molecular world, it is possible to switch between different π -conjugation topologies without dissecting the macrocyclic ring. This effect is achieved by variation of internal torsional angles and is the basis of a special type of aromaticity switching (Section 6.5). While the macrocycle retains its integrity during the switching process, the π system can be said to be temporarily broken when one torsion angle becomes exactly $\pm 90^\circ$. Figure 5 shows

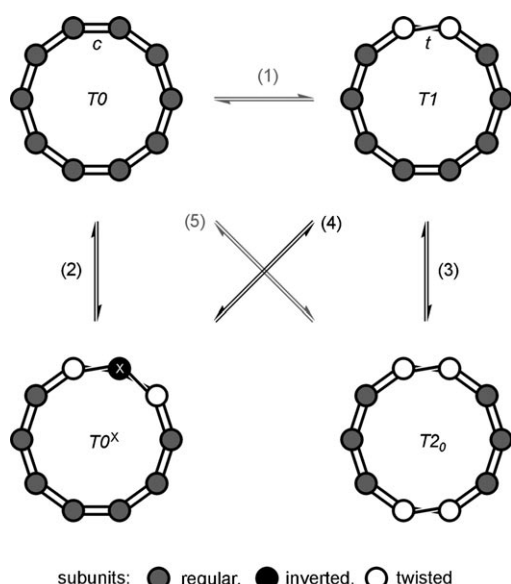


Figure 5. Generic conformational interconversion pathways in porphyrinoid systems. Circles correspond to both cyclic subunits and meso bridges. Conformations are shown in a flattened circular shape that does not correspond to the actual 3D structures. Crossed lines denote transoid linkages. X labels the inverted subunit. Pathways shown in gray have not been verified experimentally.

the simplest conversion pathways between the most important π conjugation topologies. As discussed earlier, a convex $T0$ conformation contains only cisoid inter-subunit linkages. If one linkage is distorted enough to adopt a transoid configuration ($90^\circ < |\theta| < 180^\circ$, pathway 1) one obtains a conformation with $T1$ topology, which will contain two twisted subunits (as defined in Figure 1). If a twist of opposite handedness is introduced to one of the neighboring linkages the $T1$ structure will be converted into a concave conformer $T0^X$, where X labels the subunit located between the two transoid linkages (pathway 4). Overall, a simple uniconcave structure contains two ct and one tt subunit (X). Direct $T0$ – $T0^X$ conversion can be effected by rotating subunit X relative to the macrocyclic frame (pathway 2). In another switching scenario (pathway 3), the Möbius $T1$ conformer can acquire an additional transoid linkage of identical handedness located across the macrocycle. Typically, the resulting structure folds into a figure-eight shape, creating a $T2_0$ conformer. A direct pathway from $T0$ to $T2_0$ can also be envisaged, which involves folding the planar convex conformer in such a way that the two twisted linkages are formed at once (pathway 5).

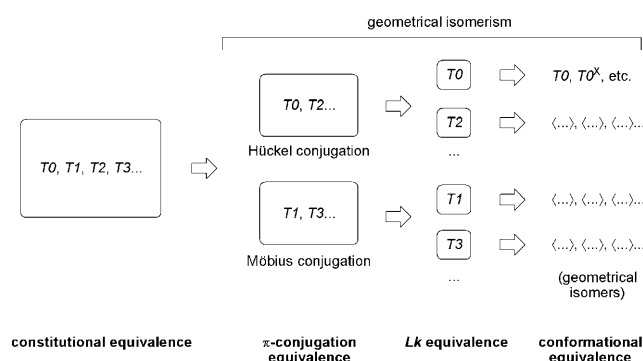
To date, several porphyrinoid macrocycles have been reported that stabilize multiple π -conjugation topologies (Table 4). In these systems, switching is actuated by a variety of chemical and physical stimuli, as discussed in detail in subsequent sections of this Review. It is of interest that direct interconversion between a Möbius $T1$ conformer and a convex $T0$ conformer (pathway 1) has not been observed in any of these systems. In all cases reported to date, $T1$ conformers are converted into concave $T0$ structures containing one (**15**-H₃, **27**-H/**28**-H₃), two (**15**-H₃, **40**-H₂/**41**-H₄, **44**-H₂) or five (**81**-H₄/**82**-H₆) inverted subunits, and the pertinent macrocycles do not stabilize convex conformers. Apparently, simultaneous accessibility of convex $T0$ and $T1$ structures is difficult to achieve because of incompatible ranges of free curvature. $T1$ structures were considered as transition states in the pyrrole inversion ($T0 \rightarrow T0^A$) of regular and N-confused porphyrins.^[89] Interconversion between $T1$ and $T2_0$ conformers, occurring through twisting of one inter-subunit linkage (pathway 3, Figure 5) was demonstrated experimentally in hexaphyrin **44**-H₂ and octaphyrin **75a**-H₆. In systems with larger τ_F values, heptaphyrin **67**-H₄ and octaphyrin **81**-H₄/**82**-H₆, the structural differences between $T1$ and $T2_0$ conformers are more profound and involve additional twists of inter-subunit linkages.

As noted earlier, different topologies of a single π -conjugated system are in fact geometrical isomers differentiable by the $\langle \rangle$ descriptor. It is therefore of interest that in this family of isomers three levels of structural equivalence can be distinguished (Scheme 5):

1. The first level stems from the topological equivalence (homeomorphism) of bands with the same parity of Lk . The edge of even- Lk bands consists of two circles whereas the edge of odd- Lk bands consists of a single circle (cf. Section 2.3). This level is important because, within the framework of the Hückel–Heilbronner description of aromaticity, each of the two equivalence classes exhibits a different type of π -conjugation: Hückel-like (Lk even), and Möbius-like (Lk odd, Section 3.4).
2. The second level, Lk equivalence, distinguishes systems whose SMC ribbons cannot be elastically deformed into each other (without cutting and pasting), as discussed in Section 2.3. A continuous deformation (known as “ambient isotopy”)^[81] between two bands exists only if they have identical linking numbers. Thus each Lk value constitutes a separate equivalence class.
3. Each equivalence class with a given Lk value can comprise several geometrical isomers characterized by different

Table 4: Porphyrinoid ring systems exhibiting multiple topologies.

Species	Topologies	Switching mechanism	Section
vacataporphyrin 15 -H ₃	$T0$, $T1$	metal coordination, acid–base	4.5
[22/24]N-fused pentaphyrin 27 -H/ 28 -H ₃	$T0$, $T1$	metal coordination, redox	5.2
[26/28]hexaphyrin(1.1.1.1.1.1) 40 -H ₂ / 41 -H ₄	$T0$, $T1$, $T2$	metal coordination, redox, acid–base	6.4
di- <i>p</i> -benzi[28]hexaphyrin 44 -H ₂	$T0$, $T1$, $T2$	solvation, temperature, acid–base, anion binding	6.5
[30]heptaphyrin(1.1.1.1.1.0.0) 62a -H ₄	$T0$, $T2$	solvation/crystal packing	7
[32]heptaphyrin(1.1.1.1.1.1.1) 67 -H ₄	$T1$, $T2$	solvation, acid–base, metal coordination	7
[32]octaphyrin(1.0.0.0.1.0.0.0) 75a -H ₆	$T1$, $T2$	metal coordination	8.2
[36/38]octaphyrin(1.1.1.1.1.1.1.1) 81 -H ₄ / 82 -H ₆	$T0$, $T1$, $T2$	acid–base, redox, metal coordination	8.2



Scheme 5. Levels of structural equivalence in π -conjugated macrocycles.

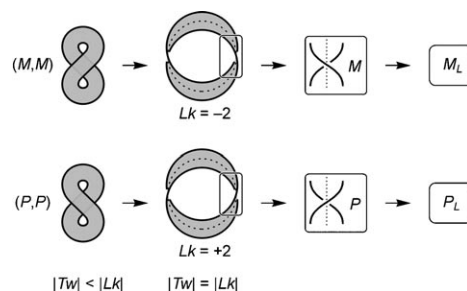
$\langle \dots \rangle$ values. In particular, the T_0 family can contain, in addition to the convex structure, a number of different concave conformers (multiple conformations are occasionally observed also for nonzero Lk values). Even though different geometrical isomers with the same Lk have isotopic SMC ribbons, the actual molecules cannot be elastically deformed into one another in such a way that the integrity of the π -system would be retained at all times. This limitation is stereochemical rather than topological in nature. Obviously, interconversion between geometrical isomers always requires that some of the torsion pass through $\pm 90^\circ$, even if a topology change is not involved.

2.6. Chirality

Any macrocycle with $|Lk| > 0$ is chiral and the sense of chirality is expressed by the sign of Lk .^[85] In molecules with nonzero Lk , inversion of enantiomers must occur with temporary breaking of the π system (in the sense discussed in Section 2.5) and this type of chirality was called “intrinsic”.^[85,90] (The term “intrinsic chirality” found earlier use in the theory of molecular graphs^[91]). Naturally, molecules with $Lk = 0$ can also be chiral but their enantiomers are interconvertible by elastic deformations that retain the integrity of the π system. If none of those deformations is chemically feasible the enantiomers will have stable configurations. Configurational stability of intrinsically chiral systems has been demonstrated by the successful chromatographic separation of enantiomers achieved for Möbius (T_1) annulenes^[92] and certain T_2 porphyrinoids (**79a-H₄** and its metal complexes, Section 8.2).^[93] In an alternative approach, the rigidity of a figure-eight structure was revealed in solution by recording a ^1H NMR spectrum in a chiral solvent (see Section 6.5).^[24]

Apparently, no general stereodescriptor has yet been proposed to distinguish the handedness of intrinsically chiral π systems. Enantiomers of the T_2 structure of **79a-H₄** (Scheme 23) were labeled as (P,P) and (M,M) to indicate the helicity of the two tetrapyrrolic loops present in **79a-H₄**.^[93] Such a designation, while perfectly accurate, may be viewed as redundant because the two loops in a T_2 conformer must have identical helicity. Given the invariance of the linking

number under elastic transformations (homotopies) of the π system, it may now be suggested that the sign of Lk be used as the preferred stereodescriptor for intrinsically chiral π -conjugated macrocycles. Thus molecules with $Lk > 0$ and $Lk < 0$ may be labeled as P_L and M_L , respectively (the subscript L distinguishes the symbols from conventional P and M descriptors). The sense of intrinsic chirality in a macrocycle is conveniently assigned by deforming the SMC ribbon into a shape characterized by $Wr = 0$ and determining the helicity of the ribbon relative to its center line using the usual IUPAC convention (Scheme 6). In the case of **79a-H₄**, the original descriptor (P,P) will be replaced with P_L .



Scheme 6. An example of the use of M_L/P_L stereodescriptors.

3. Aromaticity of Porphyrinoids

3.1. The Annulene Model

The Hückel rules, which constitute the textbook criterion of π aromaticity, were originally derived for monocyclic systems containing identical atoms. Consequently, these rules cannot be strictly applied to porphyrinoids, which contain multiple heterocyclic rings. To cope with this problem, several descriptions have been proposed,^[17] of which the so-called annulene model is the most widely used. According to this model, the ring system of a porphyrinoid is treated as a bridged heteroannulene, and the properties of the corresponding all-carbon annulene are assumed to model the aromaticity of the system in question. The “annulene in porphyrin” concept, dating back to the 1960s,^[94] was exploited with remarkable success in the research on porphyrin isomers^[95] and vinylogous porphyrins.^[31]

In the annulene model of porphyrinoid aromaticity, a conjugation pathway (CP) is searched within the π system that meets the following conditions: 1) it passes through all subunits, that is, it encompasses the macrocycle; 2) it can be filled with an alternating sequence of formal single and double bonds, that is, it can be represented by two Kekulé structures; 3) it does not involve charge separation (see Scheme 1 for representative examples). When these conditions are met, the length of the CP, denoted N , is equal to the number of π electrons in the CP and corresponds with the observed aromatic or antiaromatic character of the macrocycle, in accordance with the Hückel rules. If all macrocyclic circuits are cross-conjugated, the macrocycle will be non-aromatic. (Residual aromaticity may be observable when a CP can be found in a charge-separated structure.)^[17] In this

Review, a macrocyclic CP will be indicated with bold bonds in nearly all systems for which it can be constructed. It should be noted, however, that the possibility of drawing out an appropriate valence structure does not always imply significant macrocyclic aromaticity. In general, the CP is not identical with the smallest macrocyclic circuit (SMC), and the difference between the lengths of these two circuits $N-S$ decreases with increasing oxidation level of the macrocycle (it is worth noting that, in the case of all-pyrrole porphyrinoids, $N-S$ equals the number of amino hydrogens). The N value is given in square brackets in front of the name of the ring system (e.g. [18]porphyrin).

In the case of all-pyrrole porphyrinoids containing no confused rings,^[78] the CP passes through the iminic nitrogens and circumvents the amino NH groups. This observation is a useful mnemonic for a quick identification of the CP. However, it also implies that the selection of the CP depends on the placement of dissociable hydrogens, which creates ambiguity whenever the preferred tautomer is not known. By extension, the CP is not uniquely given in the case of conjugated acids and metal complexes, in which its selection is dependent on the placement of formal charges. Additionally, in systems containing *p*-phenylene subunits, only one side of the phenylene ring is included in the path, creating an additional source of arbitrariness. In spite of these drawbacks, the annulene model is an intuitive and effective approach to qualitative description of macrocyclic aromaticity.

3.2. Aromaticity Criteria

Quantification of aromaticity is a topic of fundamental significance in physical organic chemistry, and has been the subject of extensive theoretical and experimental investigation. Aromaticity is currently described as a multidimensional phenomenon,^[96,97] implying that in general, the aromatic character cannot be quantified using a single numerical criterion. The selection of the most useful aromaticity measure in a given case will therefore depend on its reliability and sensitivity to structural changes. The following brief summary discusses criteria that are of relevance in porphyrinoid research.

Energy-Related Criteria. Resonance energies of large aromatic systems such as porphyrins are difficult to assess experimentally^[98] and consequently, relative stabilities of porphyrinoid systems are normally estimated using high-level quantum chemical methods. It should be noted that the effect of aromatic stabilization (antiaromatic destabilization) is less pronounced for large macrocyclic aromatics than for their smaller congeners.^[99] As a result, many expanded porphyrinoids exhibit two (occasionally more) chemically stable oxidation levels. Such levels are typically related by a formal two-electron redox process, meaning that they have respectively $4n$ and $4n+2$ electron CP's. Importantly, in many cases each oxidation level is air stable or may be stabilized by structural modifications, such as change of substituents or metal coordination. Furthermore, large $4n$ electron macrocycles, even if they are destabilized relative to the $4n+2$ forms, may gain additional stabilization by transforming into

Möbius-conjugated conformers. Another consequence of extensive π -conjugation is the decreasing HOMO–LUMO gap, which affects the observed electronic transitions and redox potentials. Electronic spectra of very large porphyrinoids are often remarkably red-shifted while retaining high absorption coefficients.^[39,47,100] Two-photon absorption cross-sections have been recently found to correlate with NICS values of some porphyrinoids, and have therefore been advocated as a useful aromaticity criterion.^[101–103]

Magnetic Criteria. The importance of proton chemical shifts as an aromaticity measure was recognized in the very first NMR spectroscopic study of porphyrin derivatives.^[104] The usefulness of ^1H NMR spectroscopy in the determination of aromatic character of porphyrinoids^[17,105] relies on a number of their structural features. First, in large macrocyclic systems, the observed ring currents, both dia- and paratropic, are often of considerable magnitude, providing for their facile identification even in the presence of other effects. Second, the availability of protons attached to the periphery of the macrocycle and, more importantly, in the macrocyclic core, enables easy evaluation of ring current effects. For instance, the range of chemical shifts observed for the inner protons extends from negative values on the δ scale (frequently below -5 ppm) in strongly diatropic systems to large positive shifts (20 ppm and more) in certain paratropic porphyrinoids. Finally, the ^1H chemical shifts are remarkably sensitive to very small structural changes, enabling one to study the dependence of π -conjugation on acid-base chemistry or conformational effects. However, for exploiting the full potential of NMR spectroscopy, accurate signal assignments are needed, which are occasionally difficult to achieve, especially for large, dynamic systems, with low molecular symmetry. A computational aromaticity criterion, conceptually derived from proton shieldings is the nucleus-independent chemical shift (NICS),^[106,107] which has become a routine theoretical approach to π -conjugated systems, including porphyrins and their analogues.^[108] Calculation of actual proton shieldings is methodologically more demanding because, unlike NICS's, these values have to be directly compared with experiment. Satisfactory results can only be obtained from accurate geometries, which, in the case of large π aromatics, are not always sufficiently well reproduced by standard DFT calculations.^[109] Nevertheless, calculated ^1H NMR shifts have proven useful in several recent analyses of aromatic porphyrinoids.^[24,25,110,111] Finally, ring currents in some porphyrinoids have also been evaluated using the ipsocentric orbital model of current density.^[112] Another approach used for this purpose is the Anisotropy of the Induced Current Density (ACID) method,^[113] which has recently been applied to porphyrinoid macrocycles.^[114,115]

Structural Criteria. Aromaticity is traditionally associated with bond length equalization within the cyclic π -conjugated system, even though it is now known that the relationship between equilibrium bond lengths and aromatic stabilization is more complicated than previously thought.^[116] In large systems, especially those containing multiple rings or heteroatoms, it is more difficult to infer the extent of delocalization from geometrical parameters. Consequently, geometry-based indexes of aromaticity^[117] become particularly useful in

quantitative analysis of such systems, as has been proven for porphyrins^[108] and some porphyrin analogues.^[103,118–123] Typically used methods are the harmonic oscillator model of aromaticity (HOMA),^[103,120–124] known to give good correlation with magnetic criteria, and the harmonic oscillator stabilization energy method (HOSE) enabling estimation of canonical weights.^[118,119,125]

3.3. Conformational Effects

As long as the porphyrinoid ring system remains planar, the observed dia- and paratropic ring currents increase their magnitude with the number of involved π electrons. This feature, which is in line with theoretical predictions, is convincingly demonstrated by the series vinylogous porphyrins containing up to 34 electrons in their CP's.^[31] The strength of a ring current is often expressed in terms of $\Delta\delta$, the chemical shift difference between the most deshielded and most shielded protons. Distortions from planarity, which occur in the majority of systems discussed in this Review, generally result in diminished $\Delta\delta$ values, as a consequence of the less efficient π orbital overlap in torsionally deformed structures. Still, except for the largest systems (see Section 9), weak to moderate ring currents are often observed even in some highly nonplanar molecules, including examples of *T1* and *T2* topologies.^[23,26,126] Even relatively weak effects can be identified in those cases in which two structures of identical constitution have different oxidation levels or π -conjugation topologies and, consequently, oppositely directed dia- and paratropic shieldings.

The presence of a ring current provides analytically useful clues to the location of particular protons relative to the shielding and deshielding zones. In particular, subunit inversion swaps the protons located on the convex and concave sides of the subunit between the shielding and deshielding zones of the macrocycle. This reversal of ring current shieldings has a diagnostic value because it enables immediate identification of inverted subunits on the basis of a ¹H NMR spectrum. In fact, the first recognized instances of subunit inversion were deduced from chemical shift patterns (Schemes 1 and 13).^[19,127] In *T2_o* conformers ring currents are generally weak and complete signal assignments are seldom provided. Generally, in $(4n+2)$ -electron systems, protons located “inside” the figure-eight loops (including those residing near the crossing) are shielded in a similar fashion to that observed in untwisted *T0* systems. Conversely, protons located on the “outside” of the loops are deshielded, and these effects are qualitatively reversed in $(4n)$ -electron macrocycles.^[25,126] A theoretical analysis of ring currents in *T2_o* conformations is given in reference [11].

3.4. Möbius Aromaticity

π -Conjugation on the surface of a Möbius strip was first considered theoretically in 1964.^[83] The original analysis, based on simple molecular orbital theory, predicted that the stability rules derived by Hückel for planar aromatics would

be reversed for π -surfaces with a half-twist. As a consequence, Möbius aromaticity and antiaromaticity are defined respectively by a doubly even ($4n$) and singly even electron count ($4n+2$).^[11] Möbius aromaticity was subsequently invoked in several theoretical discussions, and proposed, sometimes controversially, as possible transition states^[128–130] or reactive intermediates.^[131] However, the first example of a stable, neutral Möbius molecule was experimentally characterized in 2003.^[87,92] The latter system was an annulene–bianthraquinodimethane hybrid, which combined planar and in-plane π -conjugation (cf. Figure 3). In 2007, it was reported that A,D-di-*p*-benzihexaphyrin (Section 6.5) shows dynamic switching between *T1* and *T2* topologies, thus constituting the second observed example of a Möbius aromatic molecule.^[24] In subsequent reports it was shown that the ability to stabilize Möbius structures is a more general feature of porphyrinoids, and that the topology adopted by the macrocycle can be controlled to some extent.^[25,26,103,110,120–123,132–134] While the occurrences of Möbius aromaticity are still relatively rare, they are more frequent than could be expected. In fact, as we will discuss in more depth later, certain instances of Möbius topology (not always coinciding with well-defined aromatic character) were published in earlier porphyrinoid literature and remained unrecognized until recently.

In its original formulation, the Hückel theory describes aromatic molecules in terms of their interatomic connectivity, effectively reducing π -conjugation to a graph-theoretical problem.^[135] This feature is preserved in the MO description of Möbius π -conjugation, in which the three-dimensionality of the twisted ring is only implicitly included by introducing a scaling factor of $\cos\theta$ to the resonance integral, whereas the half-twist appears as a phase change in the *p* orbital loop.^[83] Consequently only two types of conjugation are distinguished: the Hückel type corresponding to the untwisted π surface *T0*, and the Möbius type occurring in the surface with a single half-twist (*T1*). In topological terms, all structures *Tn* with *n* even are homeomorphic with *T0*, and as a result, the *p* orbital basis will have no phase shift in any of these topologies. Consequently, they are expected to likewise obey the Hückel rules, and indeed, such a behavior is observed experimentally in *T2_o* systems. By analogy, *Tn* surfaces with *n* odd, all of which are homeomorphic with the singly twisted Möbius band *T1* and have a 180° twist in their *p* orbital basis, should follow the reversed Hückel rules. In topological terms, the higher twist levels, characterized by knotted edges, are different embeddings of either *T0* or *T1* in the three-dimensional space. These embeddings are not ambient homotopic, that is, bands with different twist levels (either odd or even) cannot be continuously deformed into each other.

The geometrical distinction between Hückel and Möbius conjugation is simply assessed by counting the number of formal *trans* bonds in the SMC. The system has a Möbius topology (*T1*, *T3*, etc.) when the number of *trans* bonds is odd. This feature is easily verified by considering a hypothetical SMC in the form of a convex polygon, which contains no transoid bonds. By inverting a subunit we always change the configuration of two bonds at a time, therefore a *T0* conformer will always contain an even number of *trans*

bonds regardless of the inversion pattern. If we dissect the ring, twist it smoothly, and join the ends back to obtain a structure with nonzero Lk , the number of *trans* bonds will remain unchanged for even Lk values (corresponding to Hückel conjugation) and will be increased or decreased by one in the case of odd Lk values (representing Möbius conformers). Unfortunately, it is impossible to infer from the number of *trans* bonds whether the p orbital overlap between consecutive atomic centers is really effective. This information is relevant, because all systems with $|Lk| > 0$ are inherently nonplanar and many molecules with nontrivial π topologies are in fact poorly conjugated. Here we propose a simple parameter

$$\Pi = \prod_i \cos \theta_i$$

in which θ_i are the torsional angles along the SMC, which can be taken from either experimental or computed geometries. The Π parameter, which may be called “torsional π -conjugation index”, has the following features: 1) $\Pi = 1$ for a perfectly planar ring; 2) Π is positive for any Hückel (double-sided) surface regardless of its linking number, and it approaches unity for infinitely large rings with uniformly distributed torsion; 3) Π approaches zero for rings containing a “kink”, that is, a torsion very close to $\pm 90^\circ$; 4) Π is negative for any Möbius (single-sided) surface, regardless of the linking number, and it approaches -1 for infinitely large rings with uniformly distributed torsion. Möbius rings larger than 20-membered can theoretically display values of $\Pi < -0.8$ (calculated for uniformly distributed torsion). Because the resonance integral between two adjoining carbon sp^2 centers is assumed to scale with $\cos \theta_i$ in the MO description of Möbius π -aromatics,^[83] the absolute value of the Π parameter can indeed be considered a rough measure of the efficiency of π -conjugation. It should be noted that by projecting some twist into writhe, it is possible to improve the efficiency of π -conjugation.^[85] Structural data analyzed in this Review indicate that small absolute values of Π (typically smaller than 0.3) are characteristic of systems with no observable macrocyclic aromaticity. In the following discussion, the Π values given for porphyrinoid macrocycles are derived from X-ray geometries, unless stated otherwise.

In analogy to Hückel aromatics, Möbius systems display ring currents in their ^1H NMR spectra, which can have appreciable magnitudes, especially in larger rings.^[103] In most cases, however, the π overlap is inefficient and consequently, ring currents tend to be weaker than in corresponding planar macrocycles of comparable size. Even though the π surface of Möbius aromatics is inherently nonplanar, most of the actual molecules have a projection that contains no intersections, that is, one that adopts a shape of a single loop.^[11] The chemical shifts observed in some Möbius systems indicate that the axis of anisotropy cone is approximately aligned with the normal of that particular projection. The parts of the molecule that are approximately coplanar with the projection exhibit the usual sign difference between inner and outer shieldings.

4. Triphyrins and Tetraphyrins

Tetraphyrins are the most studied group of porphyrin analogues, and their chemistry has been thoroughly reviewed.^[13–15,136] In contrast, relatively few triphyrin systems have been reported, notwithstanding the remarkable synthetic progress in recent years.^[137] The present Review will focus on tetraphyrin macrocycles in which subunit inversion was observed, with a brief foray into the realm of highly strained contracted porphyrinoids. The relevant systems are summarized in Table 5 and Scheme 7.

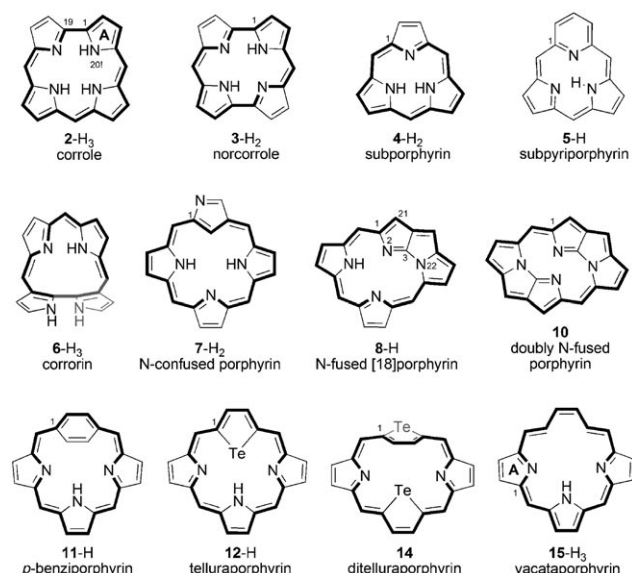
Table 5: Selected triphyrin and tetraphyrin ring systems.

Entry ^[a]	Structure ^[b]	S	τ_F	Ref.
1-H ₂	porphyrin [18]{N.N.N.N}(1.1.1.1)	16	1.19	
2-H ₃	corrole [18]{N.N.N.N}(1.1.1.0)	15	1.03	[138]
3a-H ₂	norcorrole ^[c] [16]{N.N.N.N}(1.0.1.0)	14	0.86	[139]
4bc-H ₂	subporphyrin ^[d] [14]{N.N.N}(1.1.1)	12	0.90	[36]
5d-H	subpyrporphyrin {N ^{ccc} .N.N}(1.1.1)	12	0.94	[140]
6e-H ₃	corroin	13	1.34	[141]
7bf-H ₂	N-confused porphyrin ^[d] [18]{C ^{NC} .N.N.N}(1.1.1.1)	16	1.21	[20,21]
8bf-H	N-fused [18]porphyrin	14	1.11	[22]
9f-H ₃	N-fused [20]porphyrin ^[c,e]	14	1.11	[142]
10g	doubly N-fused porphyrin	12	1.03	[143]
1bh-H	p-benziporphyrin [18]{CC.N.N.N}(1.1.1.1)	17	1.06	[144]
12i-H	21-telluraporphyrin [18]{Te.N.N.N}(1.1.1.1)	16	1.11	[145]
13j-H ₃	N-fused 21-telluraporphyrin ^[d]	14	1.14	[146]
14b	21,23-ditelluraporphyrin [18]{Te.N.Te.N}(1.1.1.1)	16	1.02	[147]
15i-H ₃	vacataporphyrin ^[f] [18]{N.N.N}(6.1.1)	17	1.73	[68]

[a] Representative substitution patterns: **a** β -Et; **b** *meso*-Ph; **c** *meso*-C₆F₅; **d** 6,16-Mes₂-11-Ph; **e** (C₆F₅)(*o*-C₆H₄NO₂)₂; **f** *meso*-Tol; **g** *meso*-C₆F₅-21,23-Br₂; **h** 5,20-Tol₂-10,15-Ph₂; **i** 5,20-Ph₂-10,15-Tol₂; **j** 5,20-Ph₂-10,15-(*p*-methoxyphenyl)₂. [b] Curly brackets contain the pattern of “inner” atoms (located on the concave sides of subunits) given in a shorthand notation. Superscripts indicate nonstandard sequence of atoms on the convex side of the subunit. [c] Free base is unknown. [d] N-confused porphyrin will be assumed to have only two dissociable protons. [e] Cross conjugated in its basic valence form. [f] For clarity, vacataporphyrin will be assumed to have three dissociable protons: two CH’s and one NH.

4.1. Contracted Systems

While contracted porphyrinoids are not as structurally diverse as the expanded systems, it is of interest to consider the amount of angular strain that can be accepted by the macrocyclic ring. The prototypical contracted system, corrole^[46,136,138] (2-H₃) has an optimum free curvature ($\tau_F = 1.03$), which provides for a relatively unstrained structure. The corrole macrocycle is also available in a number of hetero^[136,148] and carbaanalogues.^[149] Its smaller congener, norcorrole 3-H₂, containing just two meso bridges, was proposed as a

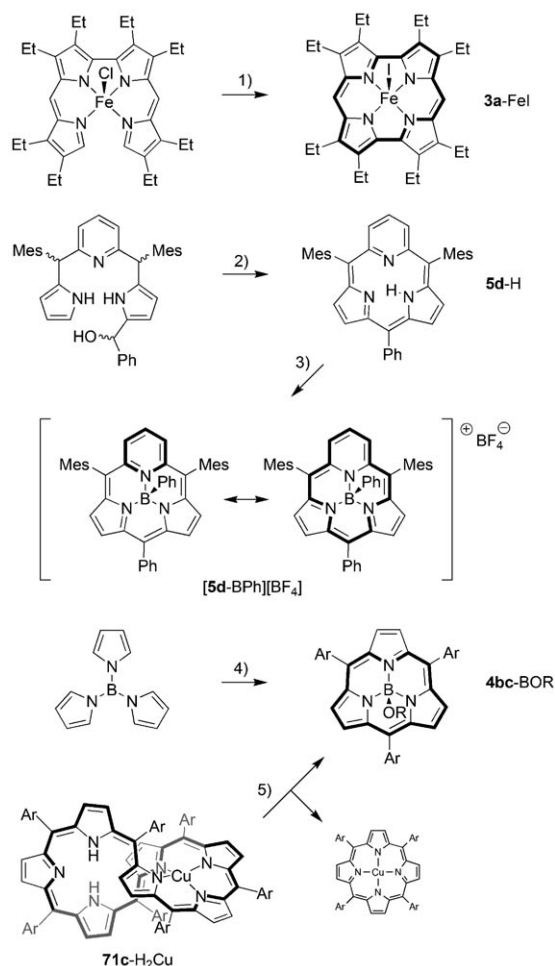


Scheme 7. Relevant tri- and tetraphyrin ring systems. Note the numbering schemes for **2-H₃** and **15-H₃** are different from those adopted in the literature.

promising synthetic target on the basis of DFT calculations, even though the macrocycle was predicted to easily convert to the corresponding phlorin-like systems by reduction or nucleophilic addition.^[150] The prediction was recently fulfilled in a remarkable synthesis of iodoiron(III) norcorrole (**3a-FeI**).^[139] This species forms spontaneously from a 2,2'-bidipyrin iron(III) complex upon axial ligand exchange (Scheme 8) and is indeed very reactive. The only decomposition product that could be isolated was a dimeric *meso-meso* linked structure, whose formation is consistent with the theoretically predicted reactivity.

On the basis of the bond length pattern observed in the DFT optimized structure, it was argued that the norcorrole ring is not an antiaromatic [16]annulenic system but should rather be viewed as a union of two nonconjugated dipyrromethene moieties.^[150] However, this statement is not supported by the values of NMR shieldings calculated for **3-H₂** at the GIAO/B3LYP/6-31G(d,p) level of theory.^[151] In particular, the predicted chemical shifts of *meso*-H and NH protons are respectively 2.15 and 37.30 ppm relative to TMS, consistent with a substantial paratropic ring current. Furthermore, the NICS shift calculated at the center of the macrocycle has a large positive value (23.4 ppm), corresponding to an antiaromatic structure.

Subporphyrins **4-H₂** and their benzo-fused analogues constitute an emerging class of aromatic contracted porphyrinoids of significant current interest.^[137] These aromatic [14]annulenic species are structurally related to subphthalocyanines, which have been known since 1972.^[152] Macrocyclizations involving pyrrole and an aldehyde (or their synthetic equivalents) preferentially yield tetraphyrins and larger macrocycles, and the formation of subporphyrin rings has so far been achieved only in the presence of a boron template, yielding complexes of the general structure **4-BX** (X = OH, OR, Scheme 8).^[36,153] An alternative approach,



Scheme 8. Syntheses of some contracted porphyrinoids and their complexes. Reagents and conditions: 1) NaI/CH₂Cl₂, then [O]; 2) BF₃/MeCN, then DDQ; 3) a) PhBCl₂, b) AgBF₄; 4) ArCHO, EtCOOH; 5) BBr₃ (excess) and EtN(iPr)₂ (excess), then MeOH, reflux.

which involves boron-induced splitting of a Cu^{II} heptaphyrin (**67c-H₂Cu**, Section 7) also yields a boron subporphyrin complex.^[154] Complexes **4-BX** adopt bowl-shaped conformations, with the bowl depth of 1.2–1.4 Å.^[137] To date, no effective procedures for the removal of boron from the subporphyrin core have been published, and the preparation of the free base **4-H** remains to be accomplished.

The hypothetical synthesis of a free-base subporphyrin from monopyrrolic precursors requires the intermediate formation of a subporphyrinogen (calix[3]pyrrole), which is apparently disfavored for steric reasons. (It is however possible to obtain cyclononatirpyrroles, which are calix[3]-pyrrole isomers containing 1,2-connected rings).^[155] Interestingly, cyclization of a linear precursor to yield a triphyrin structure is possible when one of the pyrrole rings is replaced with a pyridine unit, the latter providing a slightly larger contribution to the free curvature (Scheme 8). The resulting system, subpyrrophenin (**5d-H**) is characterized by a very crowded core, which contains the shortest NH...N hydrogen bond characterized to date with the N...N distance of 2.370(2) Å.^[140] In its most stable tautomeric form, shown in

Scheme 8, subpyrriporphyrin is not aromatic. However, its phenylboron complex [**5d**-BPh][BF₄], obtained in a reaction with PhBCl₂, exhibits diatropicity consistent with a [14]annulenic structure.^[140]

A corrole isomer, named corrorin (**6e**-H₃), was obtained as a byproduct in the synthesis of a doubly N-confused porphyrin.^[141] This macrocycle contains two directly linked 2,3-connected pyrrole rings, a structural feature seldom encountered in porphyrinoids (cf. Ref. [148]). The calculated τ_F value for corrorin is 1.34 and the actual macrocycle strongly

deviates from planarity. Interestingly, the conformation adopted by corrorin in the solid state has a Möbius topology (*T1*, Figure 6), which has apparently eluded recognition since the original report was published.^[141] As corrorin is formally a [14]annulenic system, it can be considered the smallest Möbius π -conjugated ring characterized to date. Given its *T1* topology, corrorin should be an antiaromatic system. However, the ¹H chemical shifts show no presence of a macrocyclic ring current. Similarly, NICS values calculated inside the large ring correspond with an effectively nonaromatic structure.^[151]

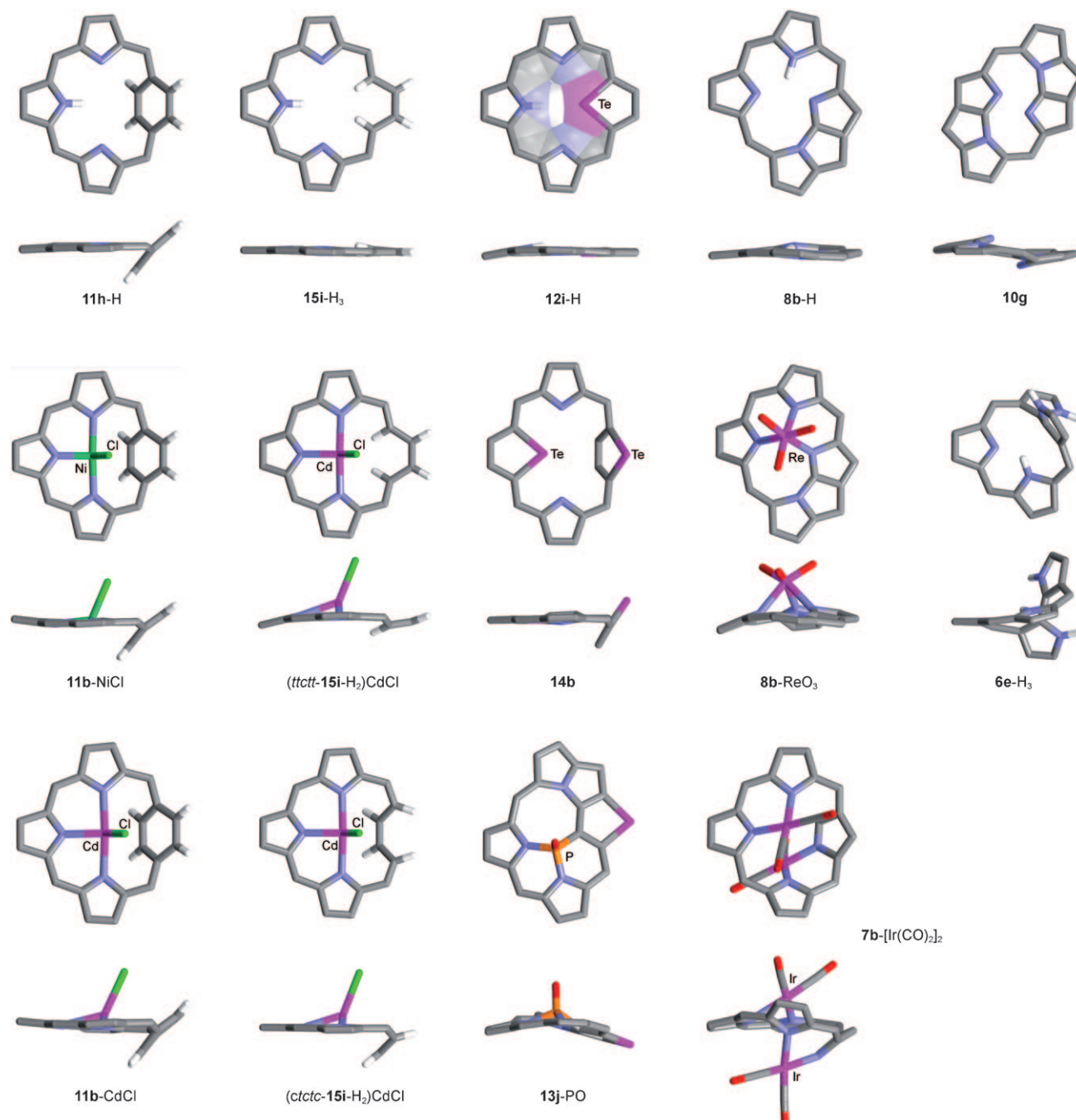


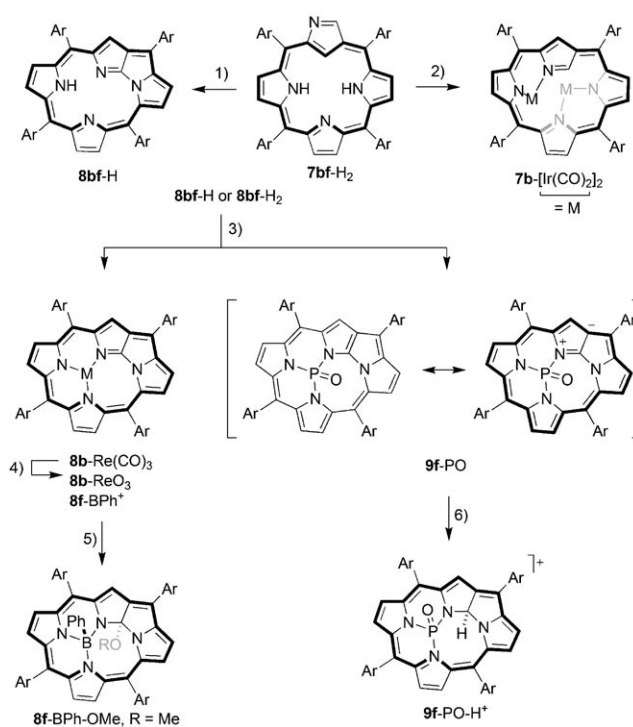
Figure 6. Three-dimensional structures of selected tri- and tetraphyrins. Coordinates have been taken from X-ray structural data, with the exception of (*ctctc*-**15e**-H₂)CdCl for which a DFT geometry was used. In most cases solvent molecules and peripheral substituents are removed for clarity.

Macrocyclic π -conjugation could apparently be quite effective, given that the Π parameter has a value of -0.33 , comparable with those predicted for Möbius conformers of vacatoporphyrin (Section 4.5). It may therefore be proposed that the lack of expected paratropicity is caused by the annelation effect of 2,3-connected pyrrole rings.^[156,157]

4.2. N-Confused and N-Fused Porphyrins

N-confused porphyrin^[20,21,158,159] (**7**-H₂) is an important porphyrin isomer characterized by rich coordination chemistry and unique reactivity traits. It is also a prototype of many related systems, including expanded N-confused,^[159] multiply N-confused,^[159] and X-confused macrocycles.^[18,160] Among the most remarkable reactions of **7**-H₂ is the ring fusion process, first reported in 1999,^[22,161] and subsequently observed in other porphyrinoid systems.^[143,146,162–166] Formally, ring fusion begins with the inversion of a cyclic subunit (most often an N-confused or regular pyrrole) that is separated by a one-carbon meso bridge from a nonconfused pyrrole ring. In the second stage, a bond is formed between the nitrogen of the adjacent pyrrole and the nearest carbon atom of the inverted subunit. In the case of N-confused porphyrin, the fusion reaction leads to the N-fused porphyrin **8**-H, in which there are three fused five-membered rings forming a *H*-pyrrolo[3,2-*b*]pyrrolizine unit. As a consequence of fusion, the SMC is reduced from 16 to 14 atoms, but the length of the CP remains unchanged ($N=18$) and **8**-H is aromatic. τ_F calculated for **8**-H using an appropriate pyrrolopyrrolizine increment is 1.11, showing that the ring-fused structure is actually quite feasible. Nevertheless, the geometric parameters of the **8**-H skeleton indicate a certain amount of angular strain caused by the shape of the fused fragment, and by steric crowding in the much smaller macrocyclic core (Figure 6).

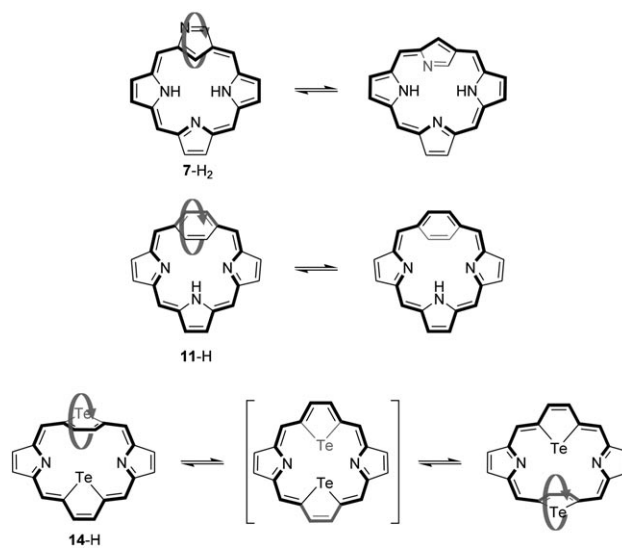
The original synthesis of **8b**-H consists of a double bromination of the N-confused pyrrole of **7b**-H₂, elimination of HBr (during which the actual fusion occurs), and an optional reductive debromination with pyridine.^[161] Subsequent research showed that coordination of metallic and non-metallic elements with small ionic radii is also capable of inducing ring fusion (these complexes can also be made starting directly from the fused ligand). Examples reported to date include **8b**-Re(CO)₃^[167] (oxidizable to **8b**-ReO₃^[168], Figure 6), **8f**-BPh⁺Cl[−],^[169] and **9f**-P=O.^[142] The phenylboron species, is cationic and easily undergoes nucleophilic addition at position 3, while retaining uninterrupted macrocyclic conjugation. In the phosphoryl complex **9f**-PO, the oxidation level of the N-fused ligand corresponds to that of isophlorin ([20]porphyrin) and the macrocyclic ring in this complex is isomeric with that of porphyrin. In fact, **9f**-PO exhibits moderate paratropicity, which can be explained in terms of a charge-separated structure (Scheme 9). **9f**-PO is selectively protonated at position 3, leading to a diatropic monocation **9f**-PO-H⁺. A related phosphoryl complex of N-fused 21-telluraporphyrin was recently prepared (**13j**-PO, Figure 6).^[146] Additionally, N-fused derivatives with broken macrocyclic conjugation were obtained by silylation of **8f**-H or **7f**-H₂.^[170] Quite interestingly, the N-fusion reaction can be reversed



Scheme 9. Reactions of N-confused porphyrin leading to ring inversion and fusion. Reagents and conditions: 1) a) NBS, b) pyridine, Δ ; 2) [IrCl(CO)₂(*p*-toluidine)], AcONa, toluene/THF, Δ ; 3) [Re₂(CO)₁₀], *o*-dichlorobenzene, Δ or PhBCl₂, toluene, Δ or PCl₃, toluene, Δ ; 4) Me₃NO, *o*-dichlorobenzene, Δ ; 5) MeONa/MeOH; 6) HBF₄/Et₂O.

under certain conditions, leading back to N-confused porphyrin derivatives.^[161,170]

While the formation of **8**-H implies the accessibility of a ring-inverted conformer of N-confused porphyrin (Scheme 10), such a structure has as yet eluded experimental verification. It was however found that the calculated activation barrier to inversion of N-confused pyrrole in **7**-H₂



Scheme 10. Subunit inversion in N-confused porphyrin (**7**-H₂), *p*-benziporphyrin (**11**-H), and ditelluraporphyrin (**14**).

(up to 24.5 kcal mol⁻¹) is lower than an analogous barrier for inversion of nonconfused pyrrole in **1-H₂** (up to 49.1 kcal mol⁻¹).^[89,171] Interestingly, an inverted conformation was stabilized in the bimetallic complex **7b**-[Ir(CO)₂]₂, in which one of the iridiums bridges the outer nitrogen with one of the inner nitrogens (Figure 6).^[172]

A doubly N-fused porphyrin **10g** was recently prepared from a doubly N-confused porphyrin by two consecutive fusion steps.^[143] This remarkable system may be viewed as a bridged [18]annulene, in which all the bridges are contained inside the 18-membered ring. The steric crowding in the macrocyclic cavity, caused by double fusion, is partly alleviated by an out-of-plane distortion of the core (Figure 6), leading to a non-bonding N...N distance of 2.368 Å. **10g** is conspicuous for its extremely small HOMO–LUMO gap (1.24 eV, measured electrochemically), comparable with that of [38]annulene. This feature is further manifested by an electronic absorption at 1300 nm, which is uniquely red-shifted for an [18]annulenoid system.^[143]

4.3. *p*-Benziporphyrin

Porphyrin analogues into which one or more benzene rings are incorporated as cyclic subunits are known as benziporphyrins.^[173] The first examples of such macrocycles^[174,175] contained 1,3-connected benzene units (*m*-phenylenes), whose curvature, expressed in terms of τ_{subunit} increments, approximates that of pyrrole, leading to a relatively unstrained macrocyclic structure. However, *m*-benziporphyrins are devoid of macrocyclic aromaticity, because no proper conjugation pathway can be constructed involving a *m*-phenylene subunit.^[17] Replacing this subunit with a *p*-phenylene ring creates an isomeric structure, *p*-benziporphyrin (**11bh-H**).^[144,173,176] which, in contrast to the *meta* isomer, is formally an expanded porphyrinoid (*S* = 17). In spite of the favorable value of τ_F , *p*-benziporphyrin is nonplanar, with the *p*-phenylene ring tilted at ca. 45° relative to the macrocyclic plane (**11h-H**, Figure 6). While this tilting of *p*-phenylene undoubtedly affects macrocyclic π -conjugation, *p*-benziporphyrins exhibit significant diatropic ring currents. The aromatic character of **11b-H** was rationalized in terms of a quinoidal canonical structure, contributing to the conjugation along the macrocyclic pathway.^[144] The diatropic character of the macrocycle induces a significant differentiation of chemical shifts of the “inner” and “outer” phenylene protons, which resonate respectively at 2.32 and 7.68 ppm.

In the free base **11b-H**, the *p*-phenylene ring oscillates between two equivalent positions, and at room temperature the process is so rapid that the phenylene ring is represented by a single signal in the ¹H NMR spectrum.^[144] Functionally, this seesaw motion of the phenylene is similar to the ring inversion process, except that the two exchanging structures are identical (Scheme 10). The internal rotation of the phenylene can be locked by metal coordination, as demonstrated for chlorocadmium(II) and chloronickel(II) complexes (**11b**-CdCl and **11b**-NiCl, Figure 6).^[144,176] In these species, the metal ion is kept at a close distance to the phenylene ring, but the proximity does not result in a

significant change of the tilting angle. A detailed NMR spectroscopic analysis carried out on the paramagnetic **11b**-NiCl revealed a conformational process analogous to that observed in the free base.^[177] In an analogous nickel(II) complex of *m*-benziporphyrin, the exchanging conformers are not structurally equivalent, and have significantly different populations.

Two heteroanalogues of *p*-benziporphyrin have been reported, 24-thia-*p*-benzi[18]porphyrin^[178] and 22,23,24-trithia-*p*-benzi[20]porphyrin.^[179] The latter macrocycle does not have features of either aromatic or antiaromatic system. *p*-Phenylene rings have also been incorporated into a number of larger ring systems, discussed in subsequent sections of this Review.

4.4. Telluraporphyrins

21-Telluraporphyrin **12i-H**, reported in 1995,^[145] is the ultimate species in the series of chalcogen-containing mono-heteroporphyrins.^[13] Because of the dimensions of the tellurium atom, the shape of the tellurophene ring differs significantly from that of pyrrole. In particular, the bonds emanating from α positions are nearly parallel, and consequently, the τ_{subunit} increment calculated for tellurophene is only 0.046. Nevertheless, the macrocycle of telluraporphyrin is nearly planar because the tellurium snugly fits into the macrocyclic core (Figure 6). The situation is different in 21,23-ditelluraporphyrin **14b**, which contains two tellurophene rings on the opposite sides of the macrocycle.^[147] Here, one of the tellurophene units is inverted, pointing the bulky Te atom away from the macrocyclic core. The angle between the plane of the inverted tellurophene ring and the plane formed by meso carbons is 57°, slightly larger the corresponding angles observed in *p*-benziporphyrins. In spite of the out-of-plane distortion, the ¹H NMR spectrum of **14b** shows clear symptoms of macrocyclic diatropicity, with the outer and inner β -tellurophene protons resonating at 8.53 and 6.08 ppm, respectively. In solution, the two tellurophene rings in **14b** undergo rapid exchange, leading to a coalescence of the β -tellurophene signals. On the basis of variable-temperature NMR data, the process was postulated to occur with the intermediacy of a convex conformer that is probably highly nonplanar (Scheme 10). Additionally, the dication **14b**-H₂²⁺ also adopts a convex conformation and is strongly diatropic. It is of interest that ditelluraporphyrin is characterized by τ_F = 1.02, which is a very small value for a system undergoing ring inversion. The concave conformer yields τ_{FI} = 0.93, indicating that the preference for ring inversion minimizes steric repulsions in the core rather than angular strain.

4.5. Vacataporphyrin

Refluxing 21-telluraporphyrin (**12i-H**) in a mixture of *o*-dichlorobenzene and 20% hydrochloric acid results in the removal of tellurium and formation of an aromatic [18]triphyrin(6.1.1) **15i-H₃**.^[68] This compound, which may be considered a porphyrin-annulene hybrid, was named vacata-

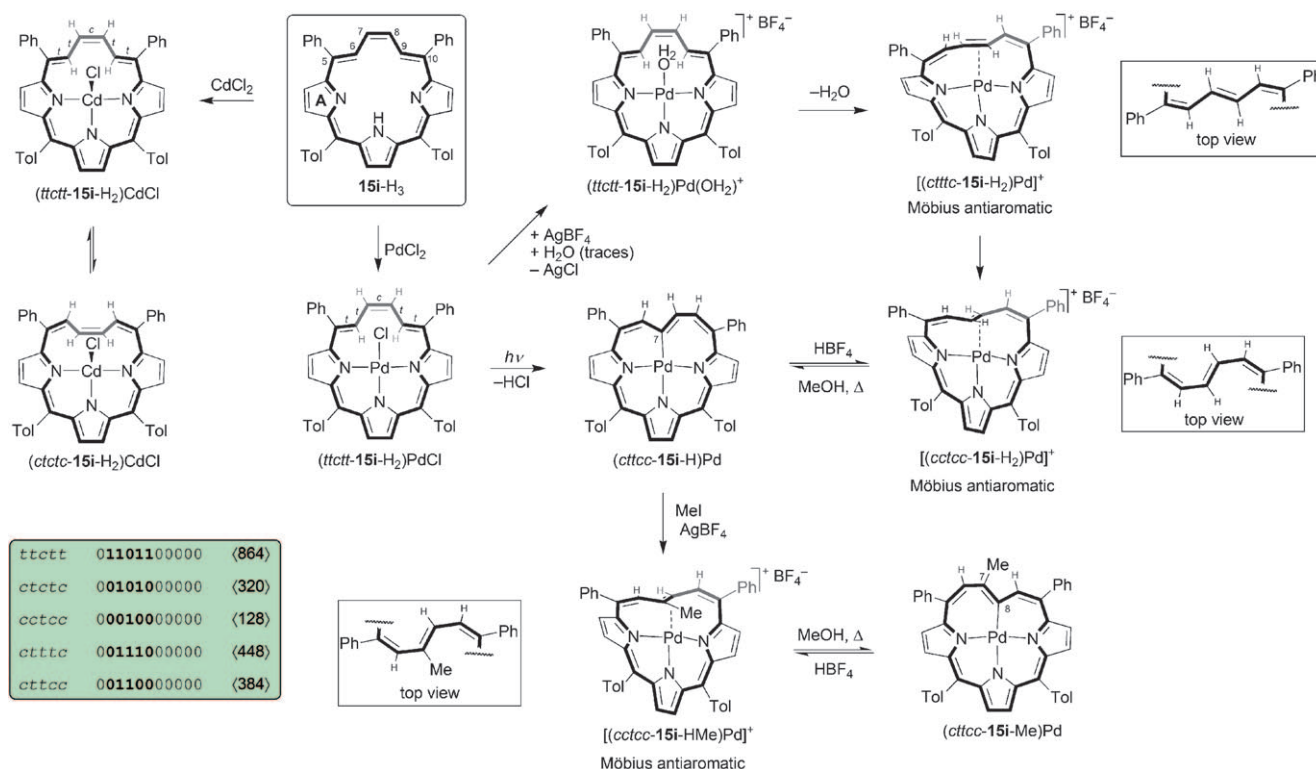
porphyrin (from Polish *wakat* = vacant post). The “vacancy” refers to the absence of one donor atom in a porphyrin-like structure. An alternative name “butadieneporphyrin” refers to one pyrrole ring being replaced by a butadiene fragment.^[180] If one adheres to the systematic description of porphyrinoid structure **15i-H₃** is more appropriately viewed as a triphyrin containing a six-carbon meso bridge. This bridge, which will be called “triene” even though it does not show any significant bond alternation, retains the *trans-trans-cis-trans* (*ttctt*) configuration present in **12i-H**. However, the configurational lability of the triene fragment has important consequences for the coordination chemistry of vacataporphyrin.^[180]

Vacataporphyrin coordinates cadmium(II) to yield a chlorocadmium complex (**15i-H₂**)-CdCl, in which the cadmium is bound by three pyrrolic nitrogens.^[181] The product is a mixture of two conformers: (*ttctt*-**15i-H₂**)-CdCl, which retains the configuration of the triene bridge found in the free base, and (*ctctc*-**15i-H₂**)-CdCl, in which the formal “butadiene subunit” is inverted (Scheme 11). These two conformers can be called respectively “convex” and “concave”. (Strictly speaking, they are both biconcave, because each methine carbon is formally a separate subunit according to the convention proposed in Section 2.2). Exchange between the two conformers is slow on the NMR time scale, and the position of the equilibrium is photochemically controlled. For samples stored in the darkness, the molar ratio of *ttctt*:*ctctc* settles at 2:5 after one day, and is shifted to 6:1 when the sample is exposed to daylight. DFT models indicate that the vacataporphyrin macrocycle is only slightly puckered in (*ttctt*-**15i-H₂**)-CdCl. In contrast, the butadiene unit is tilted out of

the plane in the concave conformer (*ctctc*-**15i-H₂**)-CdCl, resembling the structure of chlorocadmium *p*-benziporphyrin **11b**-CdCl (Figure 6).

The chloropalladium(II) complex of vacataporphyrin (*ttctt*-**15i-H₂**)-PdCl is structurally related to the Cd species, except that the tendency of palladium(II) to adopt a square-planar coordination environment induces a more decisive distortion of the triene unit (Figure 7).^[110] Upon irradiation with visible light, (*ttctt*-**15i-H₂**)-PdCl undergoes an internal carbopalladation reaction accompanied by the elimination of a HCl molecule (Scheme 11). In the resulting species, (*ctctc*-**15i-H**)-Pd, the palladium(II) forms a σ bond with position C(7), and the configuration of the triene unit is changed so that there are no C–H bonds in the macrocyclic core. The aromatic (*ctctc*-**15i-H**)-Pd is reversibly protonated at the metallated carbon, producing a new species, [*ctctc*-**15i-H₂**]-Pd]⁺ which is paratropic. The paratropicity of this cation is explained in terms of a Möbius topology adopted by the macrocycle, which leads to the reversal of ring current effects (the electron count in the conjugation pathway is unchanged by protonation). An analogous conformational change occurs when (*ctctc*-**15i-H**)-Pd is treated with MeI and AgBF₄ (Scheme 11). The methyl group is added to the metallated carbon C(7) and the Pd–C bond is cleaved to yield another antiaromatic Möbius species [*ctctc*-**15i-HMe**]-Pd]⁺. Deprotonation of this cation leads to (*ctctc*-**15i-Me**)-Pd, which is simply a methylated derivative of (*ctctc*-**15i-H**)-Pd.

One additional reactivity route, which takes the vacataporphyrin macrocycle through two distinct Möbius antiaromatic states, begins with the exchange of the chloride ligand in (*ttctt*-**15i-H₂**)-PdCl using AgBF₄. The chloride is replaced with



Scheme 11. Reactivity of vacataporphyrin and its complexes. Numerical descriptors for the observed conformers are given in the box (see Section 2.4).

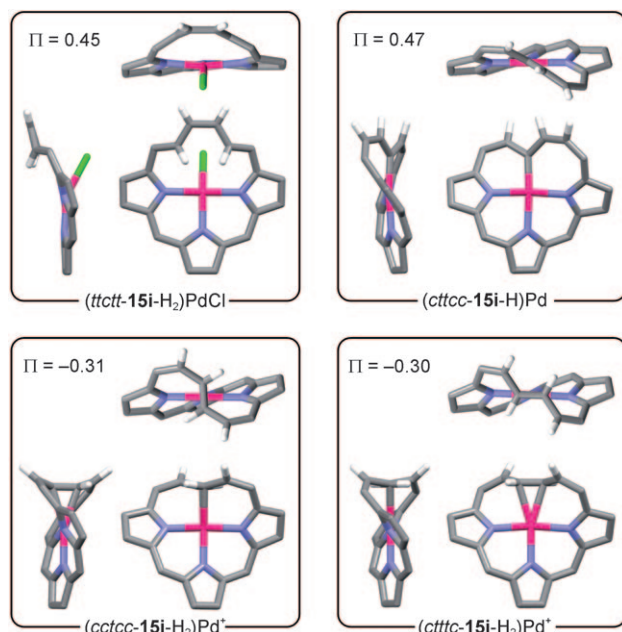
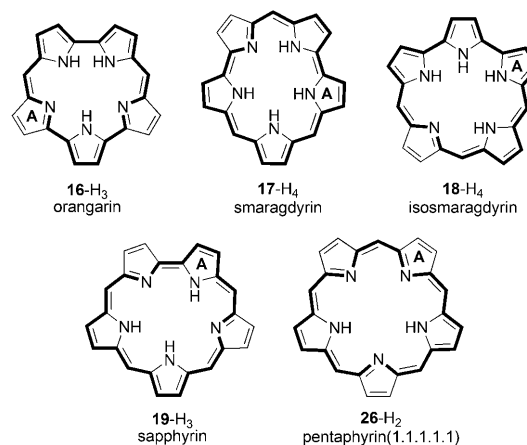


Figure 7. Three-dimensional structures of relevant Pd complexes of vacataporphyrin. The images are based on published coordinates taken from an X-ray structure (the PdCl complex) and DFT modeling (remaining structures).^[110] Substituents and the majority of hydrogen atoms are removed for clarity. Connectivity of the Pd atom is not intended to illustrate the actual valence structure.

a water molecule (from water traces present in the sample) furnishing an unstable cation $(ttctt-15i-H_2)-Pd(OH_2)^+$. That latter species undergoes water elimination from the Pd center, with a concomitant change in the configuration of the triene fragment. The product of this transformation, $(cttcc-15i-H_2)-Pd^+$, is another Möbius antiaromatic species, which ultimately rearranges to $(cctcc-15i-H_2)-Pd^+$. DFT modeling of Pd vacataporphyrins reveals that in the Möbius forms $(cctcc-15i-H_2)-Pd^+$ and $(ctttc-15i-H_2)-Pd^+$, the metal center is π -bonded to the C(7)–C(8) bond of the triene unit (Figure 7). In each case, the macrocycle acquires C_2 symmetry characteristic of many Möbius conformers.

5. Pentaphyrins

It is possible to construct eight pentaphyrin structures containing only one-carbon meso bridges. To date, five of these ring systems have been reported in the literature (Scheme 12, Table 6). The two systems of primary interest are sapphyrin (**19**-H₃) and pentaphyrin(1.1.1.1.1) (**26**-H₂), whose rich chemistry will be discussed in some detail below. Orangarin (**16a**-H₃),^[55] smaragdyrin (**17a**-H₄),^[56,182,183] and isosmaragdyrin (**18a**-H₄),^[49] are characterized by τ_F values smaller than that of porphyrin and consequently yield only convex conformations that are essentially planar. Orangarin, a [20]annulenoid antiaromatic macrocycle,^[55] is markedly paratropic, as evidenced by its center NICS value of 43 ppm.^[102] In spite of their aromatic character, smaragdyrins and their oxa analogues are unstable towards acids and light,^[56,182] but they can be made more robust by appropriate



Scheme 12. Selected pentaphyrin ring systems. The choice of tautomers is arbitrary.

Table 6: Pentaphyrin ring systems discussed in the text.

Entry ^[a]	Structure ^[b]	S	τ_F ^[c]	Ref.
16a -H ₃	orangarin [20]{N.N.N.N.N}(1.0.1.0.0)	17	0.99	[55]
17a -H ₄	smaragdyrin [22]{N.N.N.N.N}(1.1.0.1.0)	18	1.16	[56]
18a -H ₄	isosmaragdyrin [22]{N.N.N.N.N}(1.1.1.0.0)	18	1.16	[49]
19ab -H ₃	sapphyrin [22]{N.N.N.N.N}(1.1.1.1.0)	19	1.33	[48]
20a -H ₂	[22]{N.N.O.N.N}(1.1.1.1.0)	19	1.35	[189]
21a -H ₂	[22]{N.N.S.N.N}(1.1.1.1.0)	19	1.28	[189]
22a -H ₂	[22]{N.N.Se.N.N}(1.1.1.1.0)	19	1.26	[190]
23c -H	[22]{S.N.S.N.N}(1.1.1.1.0)	19	1.24	[191]
24b	[22]{Se.N.O.N.Se}(1.1.1.1.0)	19	1.22	[192]
25b -H	[22]{N.Se.N.Se.N}(1.1.1.1.0)	19	1.20	[193]
26a -H ₂	pentaphyrin [22]{N.N.N.N.N}(1.1.1.1.1)	20	1.49	[37]
27def -H	N-fused [22]pentaphyrin	13	1.37	[162]
28def -H ₃	N-fused [24]pentaphyrin	13	1.37	[162]

[a] Representative substitution patterns: **a** β -alkyl; **b** *meso*-Ph; **c** *meso*-Tol; **d** *meso*-C₆F₅; **e** *meso*-(2,6-dichlorophenyl); **f** *meso*-CF₃. [b] For explanations, see footnote [b] of Table 5. [c] Free curvature without inversions (Section 2.1).

peripheral substitution.^[183–188] Interestingly, no pentaphyrins containing less than two meso carbons have yet been reported. Hypothetical pentaphyrins (1.0.0.0.0) and (0.0.0.0.0) yield τ_F values of 0.83 and 0.66, respectively. While the latter value is likely too small for ring closure, the (1.0.0.0.0) structure might be accessible through synthesis, given that its free curvature is slightly larger than that of cyclo[6]pyrrole (Section 6.1).

5.1. Sapphyrins

The first sapphyrin was serendipitously discovered during the work on the synthesis of vitamin B₁₂.^[48,182] The sapphyrin ring, formally derived from the porphyrin by simple insertion of one pyrrolic subunit, was thus the first expanded porphyrin ever reported. The macrocyclic core of sapphyrin, which is larger than that of porphyrin, is apparently less suited for metal ion coordination, instead offering good anion binding properties when fully protonated.^[194,195]

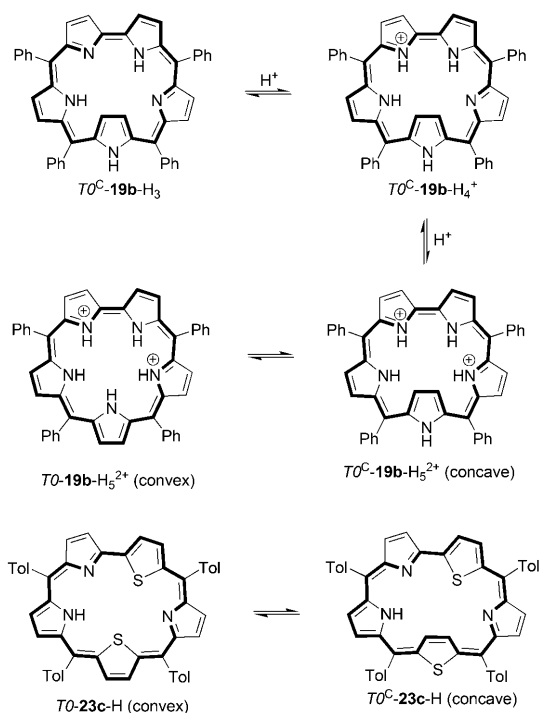
Two conformations have been observed experimentally in sapphyrins and their heteroanalogues: convex ($\tau_F = 1.33$) and concave ($\tau_{FI} = 1.03$), the latter containing an inverted subunit (ring C). The relative stability of these conformers depends on several factors, notably peripheral substitution, core modifications, and protonation state, and has been the subject of several experimental and theoretical investigations.^[127,196–199] In particular, only convex conformations have so far been identified in β -substituted systems, suggesting that the inversion of β -substituted subunits is energetically unfavorable because of the resulting steric interactions with the core. DFT calculations carried out for the free-base 12,13-dimethylsapphyrin (i.e. bearing two Me groups on ring C) showed that the concave conformer is over 15 kcal mol⁻¹ higher in energy than the convex form (the difference was 11 kcal mol⁻¹ in the case of the respective dication).^[198]

The same study showed that *meso*-methyl substituents flanking ring C have an opposite effect: the concave conformer becomes more stable than the convex form.^[198] However, the conformational preferences of real-world *meso*-substituted sapphyrins do not follow a simple pattern. Free-base *meso*-tetraphenylsapphyrin (**19b**-H₃)^[127] and its monocation obtained in the presence of various acids (HF, HCl, TFAH, DCAH) exist exclusively as the concave conformers *T0*^C (Scheme 13).^[127,196] Further titration with acids results in the formation of a dication which forms an equilibrium mixture of convex and concave conformations. The position of this equilibrium is dependent on the choice of solvent, and can be additionally varied by controlling the amount of added acid. In chlorinated solvents (CDCl₃, CD₂Cl₂) a convex dication forms initially, and it is converted to a concave

form at higher acid concentrations. Interestingly, the order of events is reversed in a more polar solvent, [D₆]DMSO. One of the factors that seems to play a role in the observed behavior of sapphyrin dications is the reversible anion binding in the core, yielding hydrogen-bonded adducts similar to those characterized structurally for β -substituted systems (e.g. [**19a**-H₅(F)]⁺ and [**22a**-H₄]Cl₂, Figure 8).^[190,200,201] Association of acid molecules may be another contributing factor, leading to conformational effects qualitatively similar to those controlling the recently reported three-level aromaticity switch based on di-*p*-benzihexaphyrin (Section 6.5).

The propensity of heterosapphyrins for ring inversion strongly depends on the identity and placement of heteroatoms.^[190,192,193,202,203] The effect of heteroatom replacement on the geometry of the macrocycle is relatively insignificant in the case of oxygen but can be quite pronounced for heavier chalcogens. For instance, tetratolyl-25,27-dithiasapphyrin (**23c**-H) exhibits a temperature dependent equilibrium in solution (Scheme 13), switching between the convex ($\tau_F = 1.24$) and concave conformer ($\tau_{FI} = 1.06$).^[191] The molar fraction of the concave species is 0.87 (298 K, [D₂]-DCM) and increases as the temperature is lowered. The preference for structures inverted at ring C is also observed for a number of *meso*-substituted sapphyrins containing bulky heteroatoms (S, Se) in rings A and E (e.g. in **24b**, Figure 8).^[192,203] Conversely, *meso*-substituted 26,28-diheterosapphyrins, such as **25b**-H, preferentially adopt convex conformations (Figure 8).^[193]

In analogy to sapphyrin-anion adducts, metal complexes of sapphyrins adopt convex conformations to meet the steric demands of the coordinated metal ions. In these complexes, the macrocycle exhibits a varying degree of nonplanarity, dependent on the binding mode. The uranyl complex of oxasapphyrin **20a**-UO₂, characterized in the solid state^[204] (Figure 8), shows a slight saddle-type distortion likely resulting from the excessive free curvature of the macrocycle and the inward compression of the core caused by metal coordination. Such an interpretation is supported by the much more pronounced distortion observed in the analogous pentaphyrin(1.1.1.1.1) complex **26a**-UO₂,^[205] in which the free curvature of the macrocyclic ring is even larger. Interestingly, the sapphyrin core is capable of binding two metal centers simultaneously. In the thiasapphyrin complex **21a**-Co₂Cl₂, the two Co^{II} ions lie virtually in the plane of the macrocycle, while being linked by two μ_2 -bridging chloride anions.^[206] Conversely, the two Rh(CO)₂ groups in the complex **21a**-[Rh(CO)₂]₂ are strongly tilted and lie on the opposite sides of the macrocyclic plane.^[206]



Scheme 13. Protonation and conformational equilibria in sapphyrins **19b**-H₃ and **23c**-H.

5.2. Pentaphyrins(1.1.1.1.1) and Their N-Fusion Products

The first pentaphyrin(1.1.1.1.1) (**26a**-H₂) was reported in 1983 in the form of a β -substituted derivative.^[37] This compound was found to be aromatic, in line with the [22]annulenic formulation, which is the typical oxidation level for pentaphyrins. [24]pentaphyrins(1.1.1.1.1) were occasionally reported and characterized as unstable, nonaromatic macrocycles.^[207–209] The ¹H NMR data reported for **26a**-H₂ are

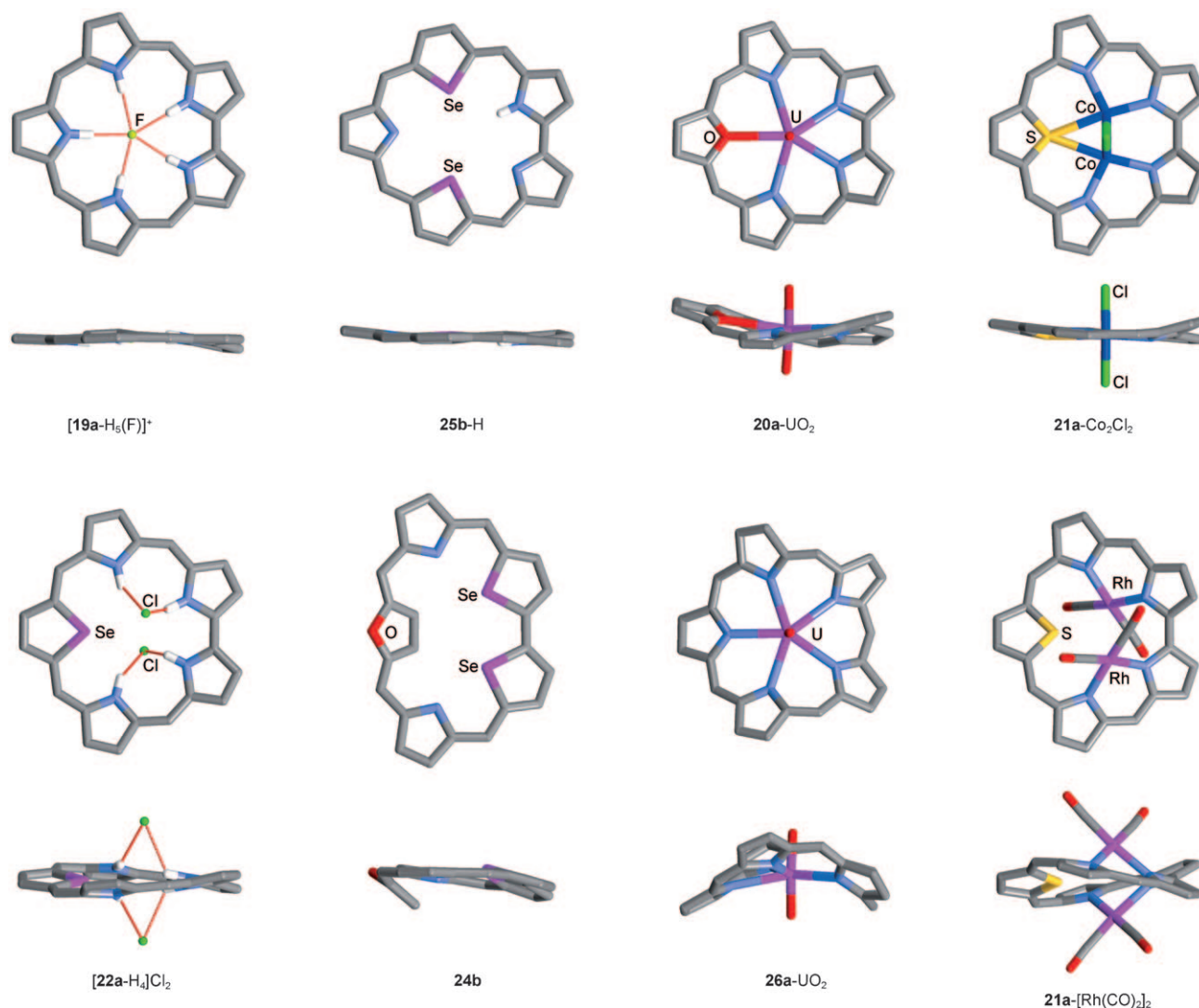
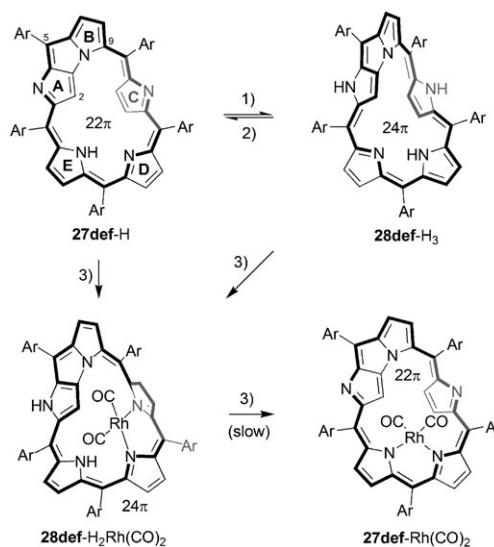


Figure 8. Three-dimensional structures of selected pentaphyrins. Coordinates were taken from X-ray structural data. Solvent molecules and peripheral substituents are removed for clarity.

consistent with a convex conformation. With a very high value of $\tau_F = 1.49$, the macrocycle is likely nonplanar. The system was not characterized crystallographically, however, the macrocycle was indeed shown in a convex conformation in a related complex **26a-UO₂**, discussed above.^[205]

On the basis of ¹H NMR spectroscopic data it was proposed that pentaphyrins with a mixed *meso*- β substitution pattern retain convex conformations both as free bases and when protonated.^[208,209] In contrast, attempts to prepare a fully *meso*-substituted pentaphyrin resulted in the isolation of N-fused systems **27def-H** and **28def-H₃**.^[120,162,210,211] The generality of this reaction was shown in subsequent work on N-confused pentaphyrins, which yielded a number of singly and doubly fused macrocycles.^[164,212] **27def-H** and **28def-H₃** constitute two oxidation levels of N-fused pentaphyrin, corresponding to 22- and 24-electron CPs, which are interconvertible by chemical oxidation and reduction (Scheme 14).^[162,210] Interestingly, N-fused pentaphyrin forms two dicarbonyl rhodium(I) complexes, **27def-Rh(CO)₂** and **28def-**



Scheme 14. Structures and reactivity of N-fused pentaphyrins. Reagents: 1) NaBH₄; 2) DDQ; 3) $[\text{RhCl}(\text{CO})_2]_2$, NaOAc.

$\text{H}_2\text{Rh}(\text{CO})_2$, which differ not only in the oxidation level of the macrocycle but also in the binding mode of the Rh center (Scheme 14).^[210] **27def-H** and **27def-Rh(CO)₂**, possess 22-electron conjugation pathways and exhibit sizable diatropic ring currents characteristic of aromatic systems. The behavior of the 24-electron systems **28def-H₃** and **28def-H₂Rh(CO)₂** is more complicated. Although some of these species display moderate paratropicity consistent with their [24]annulenoid structures, in others marked diatropicity is observed. While this important observation was made in the initial report,^[210] its significance was only appreciated in a later reinvestigation of published data.^[120]

Figure 9 shows the family of conformations adopted in the solid state by the structurally characterized N-fused pentaphyrin species. The aromatic macrocycle of **27e-H** (gray) displays a $T0^C$ conformation and is essentially planar, except

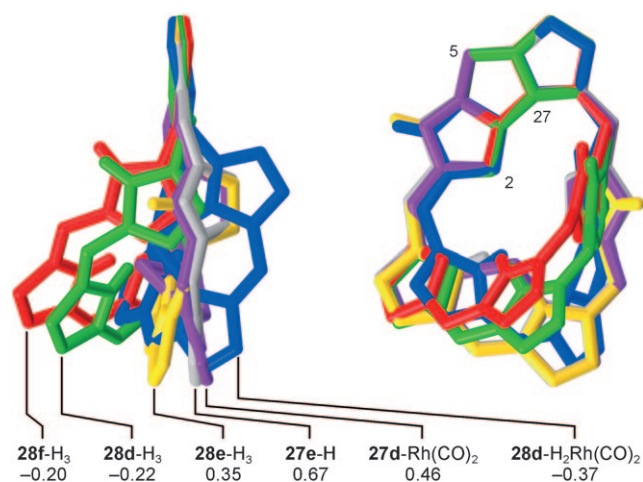


Figure 9. The family of structurally characterized conformers of N-fused pentaphyrins and their complexes. The structures are overlaid so as to closely match the positions 2-C, 5-C, and 27-N. Substituents, ligands, and hydrogen atoms (except for NH's) have been omitted for clarity. Π values are given below structure symbols.

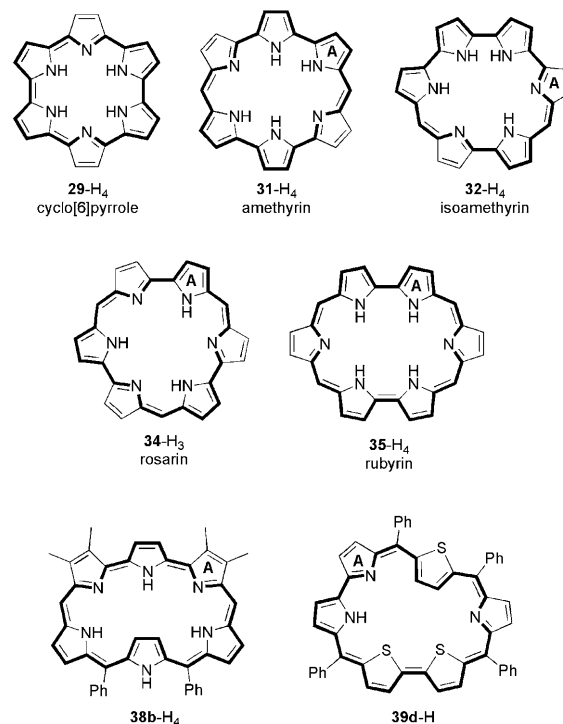
for the tilted ring C, which contributes to the lowering of the Π parameter (0.67). The corresponding rhodium complex **27d-Rh(CO)₂** has a similar structure, albeit slightly more nonplanar as a consequence of metal coordination ($\Pi = 0.46$). The distortion is even more significant in the structure of fused [24]pentaphyrin **28e-H₃**, likely because this $4n$ -electron system does not benefit from the planarizing effect of Hückel aromaticity. Two other N-fused [24]pentaphyrins **28f-H₃** and **28d-H₃**, bearing respectively CF_3 and C_6F_5 substituents were isolated in the solid state in the form of Möbius ($T1$) conformers. However, the low absolute values of Π (−0.20 and −0.22, respectively) suggest that the macrocyclic conjugation may be relatively ineffective in these structures. Interestingly, solution ^1H NMR spectra of the three species **28def-H₃** show characteristics of moderate paratropicity, indicative of the prevalence of $T0$ conformations. It should be noted, however, that the chemical shifts recorded for these macrocycles show significant variability that seems unlikely to originate from a simple substitution effect. For instance, the

signal of 29-H (NH proton of ring E) resonates at 16.98, 13.73, and 9.26 (or possibly 8.05) ppm in **28e-H₃**, **28d-H₃**, and **28f-H₃**, respectively. Such variability indicates a possible equilibrium between $T1$ and $T0$ conformations, controlled by meso substitution. The $T1$ contribution in **28f-H₃** is particularly large, as can be inferred from the noticeable diatropic shielding of the inner proton 1-H, whose signal appears at 3.09 ppm. The availability of the Möbius conformation is clearly demonstrated by the rhodium complex **28d-H₂Rh(CO)₂**, which revealed a $T1$ -type structure in the solid state ($\Pi = -0.37$) and was also found to be diatropic in solution. The type of out-of-plane distortion present in **28d-H₂Rh(CO)₂** is however qualitatively different from those observed for the two Möbius free bases **28f-H₃** and **28d-H₃**. The case of N-fused pentaphyrin exemplifies a $T0$ - $T1$ transition that is associated with a relatively simple conformational change (Figure 5, pathway 4) and with an energy gap so small that it can be easily influenced by metal coordination, peripheral substitution or crystal packing forces.

6. Hexaphyrins

6.1. Rings With Up To Two Meso Bridges

To date, three hexaphyrin ring systems with small τ_F values have been reported (Scheme 15, Table 7). Cyclo[6]pyrrole **29a-H₄**, or [22]hexaphyrin(0.0.0.0.0.0) contains no meso bridges and is the smallest member of the cyclopyrrole family.^[38] While the value of τ_F for this structure is only 0.79 indicating a fair amount of angular strain, it is readily appreciated that the geometry of the SMC in **29a-H₄**



Scheme 15. Structures of selected hexaphyrins. The choice of tautomers is arbitrary.

Table 7: Hexaphyrin ring systems discussed in the text.

Entry ^[a]	Structure ^[b]	S	τ_F ^[c]	Ref.
29a-H₄	cyclo[6]pyrrole [22]{N.N.N.N.N.N}(0.0.0.0.0.0)	18	0.79	[38]
30a-H₂	[20]{N.N.N.N.N.N}(0.0.0.0.0.0) ^[d]			[213]
31a-H₄	amethyrin [24]{N.N.N.N.N.N}(1.0.0.1.0.0)	20	1.12	[55]
32a-H₄	isoamethyrin [24]{N.N.N.N.N.N}(1.0.1.0.0.0)	20	1.12	[57]
33a-H₂	[22]{N.N.N.N.N.N}(1.0.1.0.0.0) ^[d]			[57]
34b-H₃	rosarin [24]{N.N.N.N.N.N}(1.0.1.0.1.0)	21	1.29	[40]
35ac-H₄	rubyrin [26]{N.N.N.N.N.N}(1.1.0.1.1.0)	22	1.46	[43]
36d-H₂	[26]{N.S.N.N.S.N}(1.1.0.1.1.0)	22	1.37	[220]
37d	[26]{Se.N.Se.Se.N.Se}(1.1.0.1.1.0)	22	1.21	
38b-H₄	[26]{N.N.N.N.N.N}(1.1.1.1.0.0)	22	1.46	[50]
39d-H	[26]{N.S.N.S.S.N}(1.1.1.0.1.0)	22	1.32	[59]
40acdef-H₂	hexaphyrin [26]{N.N.N.N.N.N}(1.1.1.1.1.1)	24	1.79	[221]
41cef-H₄	[28]{N.N.N.N.N.N}(1.1.1.1.1.1)	24	1.79	
42g-H	[28]{S.N.S.N.S.N}(1.1.1.1.1.1)	24	1.66	[163]
43c-H₂	[26]{C ^{CN} .N.C ^{CN} .N.C ^{CN} .N} (1.1.1.1.1.1) ^[e]	24	1.84	[222]
44h-H₂	A,D-di- <i>p</i> -benzihexaphyrin [28]{CC.N.N.CC.N.N}(1.1.1.1.1.1)	26	1.53	[24]
45i	[30]{CC.S.S.CC.S.S}(1.1.1.1.1.1)	26	1.35	[179]

[a] Representative substitution patterns: **a** β -alkyl; **b** β -alkyl-*meso*-aryl; **c** *meso*-C₆F₅; **d** *meso*-Ph; **e** *meso*-C₆F₅- β -F; **f** 5,10,20,25-(C₆F₅)₄-15,30-(2-thienyl)₂; **g** *meso*-(2,6-C₆H₃Cl₂); **h** 5,15,20,30-Mes₄-10,25-Ph₂; **i** 5,15,20,30-(C₆F₅)₄-10,25-(2,6-C₆H₃F₂)₂. [b] For explanations, see footnote [b] of Table 5. [c] Free curvature without inversions (Section 2.1). [d] Free base unknown. [e] Not isolated.

resembles the preferred conformation of [18]annulene. In analogy to the higher cyclopyrroles, **29a-H₄** is obtained in an oxidative, anion-templated coupling reaction of α -free bipyrrroles, in which the macrocycle size can be controlled by the choice of the templating ion. **29a-H₄**, isolated as trifluoroacetate or chloride salts, shows ruffled conformations in the solid state (Figure 10). The macrocyclic core of **29a-H₄** provides a nearly perfect fit for the uranyl cation, yielding a complex **30a-UO₂** with a virtually planar conformation of the hexapyrrolic ring, which is in striking contrast to the ruffled complexes of sapphyrin and pentaphyrin described above (Figure 10).^[213] Importantly, the insertion of uranyl occurs with oxidation of the macrocycle to a [20]annulenoid system with distinct paratropicity.

Amethyrins (**31a-H₄**)^[55,214–217] and their isomers isoamethyrins (**32a-H₄**)^[57,213,218,219] possess two *meso* bridges in their structure ($\tau_F = 1.12$). These macrocycles have [24]annulenoid substructures and are hence antiaromatic. All systems reported to date, whether free ligands, acid salts, or metal complexes, exhibit only convex conformations (Figure 10), which however can occasionally show a fair degree of nonplanarity. Amethyrins form structurally diverse dinuclear complexes with B^{III}, Zn^{II}, Co^{II}, Cu^{II}, and Rh^I.^[55,214,215,217] In these systems, metal coordination was reported to consistently occur without affecting the oxidation level of the macrocycle. In contrast, the formation of uranyl, neptunyl, and dinuclear copper(II) complexes of isoamethyrin was

accompanied with a change of the oxidation level to a [22]annulenoid structure corresponding to the hypothetical free base **33a-H₂**.^[57,213,219]

6.2. Rosarin

The skeleton of hexaphyrin(1.0.1.0.1.0) known as rosarin (**34-H₃**) possesses threefold symmetry and can be thought of as composed of either three directly linked dipyrromethenes or of three *meso*-bridged bipyrrrole units (Scheme 15). In spite of these potentially interesting structural features, rosarins received relatively little attention in the literature^[40,42,223] (higher homologues of rosarin are discussed in Section 9.2). The τ_F value of the rosarin ring is 1.29, comparable with that of sapphyrin, and is in the range of stable convex conformations. However, the conformation of the rosarin triacid, which forms a hydrogen-bonded aggregate, [**34b-H₆**]Cl₂(H₂O)₂⁺, in the solid state is highly nonplanar (Figure 10),^[40] which is partly due to the absence of aromatic stabilization and partly to the effect of simultaneous *meso*- and β -substitution. Interestingly, the solid state conformer has in fact the Möbius topology (*T1*), but the modest value of $\Pi = -0.14$ corresponds to rather ineffective π -conjugation. Consistent with the solid state structure, the system was reported to exhibit neither dia- nor paratropic character in solution.

6.3. Rubyrins

In a hexaphyrin structure, four single-carbon *meso* bridges can be distributed in three different ways. The (1.1.0.1.1.0) pattern corresponds to the macrocyclic structure known as rubyrin (**35-H₄**),^[43] which has been realized in numerous structural variants. Examples of the two isomeric patterns have also been reported, namely (1.1.1.1.0.0) (e.g. **38b-H₄**, Scheme 15)^[50,54,224,225] and (1.1.1.0.1.0) (e.g. **39d-H**, Scheme 15).^[59] In its all-pyrrole incarnation, each of these three isomeric ring systems is characterized by $\tau_F = 1.46$, which indicates that convex conformations will have to accept a fair amount of angular strain. By introducing one or two ring inversions, the free curvature of an all-pyrrole structure is reduced to $\tau_{FI} = 1.19$ and 0.93, respectively. These values indicate the viability of uni- and biconcave conformations, which indeed are observed experimentally. The principal oxidation level of rubyrin and its isomers is that of an aromatic [26]annulenoid, although oxidation to an antiaromatic 24-electron structure was reported in some cases.^[45] Systems containing the related (2.0.0.2.0.0) *meso* pattern are also known.^[226–228]

The first rubyrins to be reported were β -substituted macrocycles, obtained from bipyrrrole-containing precursors. These systems included the generic all-aza system **35a-H₄**^[43] and its dicationic all-thia analogue.^[12,229] **35a-H₄**, isolated in the solid state as a dichloride salt, revealed a relatively planar conformation, which is likely stabilized by hydrogen bonding (Figure 10). A number of *meso*-substituted rubyrins were subsequently synthesized by utilizing an oxidative coupling reaction of appropriate tripyrranes.^[220] These systems, con-

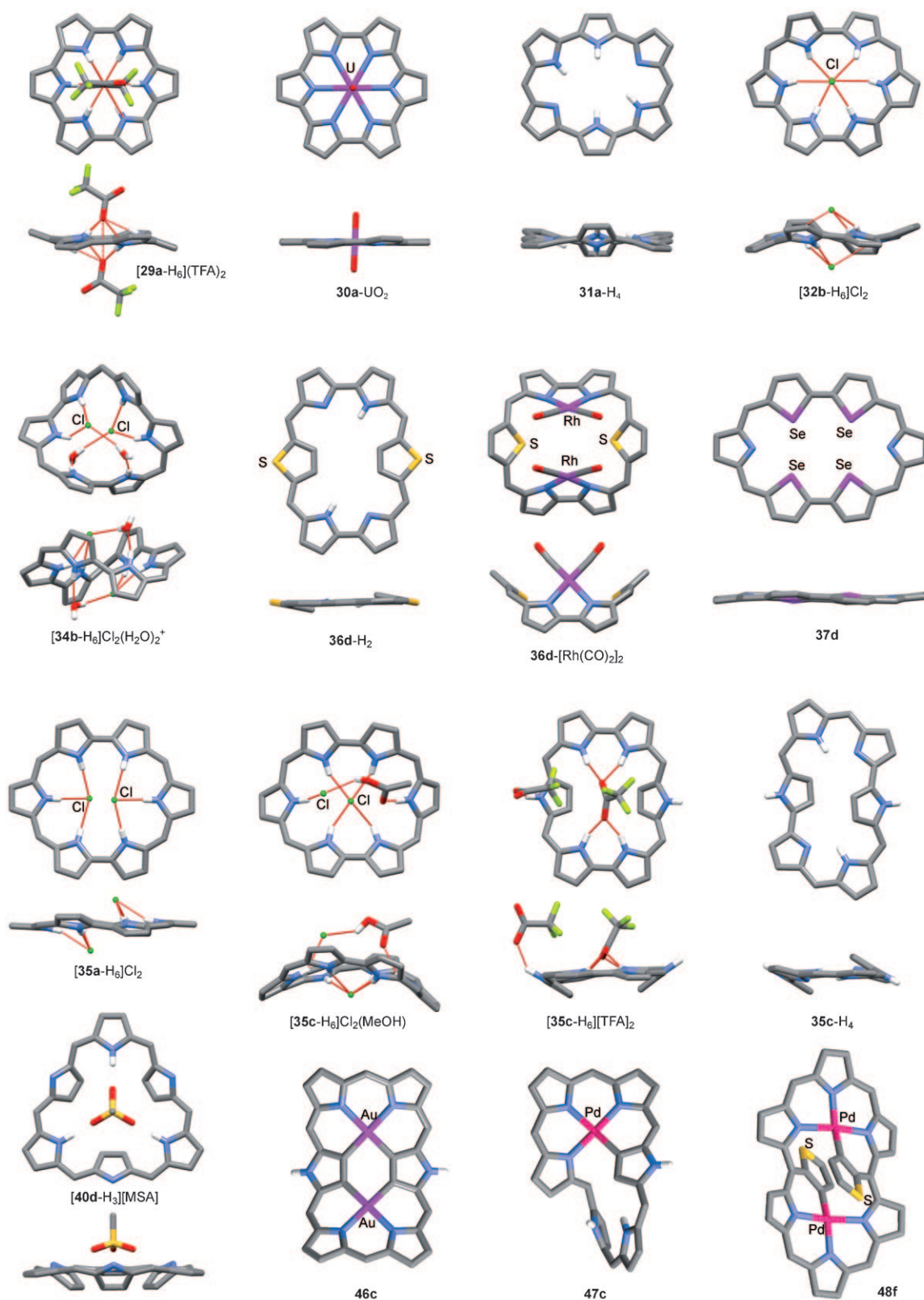


Figure 10. Three-dimensional structures of selected hexaphyrins. Coordinates have been taken from X-ray structural data. Solvent molecules and peripheral substituents are removed for clarity. The third chloride anion in the structure of $[34b-H_6]Cl_3 \cdot 2H_2O$, which is not hydrogen bound to the macrocyclic core, is not shown.

taining various patterns of core heteroatoms, show striking conformational diversity, which can often be controlled. For

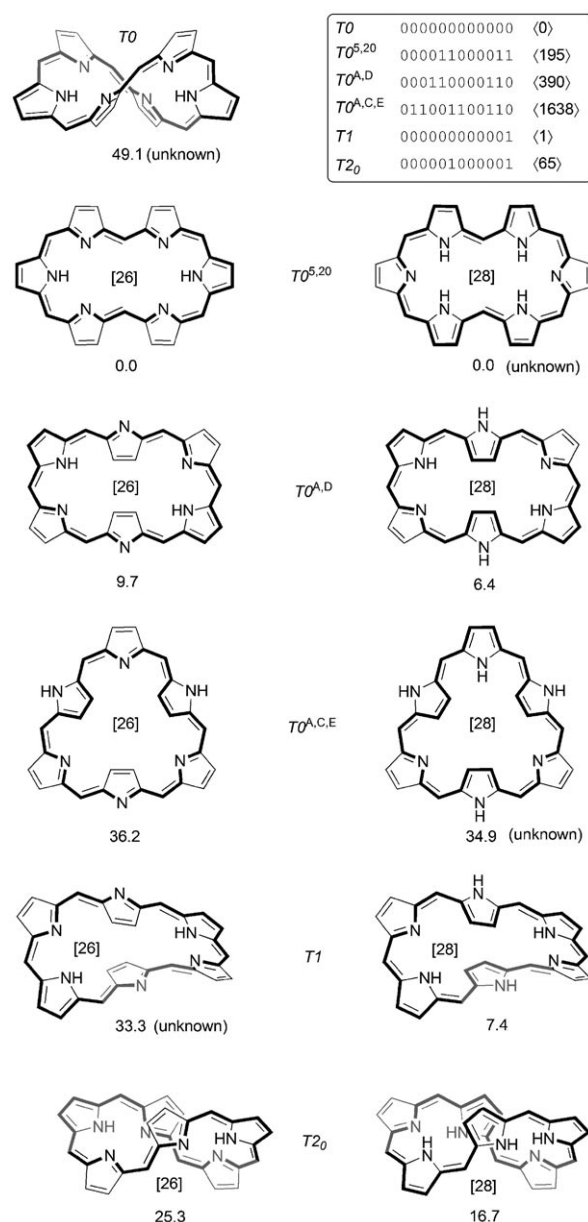
instance, a series of diheterorubyrins was obtained, exemplified here by the dithia species **36d-H₂**, in which both

nonpyrrolic rings are inverted ($T0^{B,E}$ conformer, Figure 10).^[220] (The behavior of a dioxa analogue is apparently different.)^[33] In these systems, conversion to the convex conformer is possible by protonation of the free base with TFAH. Additionally, **36d**-H₂ was transformed into a convex conformation by coordinating two rhodium centers, to yield **36d**-[Rh(CO)₂]₂ (Figure 10).^[230] *meso*-Aryl rubyrins containing four bulky heteroatoms, such as the tetraselena species **37d** adopt a convex conformation even in the free base form (Figure 10).^[231,232]

The conformational potential of *meso*-aryl rubyrins was elegantly revealed in a study of the tetrakis(pentafluorophenyl) derivative **35c**-H₄.^[44] The free base was found to adopt a biconcave $T0^{A,D}$ conformation in the solid state (Figure 10). Interestingly, the conformation is different in two acid salts of this rubyrin, [**35c**-H₆]₂Cl₂(MeOH) and **35c**-H₆-(TFA)₂, both of which were characterized crystallographically. The trifluoroacetate species stabilizes another biconcave conformation, $T0^{B,E}$, which different from that found in the free base. In contrast, a convex conformer is found in the chloride salt and it exhibits a higher degree of ruffling than the β -substituted precedent [**35a**-H₆]₂Cl₂. The effect of counteranion on the observed conformation, which is also preserved in solution, results from matching between the geometry of the anion and the hydrogen bonding pattern provided by a particular conformer. **35c**-H₄ can therefore be viewed as a flexible anion receptor, with unique conformational adaptability. Upon metallation with zinc(II) acetate, **35c**-H₄ yields two dinuclear complexes with different oxidation levels, [24]- and [26]annulenoid, both of which stabilize a convex conformation.^[45]

6.4. Hexaphyrins(1.1.1.1.1.1)

Hexaphyrins possessing six *meso* bridges are among the most structurally diverse classes of porphyrinoids. This diversity stems from the easy access to a number of distinct conformations (Scheme 16), which can be controlled with a variety of chemical factors. Interestingly, the conformers observed experimentally for all-aza systems do not include the convex structure, the absence of which is rationalized in terms of the high free curvature of the macrocycle ($\tau_F = 1.79$). Instead, the hexaphyrin ring provides for two biconcave conformations $T0^{5,20}$ (dumbbell) and $T0^{A,D}$ (rectangular), triconcave structure $T0^{A,C,E}$ (triangular), Möbius conformer $T1$, and a figure-eight structure $T2_0$ (Scheme 16). The chemistry of hexaphyrins is further enriched by their acid-base and coordination properties, and by the availability of two oxidation levels corresponding to a [26]- and [28]annulenoid. (A dinuclear oxyphosphorus complex of [30]hexaphyrin has recently been reported to adopt a $T1$ conformation.)^[115] Below we will mainly focus on the all-aza systems, and some of their heteroanalogues, leaving out the majority of macrocycles containing N-confused pyrroles.^[233,234] The conformational behavior of the latter family of compounds is largely similar to that of their nonconfused congeners. A special case of hexaphyrin containing two *p*-phenylene rings is discussed separately in the following section.



Scheme 16. Generic conformations of all-aza hexaphyrins(1.1.1.1.1.1) **40**-H₂ (left) and **41**-H₄ (right). Values correspond to relative energies (kcal mol⁻¹, B3LYP/6-31G**) calculated for unsubstituted structures.^[151] No stable minimum could be located for the 28-electron $T0$ structure. Where possible, experimentally observed tautomers were chosen.

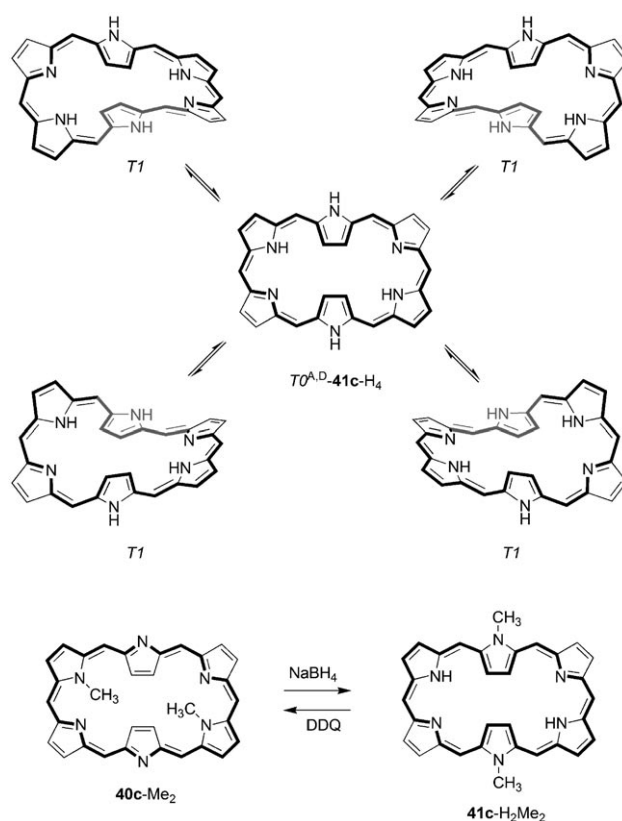
The first hexaphyrins were obtained in 1983 as β -substituted aromatic macrocycles with a 26 electron conjugation pathway (**40a**-H₂).^[12,221,235] In the absence of X-ray structural analyses, ¹H NMR spectra of these systems provided convincing evidence for the adoption of the biconcave $T0^{5,20}$ conformation. As the substitution patterns of some of the **40a**-H₂ derivatives were unsymmetrical, the double inversion of *meso* bridges led to positional isomerism, which could be observed spectroscopically. Analogous conformations of the macrocycle were attributed to Ni^{II} and Zn^{II} complexes of **40a**-H₂, obtained in the initial exploration of

its coordination chemistry. Interestingly, coordination of palladium(II) to **40a**-H₂ was shown to result in a species with the $T0^{A,D}$ conformation, which was the first example of subunit inversion reported in the literature (Scheme 1).^[19]

While the structural analysis contained in these early studies was solely based on solution NMR spectroscopy and steric considerations, the viability of the two biconcave structures, $T0^{5,20}$ and $T0^{A,D}$, was later verified in the solid state for *meso*-substituted systems. In particular, the initial structural report on a perfluorophenyl species **40c**-H₂^[236] revealed a $T0^{A,D}$ structure (Scheme 16) slightly twisted out of plane. A related system, **40d**-H₂, was only partly characterized due to its instability.^[237] Interestingly, that latter species becomes much more stable in the form of an ion-pair complex [**40d**-H₃][MSA], in which the methanesulfonate anion is symmetrically bound inside the bowl-shaped cavity of the triconcave conformation $T0^{A,C,E}$ (Figure 10).^[222] The perfluorinated hexaphyrin **40e**-H₂, itself incompletely characterized because of poor solubility, was reduced with sodium borohydride to the corresponding [28]hexaphyrin **41e**-H₄.^[238] That latter system is antiaromatic and adopts a figure-eight conformation ($T2_0$). An analogous redox couple was later characterized for *meso*-trifluoromethyl derivatives, and it was found that the $T2_0$ conformer is stabilized at both oxidation levels.^[211]

An unusual feature of the [28]hexaphyrin **41c**-H₄, isolated alongside **40c**-H₂ in 1999, was that its ¹H NMR spectrum indicated the presence of a diatropic ring current, in spite of a 4*n*-electron conjugation pathway.^[236] This striking observation remained a mystery until nine years later, when the solution structure of **41c**-H₄ was reinvestigated by means of low-temperature NMR spectroscopy and other physical methods.^[121,123] It was shown that **41c**-H₄ rapidly switches among four equivalent Möbius conformations ($T1$) in such a way that the positions of inverted rings in the intermediate $T0^{AD}$ structure are retained (Scheme 17). Consequently, the dynamically averaged room-temperature spectrum of **41c**-H₄ has the same symmetry as the spectrum of **40c**-H₂.

Extensive synthetic exploration of hexaphyrin chemistry, involving variation of substituents, peripheral fusion reactions and substitution of nitrogens, revealed additional instances of the conformations discussed above including the much sought-after Möbius structure.^[122,133,165,239–243] For instance, a redox-actuated switching process between two non-equivalent $T0^{A,D}$ configurations was reported for the *N,N*-dimethyl derivative of **40c**-H₂ (Scheme 17) and described as a caterpillar motion of the macrocycle.^[240] Another redox couple related to **40c**-H₂ and **41c**-H₄, containing four additional β -phenyl groups, was observed to switch between $T0^{A,D}$ and $T2_0$ structures.^[133] In the [28]electron species, an additional transformation into the $T1$ structure was induced by addition of trifluoroacetic acid. Interesting observations were made upon introduction of a variety of thienyl substituents into the hexaphyrin structure.^[243] It was found that **40f**-H₂, containing two 2-thienyl substituents, adopts the $T0^{5,20}$ conformation, previously unobserved in *meso*-substituted systems. This preference apparently relies on a subtle energetic balance, and is easily affected by small structural modifications. Specifically, the use of 3-thienyl substituents results in a



Scheme 17. Conformational behavior of the free base **41c**-H₄ (top) and the redox-actuated caterpillar motion in **40c**-Me₂ (bottom). Each of the four $T1$ structures of **41c**-H₄ represents one of two enantiomers. In all structures, *meso* substituents have been removed for clarity.

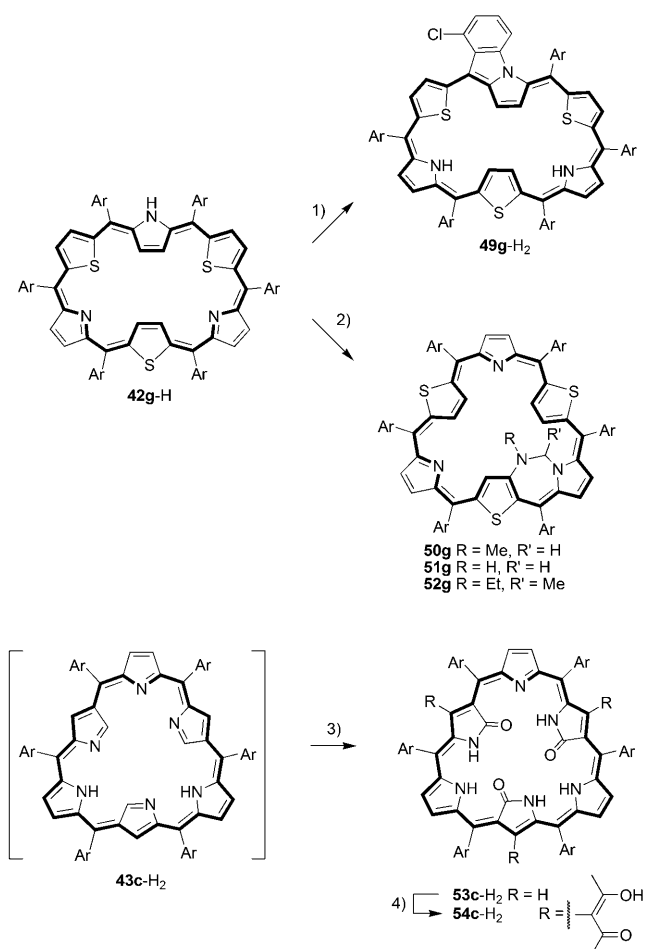
temperature-dependent equilibrium between the $T0^{A,D}$ and $T0^{5,20}$ structures, and when 3-methyl-2-thienyl substituents are introduced, only the $T0^{A,D}$ structure is observed. The reduced species **41f**-H₄ was characterized in the solid state, revealing a Möbius $T1$ conformation, originally described only as “highly distorted”.^[243] The ¹H NMR spectrum of **41f**-H₄ was dynamically broadened under ambient conditions; however, no further insight was sought into the solution structure of this species.

The structural outline of the $T0^{A,D}$ conformer may be viewed as a result of merging two partially overlapping porphyrin-like cores. While this analogy appears only pictorial at first glance, the resulting structural paradigm actually dominates the coordination chemistry of hexaphyrins because of the fortunate reactivity of pyrrolic β positions. A number of mono- and dinuclear complexes of *meso*-substituted macrocycles with such ions as Au^{III} (e.g. **46c**, Figure 10), Cu^{III}, Rh^I, Rh^{III}, and Hg^{II} have been reported, in which square-planar coordination is achieved by means of β -metallation of the inverted pyrrole rings A and D. The conformations stabilized by metal coordination are not limited to $T0^{A,D}$. Mononuclear Ni^{II} and Pd^{II} complexes of **41c**-H₄ (e.g. **47c**, Figure 10) are isostructural examples of Möbius conformers $T1$ ($\Pi = -0.37$ and -0.38 , respectively).^[244] In spite of the marked diatropicity of these interesting systems, their Möbius aromatic character was not recognized in the original report.^[103] Recent

work on thienyl-substituted hexaphyrins revealed that these untypical substituents can play a structural role in stabilizing metal complexes. In the bis-palladium(II) complex of **40f**-H₂ (**48f**, Figure 10), the macrocycle adopts the $T0^{5,20}$ conformation, with each of the thienyl groups providing a carbon donor that completes the coordinating environment of Pd^{II}.^[243]

The experimental results summarized above are in qualitative agreement with the theoretically predicted conformational preferences of the unsubstituted hexaphyrin ring and their dependence on the oxidation level (Scheme 16).^[151] Conformer $T0^{5,20}$ is energetically preferred for both [26]- and [28]annulenoid rings but its stability will crucially depend on the absence of meso substituents. Accordingly, in the majority of meso-substituted systems, $T0^{A,D}$ is the preferred structure. One exception from this rule is provided by an internally bridged hexaphyrin derivative,^[245] in which the $T0^{5,20}$ conformer is enforced by a covalent link between positions 5 and 20. Interestingly, there is a significant difference in the relative stability of $T1$ conformers at the [26] and [28] oxidation levels (33.3 and 7.4 kcal mol⁻¹, respectively). This difference is attributable to the combined effect of aromatic stabilization in the Möbius $4n$ electron system and antiaromatic destabilization in the $4n+2$ electron system. The $T2_0$ structures of both oxidation levels are relatively unstable, likely because the free curvature of the hexaphyrin ring ($\tau_F = 1.79$) is smaller than the optimum for a figure-eight conformer. It should be noted, that the calculated energy of the unobserved convex conformer of **40**-H₂ (which is predicted to have a strong saddle distortion) is particularly high (49.1 kcal mol⁻¹).

A number of analogues of hexaphyrin(1.1.1.1.1.1) have been reported. These include dioxo,^[246] dithia,^[247] trithia,^[163] and diselena^[247] derivatives. A variety of different conformations were claimed for the dihetero species, including some very unusual quadriconcave structures.^[246,247] However, these conformers were proposed on the basis of partial NMR assignments and were not supported by either X-ray diffraction analyses or high-level molecular modeling. [28]Trithiahexaphyrin **42g**-H adopts the $T0^{A,D}$ structure ($\tau_{FI} = 1.22$), as evidenced by the ¹H NMR spectrum recorded at 298 K.^[163] This conformation is retained in a product of intramolecular fusion with one of the 2,6-dichlorophenyl substituents (**49g**-H₂, Scheme 18). In addition, a variety of internally bridged products (**50g**, **51g**, and **52g**) were obtained from **42g**-H in the presence of Cu^I salts and aliphatic amines or DMF. These systems are of interest because they stabilize a triconcave conformation $T0^{A,C,E}$ with three inverted thiophene rings ($\tau_{FI} = 1.13$), similar to that reported for [40d-H₃][MSA] (see above). An analogous triangular conformer was recently reported as the preferred structure of hexaphyrin **53c**-H₂ (Scheme 18).^[222] This system forms in the course of spontaneous aerial oxidation of a triply N-confused hexaphyrin **43c**-H₂ and can be further derivatized to yield **54c**-H₂. The solid state structure of the latter species is similar to that of [40d-H₃][MSA], except for the arrangement of the inverted rings.



Scheme 18. Reactivity of trithiahexaphyrin **42g**-H. Reagents and conditions: 1) CuCl, DMF, reflux; 2) [Cu(MeCN)₄][BF₄], DMF, reflux, ammonium salt (**50g**, no salt added; **51g**, MeNH₃Cl; **52g**, Et₃NH₂Cl); 3) aerial oxidation; 4) [Mn(acac)₃], toluene, reflux. The conformation of **43c**-H₂ was not determined.

6.5. Aromaticity Switching in A,D-Di-*p*-benzihexaphyrin

The restricted motion of *p*-phenylene ring in the macrocyclic frame of *p*-benziporphyrin (**11**-H), may be considered a special case of ring inversion in which the two conformers related by the rotation of the phenylene are structurally identical (Scheme 10). Interestingly, when the macrocyclic frame is not planar but displays a twist along the axis of the phenylene (Figure 11, top), it becomes possible for the ring to adopt two non-equivalent orientations, differing by a 90° torsion, each of which may correspond to an actual energy minimum. If the axial twist approximates 90°, as shown in the Figure, the π -electron overlap between the phenylene ring and the frame will be appreciable in both conformations. However, by switching between the two orientations of the phenylene, a phase change of 180° is introduced to the macrocyclic π system, even though the ring has been rotated by only 90°. This observation suggests that, provided such a structural arrangement can be stabilized and controlled, it may be possible to construct a conformational aromaticity switch commuting between Hückel and Möbius conjugation.

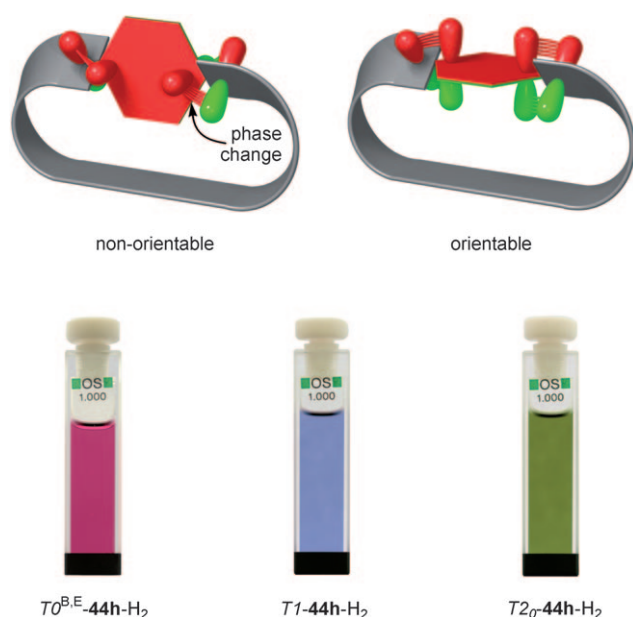
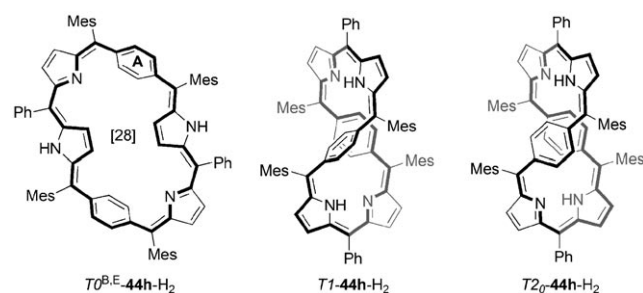


Figure 11. Top: The phenylene ring as a topology selector. Bottom: Colors of the three conformers of the free base **44h-H₂** observed in solution: $T0^{B,E}$ (transient, CH_2Cl_2), $T1$ (CHCl_3 , 32% $T2_0$), and $T2_0$ (hexane). All spectra were recorded at room temperature.

So far, this particular switching mechanism has not been demonstrated for subunits with nonzero curvature, such as the pyrrole ring. As can be appreciated from the examples discussed in this Review, topology switching in all-pyrrole expanded porphyrins involves a different type of motion, which is a combined rotation of a pyrrole and an adjacent meso bridge. As a result of this rotation, a *tt*-aligned pyrrolic subunit is transformed into a *ct*-aligned subunit (or vice versa, see Figure 1 and Figure 5), increasing or decreasing the number of *trans* bonds in the SMC by one.

The concept of topology selection outlined above, was realized in the structure of A,D-di-*p*-benz[28]hexaphyrin(1.1.1.1.1.1), **44h-H₂**,^[24,25,248] which was shown to switch between a $T2_0$ conformation with Hückel antiaromaticity and a Möbius-aromatic $T1$ conformation (Scheme 19). This system, which combines the structural features of all-pyrrole hexaphyrins and *p*-benzporphyrins, was the first porphyrinoid, in which Möbius π -conjugation was demonstrated. The ability of **44h-H₂** to switch between two different



Scheme 19. Three conformers of **44h-H₂** with different topologies of the π -surface.

aromaticity states was initially appreciated while analyzing the temperature-dependent behavior of the ^1H NMR spectrum of the free base dissolved in CDCl_3 . It was observed that on lowering the temperature, the macrocyclic ring current gradually changed from paratropic to diatropic. Such a change could in principle be caused by a tautomeric process,^[119] however, the length of the conjugation pathway is the same for all imaginable tautomers of **44h-H₂**. A conformational equilibrium was then considered and the energetic accessibility of the $T2_0$ and $T1$ structures was confirmed by DFT calculations. The two conformers differ in the relative orientation of the phenylene rings. In the Hückel structure $T2_0$, the rings are cofacial, whereas they are oriented edge-to-face in the Möbius form. That latter arrangement was also found to be stabilized in a solid state structure of **44h-H₂**.

The equilibrium between conformers $T2_0$ and $T1$ depends on the choice of solvent and temperature in a manner that is not completely understood. In deuterated chloroform, the equilibrium constant $K = [T2_0]/[T1]$ varies from 1.41×10^{-2} at 203 K to 1.43 at 343 K ($\Delta H = 19.1(4) \text{ kJ mol}^{-1}$ and $\Delta S = 58.7(1.1) \text{ J mol}^{-1} \text{ K}^{-1}$). The prevalence of $T1$ at low temperatures is also observed in other chlorinated solvents. In particular, the spectrum of pure $T1$ in the slow exchange limit can be recorded in CDFCl_2 ($[\text{D}]-\text{DCFM}$) at or below 150 K.^[25] In contrast, $T2_0$ is the principal conformation observed at room temperature for solutions of **44h-H₂** in aliphatic hydrocarbons and other solvent such as alcohols. However, variable-temperature measurements taken in $[\text{D}_{12}]\text{pentane}$ indicate that even in this solvent the Möbius conformer appears to be the dominant form at 140 K (a more detailed analysis was not possible because of severe solubility problems).^[249] Interestingly, the preference for the Möbius structure observed in solution is not reproduced by DFT calculations (B3LYP/6-31G** and KMLYP/6-31G**),^[24,25,248] which predict that the $T2_0$ conformer should be more stable by ca. 2 kcal mol^{-1} . This discrepancy may be a result of solvation effects not accounted for in the DFT calculations, or may indicate a non-negligible contribution of $\text{CH}\cdots\pi$ interactions in $T1$ -**44h-H₂**, which are known to be poorly reproduced by conventional DFT methods.

Even though the exchange between $T1$ and $T2_0$ forms of **44h-H₂** is very rapid at room temperature, the inversion of the figure-eight shape found in both conformers is either a very slow process or does not occur. Consequently, the molecule retains its handedness during topology switching. While separation of enantiomers was not attempted for **44h-H₂**, their configurational stability could be probed using ^1H NMR spectroscopy.^[24] The spectrum recorded for a (–)-limonene solution of **44h-H₂** (containing predominantly the $T2_0$ conformer) displayed two peaks corresponding to the two enantiomers. The separation between the signals is rather small, though (0.02 ppm), and other signals in the spectrum are not affected by the use of a chiral solvent. It seems that the discriminating effect of limonene does not result from a specific interaction with the solute because 1) the NH protons are buried in the macrocyclic cavity and are not easily available and 2) the solvent molecule does not contain strongly interacting groups. It may be proposed that the chiral medium imposes a slight difference in equilibrium

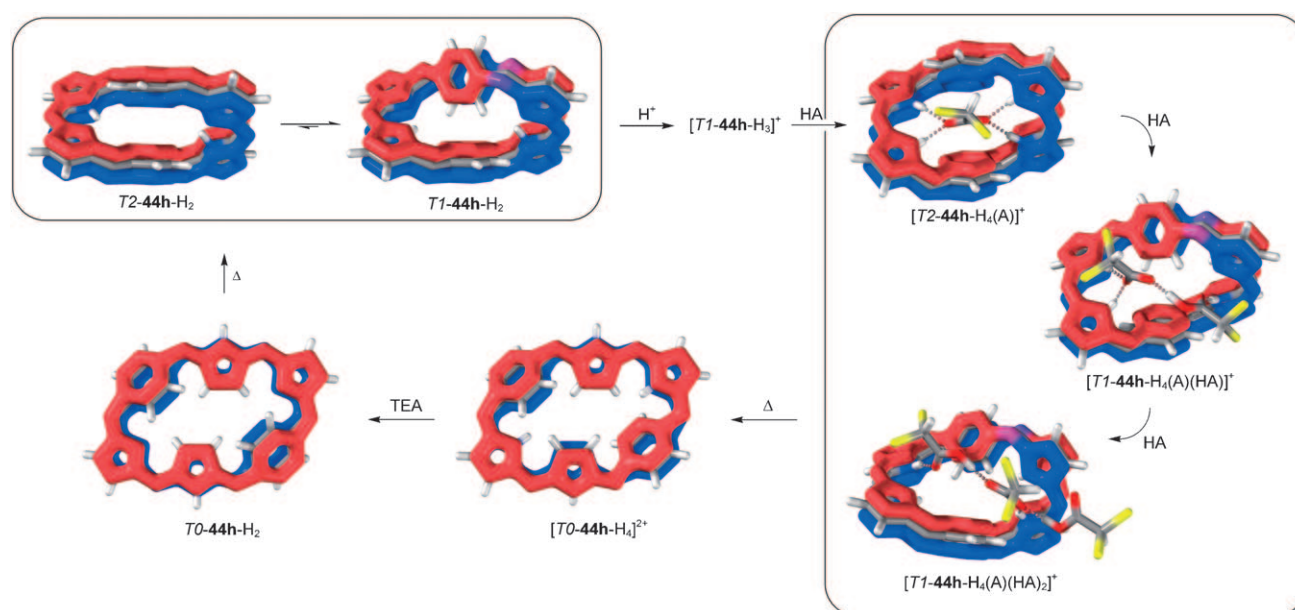


Figure 12. Switching between the three different π -conjugation topologies of A,D-di-*p*-benzihexaphyrin performed in [D]-DCFM solution at 150 K.^[25] Reversibility of some processes is not indicated. Additional symbols used: HA, acid (TFAH or DCAH); TEA, triethylamine; Δ , heating to 270 K to induce conversion, then cooling back to 150 K. DFT optimized geometries^[25] (A = DCA) are shown with peripheral substituents removed for clarity. π -Conjugation is indicated schematically in red and blue. A close-up image of $[T2_0\text{-}44\text{h-H}_4(\text{DCA})]^+$ is shown in the frontispiece.

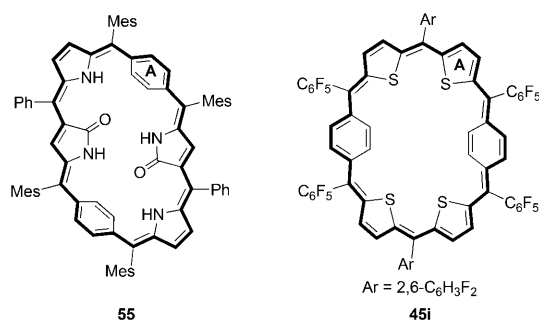
geometries of the enantiomers, which most strongly affects the strongly deshielded NH signal.

A significantly more complicated behavior was demonstrated for **44h-H₂** during protonation experiments carried out in [D]-DCFM at low temperatures (Figure 12).^[25] These experiments showed that a three- or four-step switching cycle, which involves an additional, biconcave conformation, can be realized by sequential addition of trifluoroacetic or dichloroacetic acid (TFAH or DCAH) combined with temperature changes. The principal forms involved in switching, elucidated with the help of NMR spectroscopy and DFT calculations, are summarized in Figure 12. The cycle begins with the free-base **T1-44h-H₂**, which exists as the pure Möbius conformer in [D]-DCFM at 150 K. The first protonation step leads to a monocationic species $[T1\text{-}44\text{h-H}_3]^+$, which retains the Möbius structure. This monocation, which only forms in small amounts, is converted to a new, Hückel-antiaromatic species, $[T2_0\text{-}44\text{h-H}_4(\text{A})]^+$ (A = DCA or TFA), in which the anion binds to the macrocyclic core in a manner reminiscent of that observed in the rubyrin structure **35c-H₆(TFA)₂** (Section 6.3). A cofacial arrangement of the phenylene rings is necessary to accommodate the carboxylate anion inside the macrocycle, leading to the observed change in π -surface topology. At higher acid concentrations, the antiaromatic species is replaced by two Möbius forms, $[T1\text{-}44\text{h-H}_4(\text{A})(\text{HA})]^+$ and $[T1\text{-}44\text{h-H}_4(\text{A})(\text{HA})_2]^+$, in which the anion is no longer hydrogen-bonded in the core. Instead, and aggregate consisting of two or three acid residues is bound to one of the macrocyclic grooves formed by the figure-eight structure of the macrocycle.

The three protonated species, $[T2_0\text{-}44\text{h-H}_4(\text{A})]^+$, $[T1\text{-}44\text{h-H}_4(\text{A})(\text{HA})]^+$ and $[T1\text{-}44\text{h-H}_4(\text{A})(\text{HA})_2]^+$, are metastable, and have a limited lifetime above 190 K. Thus when the

sample temperature is temporarily increased, these cationic forms undergo a conformational change to a new species, $[T0^{\text{B,E}}\text{-}44\text{h-H}_4]^+{}^{2+}$. This new biconcave conformer, containing two inverted pyrrole rings, displays distinct Hückel antiaromaticity. While the biconcave dication is stable at room temperature, the corresponding free base, **T0^{B,E}-44h-H₂**, enjoys only a fleeting existence under ambient conditions and is quantitatively converted to the equilibrium mixture of **T1** and **T2₀** conformers within just a few seconds. This unstable species could be trapped by addition of base at room temperature. Upon temporary warming of the sample to room temperature and cooling it back to 150 K, the macrocycle reverts to the **T1** conformer, thus completing the switching cycle. The **T0^{B,E}** structure of the free base is distinguished from the other two conformers by its ruby color (**T1** and **T2₀** species are respectively violet and green, cf. Figure 11, bottom).

Interestingly, the unusual conformational features of **44h-H₂** are strongly dependent on fine structural detail, and can be affected by changes in peripheral substitution.^[248,249] For instance, replacing the mesityl substituents in **44h-H₂** with more electron-donating 2,3,5,6-tetramethylphenyl groups shifts the **T1**–**T2₀** equilibrium towards the Möbius form, as can be judged from the ¹H NMR shifts of the respective free bases measured in [D]chloroform at room temperature.^[248] In a related system, **55**, containing two oxidized N-confused rings, the biconcave structure **T0^{B,E}** becomes the preferred conformation (Scheme 20).^[248] It is possible that intramolecular hydrogen bonds formed by the carbonyl groups present in **55** contribute to the stability of the **T0^{B,E}** conformer. In contrast, a convex conformation was reported for **45i**, a tetrathia analogue of **44h-H₂**.^[179] This system stabilizes an oxidation level corresponding to the [30]annulene CP and is



Scheme 20. Macrocycles structurally related to **44h-H₂**.

markedly diatropic. In the solid state, **45i** displayed a noticeable saddle-like distortion from planarity, which reflects the excessive free curvature of the ring ($\tau_F = 1.35$).

7. Heptaphyrins

To date, seven distinct meso patterns (out of 18 possible) have been reported in the heptaphyrin family (Table 8). In spite of this apparent diversity, the number of heptaphyrin systems described in the literature is small when compared

Table 8: Heptaphyrin ring systems discussed in the text.

Entry ^[a]	Structure ^[b]	S	τ_F ^[c]	Ref.
56a-H₅	cyclo[7]pyrrole [26]{N.N.N.N.N.N.N}(0.0.0.0.0.0.0)	21	0.92	[38]
57a-H₅	[28]{N.N.N.N.N.N.N}(1.0.0.1.0.0.0)	23	1.26	[58]
58b	[30]{S.N.S.S.N.S.S}(1.1.0.1.1.0.0)	25	1.37	[60]
59b-H	[30]{S.N.S.S.N.S.S}(1.1.0.1.0.1.0)	25	1.41	[60]
60b-H₂	[30]{N.S.N.N.S.S.N}(1.1.0.1.0.1.0)	25	1.46	[60]
61c-H₅	[30]{N.N.N.N.N.N.N}(1.1.1.1.0.0.0)	25	1.59	[51]
62a-H₄	[30]{N.N.N.N.N.N.N}(1.1.1.1.1.0.0)	26	1.76	[52]
63d-H	[30]{S.N.N.N.N.S.S}(1.1.1.1.1.0.0)	26	1.62	[53]
64d-H₃	[32]{S.N.N.N.N.S.S}(1.1.1.1.1.0.0)	26	1.62	[53]
65c-H₃	[30]{N.N.N.N.N.N.N}(1.1.1.1.1.1.0)	27	1.92	[51]
66e	[30]{S.N.N.S.N.N.S}(1.1.1.1.1.1.0)	27	1.79	[250]
67cfg-H₄	[32]{N.N.N.N.N.N.N}(1.1.1.1.1.1.1)	28	2.09	[100]

[a] Representative substitution patterns: **a** β -alkyl; **b** *meso*-Ph; **c** *meso*-C₆F₅; **d** *meso*-(Mes)_m(C₆F₅)_n; **e** *meso*-Mes; **f** *meso*-(C₆F₅)- β -F; **g** *meso*-(2,6-C₆H₃Cl₂). [b] For explanations, see footnote [b] of Table 5. [c] Free curvature without inversions (Section 2.1).

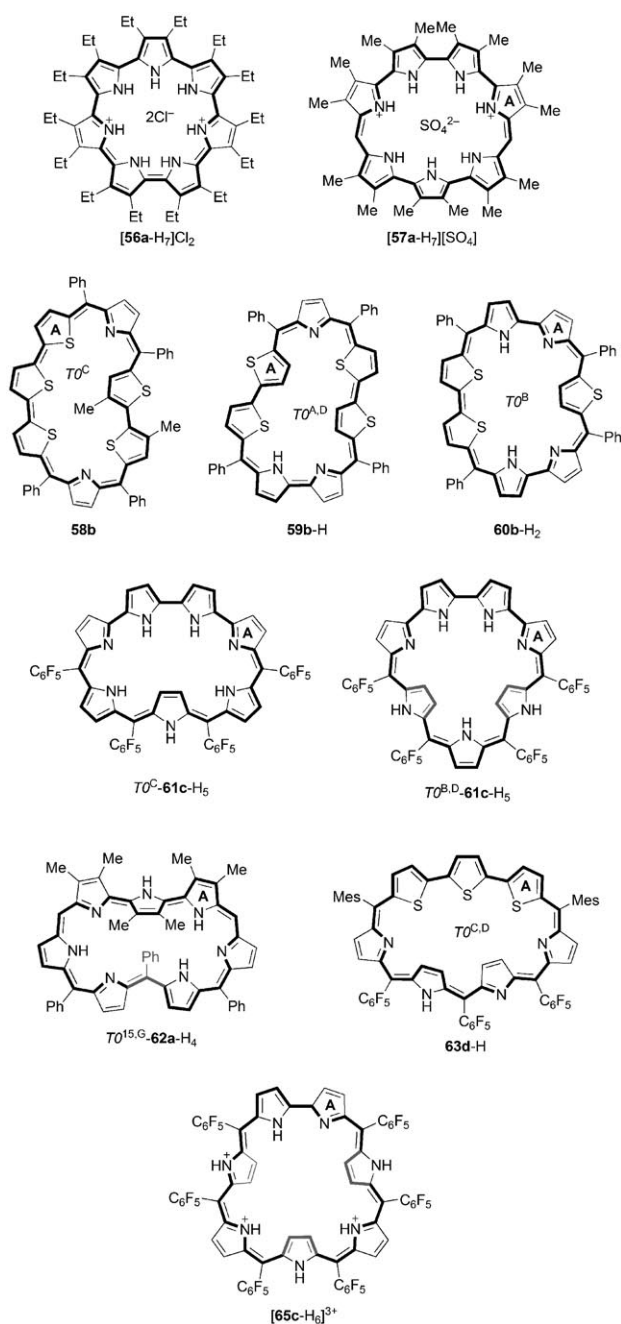
with hexa- or octaphyrins. The reason for this relative scarcity is apparently synthetic: heptaphyrins are more difficult to make using predesigned oligopyrrolic precursors, whereas direct Rothmund-style methods are low-yielding and show poor ring-size selectivity. The first reported system in the heptaphyrin class, antiaromatic [28]heptaphyrin(1.0.0.1.0.0.0) (**57a-H₅**), was obtained in an oxidative cyclization of a linear heptapyrrolic precursor.^[58] In the solid state, the sulfate salt [**57a-H₇**][SO₄] reveals a ruffled convex conformation and a sulfate anion hydrogen-bonded in the macrocyclic core. The preference of **57a-H₅** for a convex structure results from the relatively low free curvature of the macrocycle ($\tau_F = 1.26$) and is likely enhanced by β -substitution and anion binding in the

core. A structurally related system is the aromatic cyclo[7]-pyrrole (**56a-H₅**, $\tau_F = 0.92$), which forms as a scrambling product in the oxidative cyclooligomerization of bipyrrroles.^[38] The chloride salt [**56a-H₇**][Cl]₂, characterized crystallographically, displays a marked ruffling of the macrocycle, which is at least in part induced by the “sitting-atop” coordination of counteranions.

The remaining known heptaphyrins are characterized by much larger τ_F values, and consequently, they are never seen to adopt stable convex conformations. A family of heteroheptaphyrins containing up to five thiophene or selenophene rings and four meso bridges in various patterns were characterized in solution revealing a variety of diatropic quasi-planar conformations containing at least one inverted subunit.^[60] Representative examples of these systems include the uniconcave trithiaheptaphyrin **60b-H₂** ($T0^B$, $\tau_{FI} = 1.28$), biconcave tetrathia species **59b-H** ($T0^{A,D}$, $\tau_{FI} = 1.06$), and uniconcave pentathiaheptaphyrin **58b** ($T0^C$, $\tau_{FI} = 1.19$). An aromatic trithiaheptaphyrin **66e**, characterized by one “missing” meso bridge, was also reported and shown to adopt a figure-eight $T2_0$ conformation in the solid state.^[250] The symmetry and line broadening of the room temperature ¹H NMR spectrum indicated the presence of a dynamic process but the conformational behavior of **66e** was not investigated.

An interesting species containing a sequence of four meso bridges (**61c-H₅**, $\tau_F = 1.59$) was recently reported as a product of Rothmund-type condensation carried out in water.^[51] In this reaction, the compound was accompanied by another heptaphyrin **65c-H₃**, and an octaphyrin (**78e-H₅**, Section 8.2). While the selectivity of this reaction remains to be explained, it provides a potentially general route to expanded macrocycles with unsymmetrical meso patterns. The principal conformation of **61c-H₅** is the diatropic conformer $T0^C$ ($\tau_{FI} = 1.33$), containing one inverted pyrrole (Scheme 21). However, upon conversion to the trifluoroacetate salt [**61c-H₇**][TFA]₂, the macrocycle undergoes a conformational change to a doubly inverted form $T0^{B,D}$ ($\tau_{FI} = 1.06$), and an analogous transformation was proposed to explain the spectral changes observed for **61c-H₅** in partly aqueous solutions.^[51] Compound **65c-H₃**, to which a [30]annulenic formulation was assigned on the basis of mass spectrometric and X-ray structural data, is of interest because it exhibits distinct paratropicity in the free base form, in spite of the $4n + 2$ conjugation pathway. In the original report, a $T2$ conformation was proposed for **65c-H₃**, which is not consistent with the observed ring current.^[51] The above discrepancy may be explained in terms of a Möbius-type conformer $T1$, which might be structurally similar to that found for **67-H₄** (see below). The trication [**65c-H₆**]³⁺ was characterized in the solid state as a triconcave structure $T0^{B,D,F}$. ¹H NMR data show that the trication is diatropic and that the triconcave conformation likely persists in solution.

An interesting feature of the heptaphyrin family is that its members span a considerable range of free curvature values ($\tau_F = 0.92$ to 2.09). For the macrocycles with smaller values of τ_F discussed above, the excess curvature is eliminated by subunit inversions, whereas for larger τ_F values the preference for $T2$ conformers becomes apparent. Heptaphyrin **62a-H₄**,



Scheme 21. Structures of selected heptaphyrins. The choice of tautomers is arbitrary.

characterized by the (1.1.1.1.1.0.0) meso pattern ($\tau_F = 1.76$), is a borderline case displaying an interesting structural dichotomy. The conformation assigned to **62a-H₄** on the basis of solution NMR spectroscopy is a diatropic biconcave structure $T0^{15,G}$, containing an inverted pyrrole and an inverted meso bridge ($\tau_{FI} = 1.16$, Scheme 21). In contrast, in the reported crystal structure, the macrocycle adopted a figure-eight conformation $T2$ (Figure 13), and this difference was ascribed to the effect of crystal packing forces. Heteroanalogues of **62a-H₄** were reported that stabilize two oxidation levels corresponding to [30]- and [32]annulenoid CP's, exemplified here by the trithia species **63d-H** and its reduced form, **64d-**

H₃, respectively.^[53] **63d-H** was characterized in the solid state as a biconcave conformer $T0^{C,D}$ ($\tau_{FI} = 1.10$, Scheme 21), however, the X-ray structure was rather poorly resolved. The presence of two inverted pyrrole rings and diatropicity of the macrocycle were additionally confirmed in the ^1H NMR spectra of **63d-H**. In spite of the relatively high free curvature ($\tau_F = 1.64$), the reduced species **64d-H₃** was represented as a convex conformer in the original report.^[53] This assumption is not easily verified because the ^1H NMR spectrum of **64d-H₃** did not show significant para- or diatropicity. It is however noteworthy that the number of resonances observed for mesityl substituents is indicative of a nonplanar structure.

meso-Aryl-substituted [32]heptaphyrins(1.1.1.1.1.1.1) (**67-H₄**) are found among the products of direct pyrrole–aldehyde condensations^[100,238] but they are more efficiently prepared using a specially designed [3+4] method.^[251] **67c-H₄** ($\tau_F = 2.09$) adopts a figure-eight conformation ($T2_0$) in the solid state (Figure 13). The ^1H NMR spectrum of **67c-H₄** recorded in nonpolar solvents (such as hexane, toluene, or dichloromethane) indicated the prevalence of a Hückel-antiaromatic $T2_0$ conformer. In contrast, the low-temperature ^1H NMR spectra obtained in $[\text{D}_6]\text{acetone}$ corresponded to a diatropic system, ascribable to a conformational conversion to a $T1$ structure.^[132] Interestingly, a related heptaphyrin **67g-H₄**, which contains 2,6-dichlorophenyl substituents, stabilizes the $T1$ conformation also in nonpolar solvents.^[103] Upon addition of TFAH, both heptaphyrins undergo stepwise protonation, resulting in the formation of distinct mono- and tricationic species all of which show characteristics of Möbius aromaticity. The monocation [**67c-H₃**]⁺ was characterized in the solid state, revealing hydrogen-bonded interactions of the protonated macrocycle with a hydrogen bis(trifluoroacetate) anion and a TFAH dimer (Figure 13). In contrast to the free base heptaphyrins **67-H₄** and their cations, whose Möbius conformers are dynamic in solution, the mononuclear palladium(II) complex **68c** (Figure 13) is locked by metal coordination, as evidenced by the sharp ^1H NMR spectrum observed at room temperature. In **68c**, the Pd^{II} center is bound to three nitrogens and one β -pyrrolic carbon and this particular binding mode is responsible for stabilizing the twist necessary for a Möbius structure. A related complex, **67c-H₂Zn**, contains a Zn^{II} ion coordinated by four pyrrolic nitrogens and stabilizes a $T2_0$ conformation (Figure 13).^[154]

Heptaphyrins(1.1.1.1.1.1.1) display some interesting reactivity traits, exemplified earlier by the extrusion of a subporphyrin from the copper(II) complex **67c-H₂Cu** (Section 4). *meso*-Pentafluorophenyl substituents in **67c-H₄** undergo a sequence of intramolecular nucleophilic fluoride displacements (known as “fusions”) to yield a singly, doubly, and quadruply fused product (**69c-H₃**, **70c-H₂**, **71c-H₂**, respectively, Scheme 22).^[251] The first two fusion steps occur with retention of the original [32]annulenoid structure. In contrast, the formation of the ultimate product **71c-H₂** involves formal reduction of the macrocycle to a 34-electron CP. However, **71c-H₂** was characterized as nonaromatic on the basis of its ^1H NMR spectrum. The nonfused tripyrrolic section of the macrocycle in **71c-H₂** acts as a sterically hindered tripyrroline-like ligand capable of binding small cations, such as boron(III).^[251] Remarkably, a copper(II) complex **71c-Cu** has been

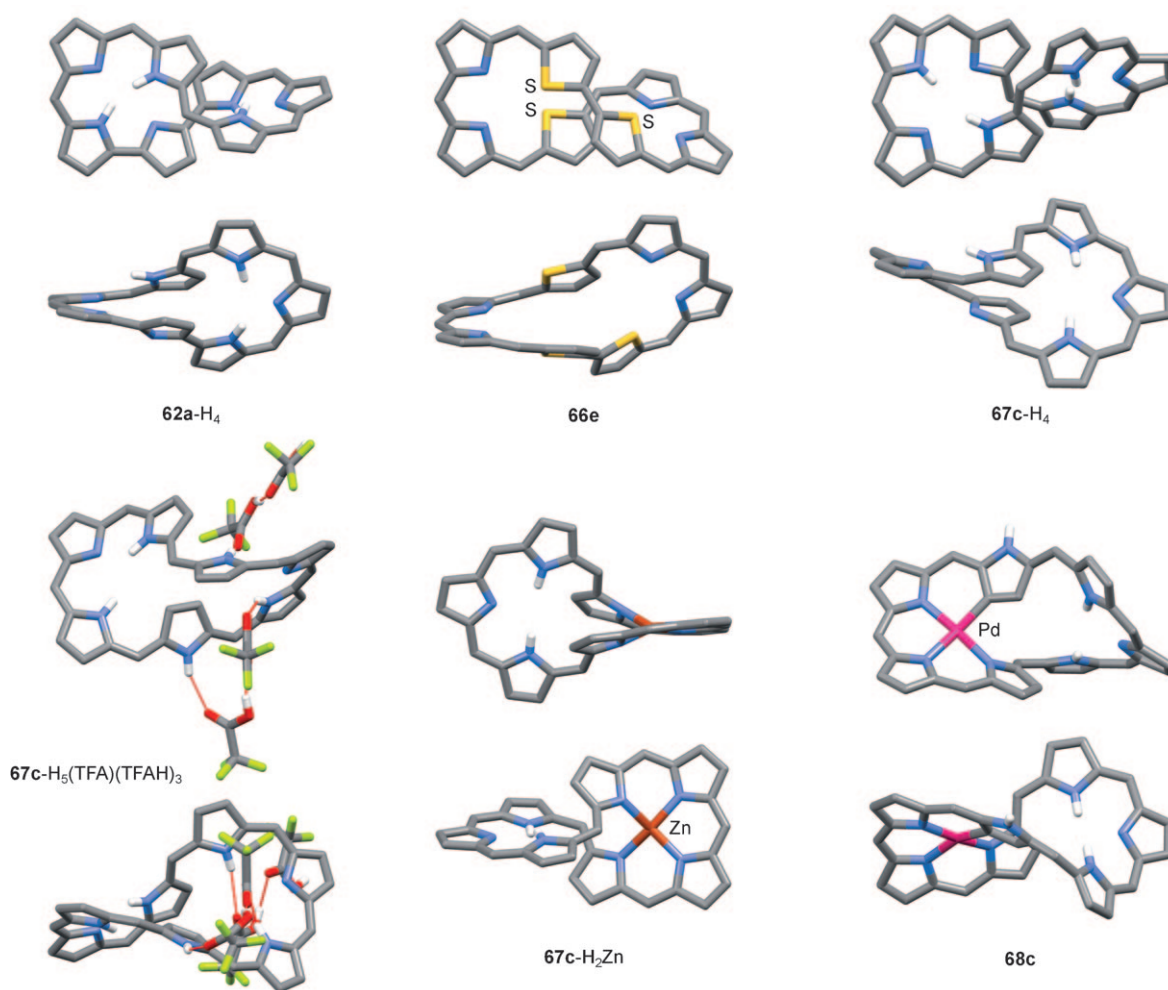


Figure 13. Three-dimensional structures of selected heptaphyrins. Coordinates have been taken from published X-ray structural data. Solvent molecules and peripheral substituents are removed for clarity.

reported recently, which stabilizes a unique T-shaped coordination geometry of the copper(II) center.^[252,253]

8. Octaphyrins

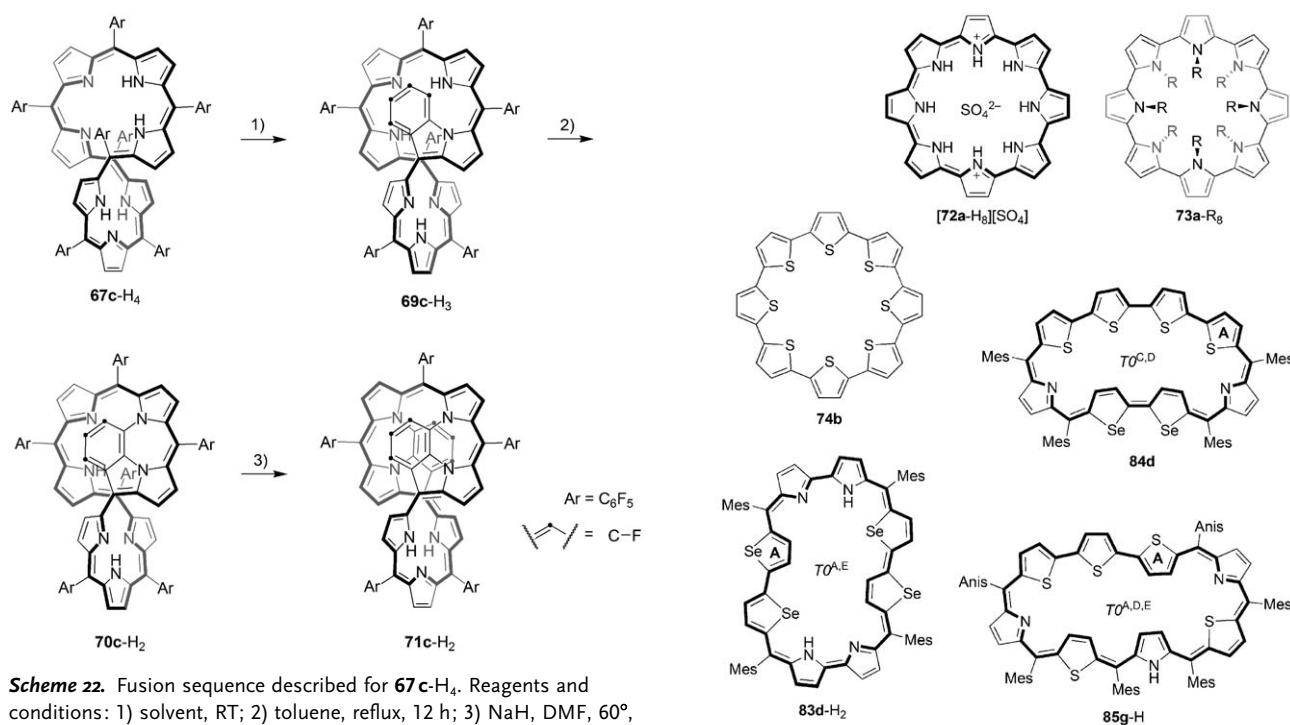
8.1. T0 Systems

Octaphyrins, the first examples of which were reported in the 1990s, are a structurally diverse class of expanded porphyrinoids (Table 9). Octaphyrin macrocycles can be conveniently classified as planar systems, in which the *T0* conformation predominates and is usually achieved with multiple subunit inversions, and figure-eight systems, which typically take *T2* and *T1* conformations. Among all-pyrrole octaphyrins, only cyclo[8]pyrrole (**72a**-H₆, Table 9) adopts a convex *T0* structure.^[39] Normally isolated and studied in the form of its sulfate salt, [**72a**-H₈][SO₄] (Scheme 23), cyclo[8]pyrrole is the most important member of the cyclopyrrole family, with emerging applications in molecular electronics,^[258] liquid crystal design,^[259] explosives detection,^[259] and anion extraction.^[260] Cyclo[8]pyrrole is a [30]annulenoid

Table 9: Octaphyrin ring systems discussed in the text.

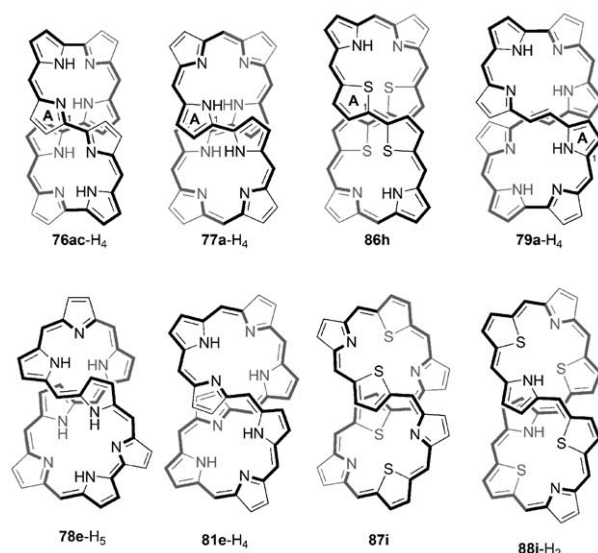
Entry ^[a]	Structure ^[b]	S	τ_F ^[c]	Ref.
72a -H ₆	[30]{N.N.N.N.N.N.N.N}(0.0.0.0.0.0.0.0)	24	1.06	[39]
73a -H ₈	[32]{N.N.N.N.N.N.N.N}(0.0.0.0.0.0.0.0)	24	1.06	[254]
74b	[32]{S.S.S.S.S.S.S.S}(0.0.0.0.0.0.0.0)	24	0.70	[255]
75a -H ₆	[32]{N.N.N.N.N.N.N.N}(1.0.0.0.1.0.0.0)	26	1.39	[58]
76ac -H ₄	[32]{N.N.N.N.N.N.N.N}(1.0.1.0.1.0.1.0)	28	1.72	[41]
77a -H ₄	[34]{N.N.N.N.N.N.N.N}(1.1.1.0.1.1.1.0)	30	2.06	[47]
78e -H ₅	[36]{N.N.N.N.N.N.N.N.N.N}(1.1.1.1.1.1.1.0)	31	2.22	[51]
79a -H ₄	[36]{N.N.N.N.N.N.N.N.N.N}(2.1.0.1.2.1.0.1)	32	2.39	[47]
80e -H ₂	[34]{N.N.N.N.N.N.N.N.N.N}(1.1.1.1.1.1.1.1)	32	2.39	[100]
81ef -H ₄	[36]{N.N.N.N.N.N.N.N.N.N}(1.1.1.1.1.1.1.1)	32	2.39	[100]
82ef -H ₆	[38]{N.N.N.N.N.N.N.N.N.N}(1.1.1.1.1.1.1.1)	32	2.39	[100]
83d -H ₂	[34]{Se.N.N.Se.Se.N.N.Se}(1.0.1.0.1.0.1.0)	28	1.48	[256]
84d	[34]{S.N.Se.Se.N.S.S.S}(1.1.0.1.1.0.0.0)	28	1.42	[61]
85g -H	[36]{S.N.S.N.S.N.S.N.S.N}(1.1.1.1.1.1.0.0)	30	1.83	[54]
86h	[34]{S.N.S.N.S.N.S.N.S.N}(1.1.1.0.1.1.1.0)	30	1.88	[257]
87i	[36]{S.N.S.N.S.N.S.N.S.N}(1.1.1.1.1.1.1.1)	32	2.21	[126]
88i -H ₂	[38]{S.N.S.N.S.N.S.N.S.N}(1.1.1.1.1.1.1.1)	32	2.21	[126]

[a] Representative substitution patterns: **a** β -alkyl; **b** partial β -alkyl; **c** β -alkyl-*meso*-Ar; **d** *meso*-Mes; **e** *meso*-C₆F₅; **f** *meso*-(C₆F₅)- β -F; **g** *meso*-(Mes)_m(*p*-C₆H₄OMe)_n; **h** *meso*-C₆F₅-*meso*-(2,6-C₆H₃Me₂); **i** *meso*-Tol. [b] For explanations, see footnote [b] of Table 5. [c] Free curvature without inversions (Section 2.1).



aromatic system, as evidenced by the diatropic ring current observed in the ^1H NMR spectrum. The electronic absorption profile of $[\mathbf{72a-H}_8][\text{SO}_4]$ is very characteristic, with a uniquely intense absorption at ca. 1100 nm ($\epsilon \approx 130\,000 \text{ mol}^{-1} \text{ cm}^{-1}$).^[39] Remarkably, when $[\mathbf{72a-H}_8][\text{SO}_4]$ is subjected to a reductive alkylation reaction it yields products of the general structure **73a-R₈** (R = Me, Et, Bn), which show no significant absorption above 325 nm.^[254] **73a-R₈** is formally a [32]annulene system but it largely behaves as a cyclic oligopyrrole with insignificant macrocyclic conjugation. In the solid state, **73a-Me₈** adopts an alternant “four up, four down” conformation with the N-alkyl groups located on both sides of the macrocycle (Figure 14). Interestingly, cyclo[8]thiophene **74b**, which may be viewed as an all-thia analogue of **73-R₈**, is a red-colored compound.^[255] The macrocycle of **74b**, which is most likely very strained ($\tau_F = 0.70$), is the smallest reported member of the cyclo[*n*]thiophene family discussed in Section 9.3.

A number of *meso*-substituted heterooctaphyrins have been reported that stabilize diverse *T₀* structures. The corresponding conformations are close to planarity and contain two or more inverted subunits (Scheme 23). Tetraheterooctaphyrins(1.0.1.0.1.0.1.0) containing four furan, thiophene, or selenophene rings (**83d-H₂** for X = Se) adopt similar *T₀^{A,E}* conformations, in which two nonpyrrolic subunits located across the macrocycle are consistently inverted.^[256] In another system, containing biselenophene and quaterthiophene subunits (**84d**), the two selenophene rings are inverted (*T₀^{C,D}* conformer).^[61] Compounds **83d-H₂** and **84d** contain [34]annulene CP's and are both aromatic. In contrast, a larger system, pentathiaoctaphyrin **85g-H** is a 36-electron antiaromatic system. It was characterized in the solid state in the form of a *T₀^{A,D,E}* conformer.^[54]



Scheme 23. Structures of selected octaphyrins. The choice of tautomers is arbitrary. In some systems, substituents have been omitted for clarity.

8.2. T₁ and T₂ Systems

The majority of porphyrinoid macrocycles adopting figure-eight conformations (*T₀* or *T₁*) are characterized by $\tau_F > 1.7$. An interesting exception is provided by octaphyrin(1.0.0.0.1.0.0.0) (**75a-H₆**, $\tau_F = 1.39$)^[58] and its diboron complex **75a-H₄**(BF₂)₂.^[217] The X-ray structure of a dichloride salt, $[\mathbf{75a-H}_8]\text{Cl}_2 \cdot 2\text{MeOH}$, revealed a distorted conformation that is formally Möbius-like (Figure 14).^[58] However, because one of the torsions along the SMC is 83° the Π parameter is only -0.03 , indicating that macrocyclic π -electron conjugation

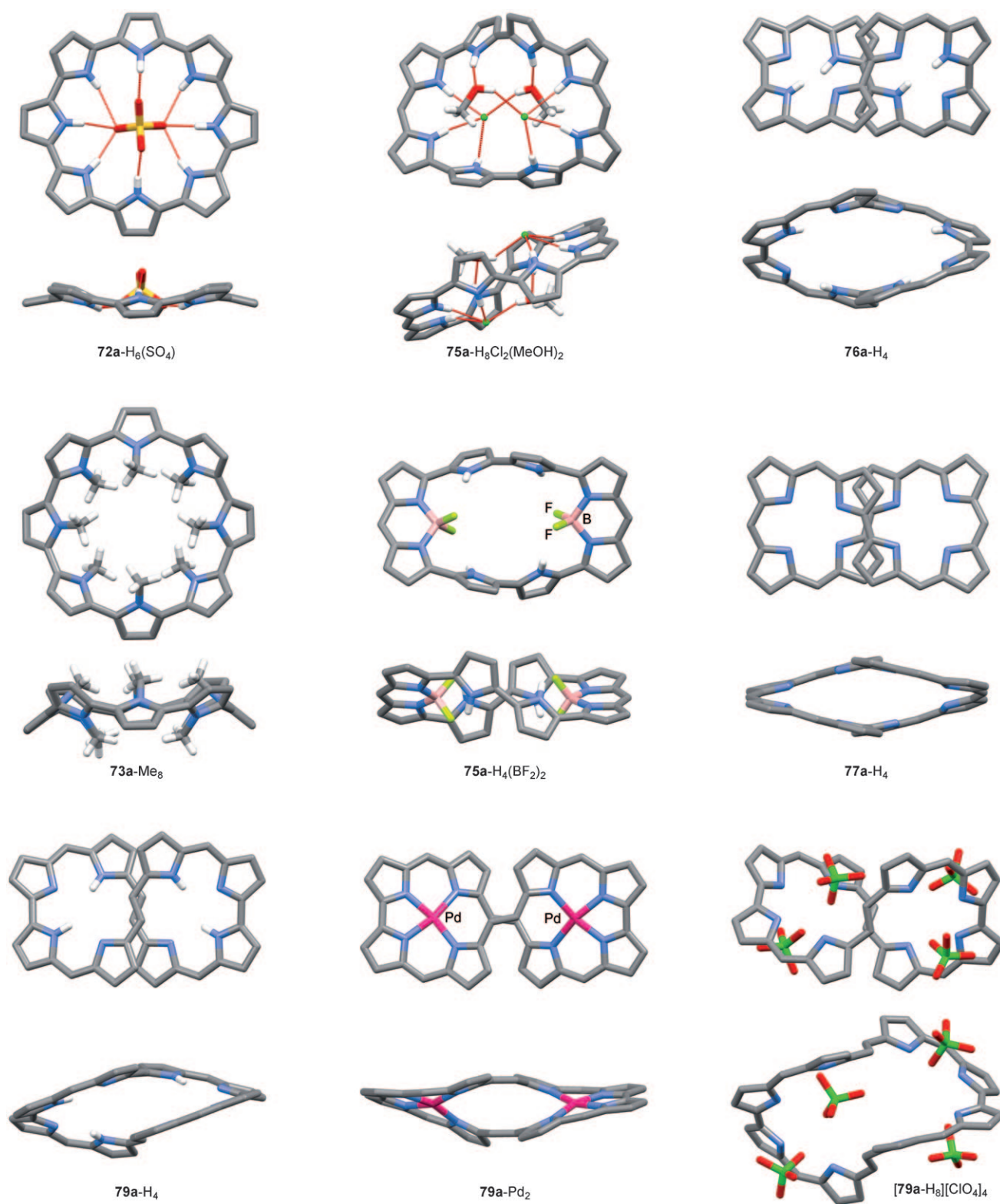


Figure 14. Three-dimensional structures of selected octaphyrins. Coordinates have been taken from X-ray structural data. In most cases, solvent molecules and peripheral substituents are removed for clarity. NH hydrogens are not shown in the structures of **77a**-H₄ and **[79a-H₈][ClO₄]**.

tion will be inefficient in **[75a-H₈]²⁺**, and indeed, the solution ¹H NMR spectra showed no signs of diatropic character. Interestingly, in the diboron complex **75a**-H₄(BF₂)₂, the conformation of the macrocycle, though fairly similar to

that observed in the dichloride salt, can be classified as *T*_{2o}, with a small value of *Π* = 0.09 (Figure 14). Even though π -conjugation along the SMC is insignificant in **[75a-H₈]²⁺** and **75a**-H₄(BF₂)₂, the octaphyrin(1.0.0.0.1.0.0.0) ring is of interest

because it constitutes a borderline case of a system that can switch between formal $T1$ and $T2$ topologies with minimal structural changes.

The figure-eight $T2_0$ structure is the trademark conformation of all-aza octaphyrin ring systems containing at least four meso carbons ($\tau_F > 1.7$) and their mono- and dinuclear metal complexes. The meso patterns reported to date include (1.0.1.0.1.0.1.0) in **76-H₄**,^[41, 42, 261–263] (1.1.1.0.1.1.1.0) in **77-H₄**,^[47] (1.1.1.1.1.1.1.0) in **78-H₅**,^[51] (2.1.0.1.2.1.0.1) in **79-H₄**,^[47, 93] and (1.1.1.1.1.1.1.1) in **81-H₄** and **82-H₆** (Scheme 23).^[67, 100, 103, 238, 264, 265] Figure-eight conformers have also been reported for certain heteroanalogues of the above systems (**86**, **87**, and **88-H₂**).^[126, 257] Representative examples of all-pyrrole structures are shown in Figure 14. Even though the $T2_0$ conformers look similar, they differ in some structural details. Depending on the constitution of the macrocycle, the subunits located at the intersection of the lemniscate can be different. In octaphyrin(2.1.0.1.2.1.0.1) **79a-H₄**, the intersection is occupied by the C=C meso bridges^[47] and the configuration of these bridges relative to the adjoining pyrrole rings is altered by metal coordination (**79a-Pd₂**, Figure 14).^[93] In other systems containing bipyrrrole or bithiophene subunits, namely **76-H₄**, **77-H₄**, and **86h**, the bonds that meet at the intersection are the direct links between cyclic subunits. Another parameter that varies between the different $T2_0$ conformers is the “intersection pitch”, that is, the vertical distance between the crossing parts of the macrocycle. This distance is fairly large in **76a-H₄** (4.6 Å), possibly because the free curvature of the macrocycle is insufficient for a fully relaxed $T2_0$ conformer. In larger macrocycles, the intersection pitch approaches the π -aromatic stacking distance (3.3 Å in **77a-H₄**, 3.5 Å in **79a-H₄**, and 3.6 Å in **86h**). The Π parameter also varies with the free curvature of the ring: it is 0.47 in **76a-H₄**, 0.72 in **77a-H₄**, 0.63 in **79a-H₄**, and 0.73 in **86h**. It therefore seems that the (1.1.1.0.1.1.1.0) ring system (**77-H₄**) provides for the relatively least strained $T2_0$ conformer. Interestingly, the corresponding τ_F value (2.06) nicely approximates that of a perfect lemniscate (Section 2.1). It should be noted, however, that the geometric parameters of the figure-eight structures are affected not only by ring curvature but also by peripheral substitution and metal coordination.

The $T2_0$ conformation can be viewed as a union of two helical fragments of identical handedness and is therefore chiral (depending on the structure, the corresponding point symmetry can be D_2 , C_2 , or C_1). Variable-temperature ^1H NMR spectra recorded in [D_8]toluene between 173 K and 373 K showed that **76a-H₄** undergoes rapid inversion.^[41] On the basis of subsequent work, the inversion was proposed to occur with the intermediacy of a tub-shaped D_{2d} -symmetric transition state (Figure 15).^[266] This mechanism is unusual because inversion is achieved by exchanging positions that are chemically inequivalent in the stationary D_2 conformer. Characteristically, because the exchange occurs without planarization, such an inversion process does not lead to dynamic averaging of the diastereotopic CH_2 signals of the ethyl substituents. In contrast to **76a-H₄**, compounds **77a-H₄** and **79a-H₄**, in which the symmetry of the macrocyclic framework is lower, are configurationally stable in solution.^[47]

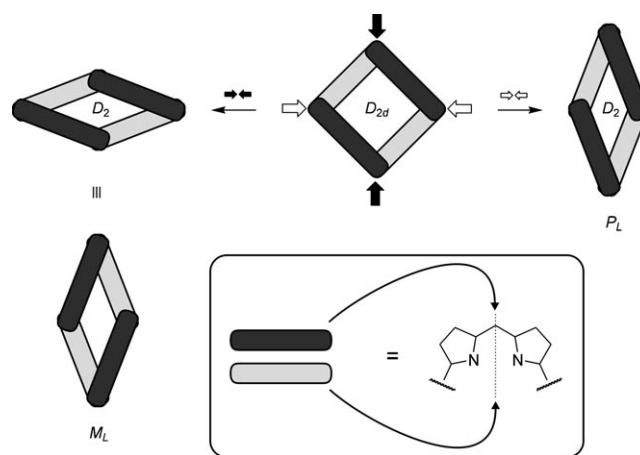
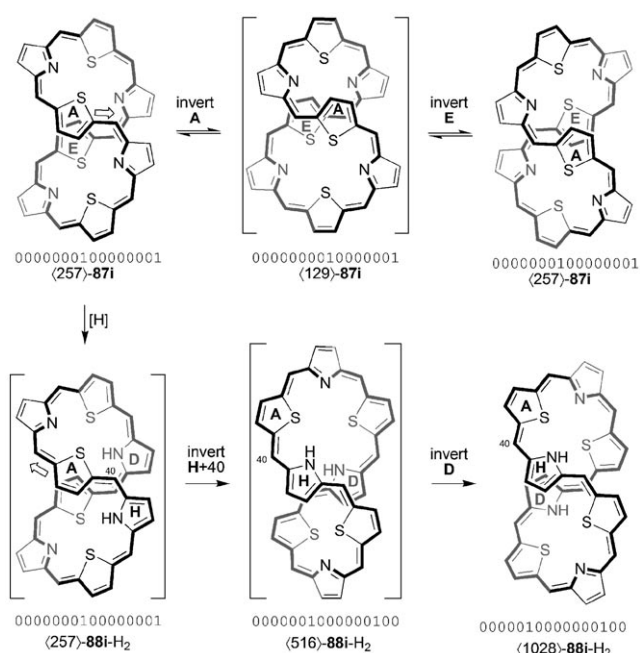


Figure 15. Inversion mechanism proposed for **76a-H₄**.^[266] The four dipyrrole subunits are viewed along the dotted line. NH protons are assumed to tautomerize rapidly.

In fact, **79a-H₄** was separated into enantiomers, which showed no significant tendency to racemize.^[93] In these systems, the inversion would require actual untwisting of the figure-eight structure, and such a process may be expected to have a higher activation barrier than that operating for **76a-H₄**.

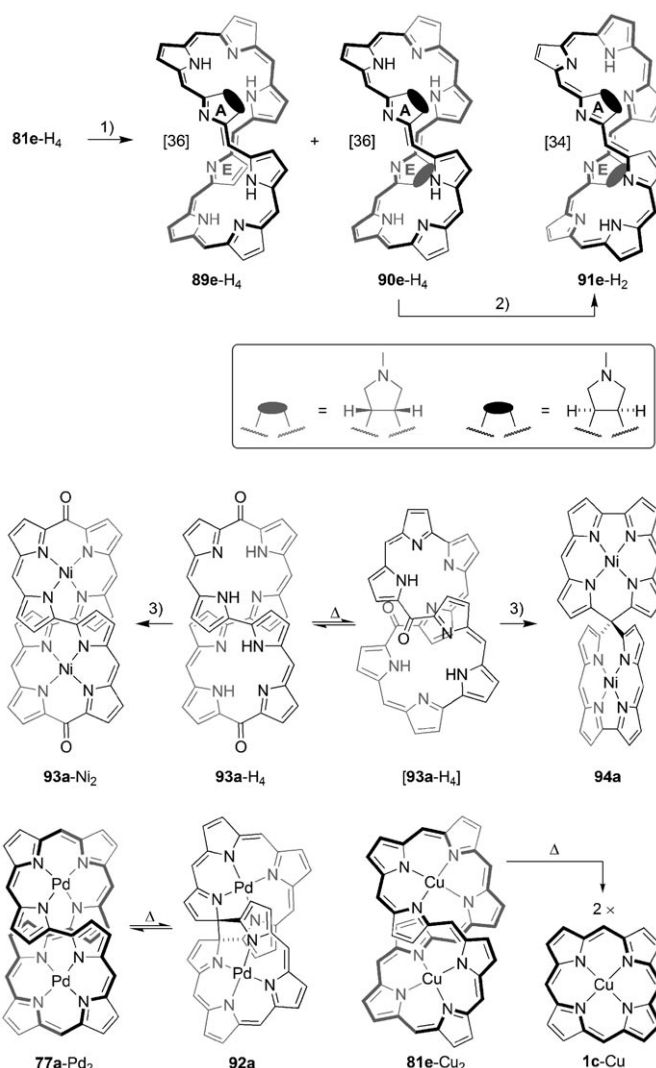
$T2_0$ conformers have also been found in numerous meso-substituted systems. All-aza octaphyrin(1.1.1.1.1.1.1.1) stabilizes three oxidation levels: **80e-H₂** ($N=34$), **81e-H₄** ($N=36$, principal), and **82e-H₆** ($N=38$).^[100] Of these three species, only **81e-H₄** was characterized crystallographically, revealing a figure-eight conformation. Such a structure can also be inferred from solution ^1H NMR spectra, which indicate that the conformer is not fluxional.^[100] An unsymmetrical $T2_0$ conformer was also identified in a related system containing one direct meso linkage, **78e-H₅**.^[51] Also in this case, the room-temperature ^1H NMR spectrum is consistent with a rigid solution structure. In contrast, thiophene-containing octaphyrins are conformationally fluxional, as evidenced by the behavior of tetrathiaoctaphyrins **86h**,^[257] **87i** and **88i-H₂**.^[126] While the solution behavior of **86h** was not conclusively explained, the structure and conformational dynamics of the latter two macrocycles were investigated in considerable detail (Scheme 24). **87i** and **88i-H₂** constitute two oxidation levels of the same ring system, 41,43,45,47-tetrathiaoctaphyrin(1.1.1.1.1.1.1.1), corresponding respectively to 36- and 38-electron CP's. Accordingly, **87i** was shown to sustain a weak paratropic ring current whereas **88i-H₂** displayed residual diatropicity. Compound **87i**, characterized structurally in solution using 2D NMR spectroscopy, was shown to adopt a $T2_0$ conformation with thiophene rings located at the intersection. The conformation is not rigid, leading to severe dynamic broadening of the ^1H NMR spectrum at room temperature. The exchange pattern observed by NOESY at low temperature showed only partial averaging of the constitutionally equivalent positions in the macrocycle. Two dynamic processes were considered, both consistent with the observed exchange. The first of them involved helix inversion, whereas in the other process the exchange was assumed to retain the helicity of the conformer.



Scheme 24. Conformational dynamics of tetrathiaoctaphyrins **87i** and **88i-H₂**. Conformations are labeled according to convention given in Section 2.4. Meso substituents are omitted for clarity. Solid arrows indicate the direction of the “conveyor belt” movement.

The latter mechanism relied on sequential inversions of thiophene rings located at the intersection combined with a conveyor-belt movement of the macrocyclic chain (Scheme 24). Such a process was considered more likely given the high rate of observed exchange.^[126] Unusually, the reduction of **87i** to **88i-H₂** leads to a different T_{20} conformation, in which the crossing of the figure-eight structure is occupied by pyrrole rings. This conformational transformation was proposed to proceed in a similar fashion to that assumed for the self-exchange of **87i** (Scheme 24). The conformation of **88i-H₂** is also fluxional, as can be judged by the line broadening observed at room temperature, however, details of this exchange process have not been elucidated.

[36]Octaphyrin(1.1.1.1.1.1.1.1), **81e-H₄**, undergoes 1,3-dipolar cycloaddition with azomethine ylide to yield pyrrolidine-fused products **89e-H₄** and **90e-H₄** (Scheme 25).^[265] The latter species was oxidized with MnO₂ to give its 34-electron counterpart, **91e-H₂**. All three systems were characterized crystallographically and found to adopt a T_{20} conformation that is distinct from the parent structure **81e-H₄**. The difference stems from a larger number of transoid inter-subunit linkages present in **89e-H₄**, **90e-H₄**, and **91e-H₂**. All figure-eight conformations shown in Scheme 23 contain two transoid links which divide the SMC into two sections of equal length (in the unsymmetrical conformer **78e-H₅**, the two sections are not equivalent). In the pyrrolidine-fused octaphyrins, however, the usual figure-eight structure is not feasible sterically. To reduce unfavorable interactions with the flanking *meso*-aryl groups the fused pyrrole rings (A and E) are “inverted” relative to their positions in **81e-H₄**. Such an arrangement results in six transoid links being present in the structure of **90e-H₄**. Using the descriptor proposed in Section 2.4, these



Scheme 25. Reactivity of selected octaphyrins. Reagents and conditions: 1) paraformaldehyde, sarcosine, toluene, reflux; 2) MnO₂; 3) Ni(OAc)₂, DMF, Δ. Peripheral substituents are omitted for clarity.

two T_{20} conformers can be differentiated as ⟨257⟩ and ⟨33667⟩, respectively.

Figure-eight octaphyrins can be envisaged as formal dimers of corresponding tetraphyrin macrocycles, such as porphyrin (**81-H₄**), 21,23-dithiaporphyrin (**87**), corrrhycene (**79-H₄**), corrole (**77-H₄**), or norcorrole (**76-H₄**), an analogy with two practical consequences. First, the formation of octaphyrin macrocycles is often a competing reaction in the syntheses of their tetraphyrin counterparts, in some cases becoming the dominant macrocyclization route.^[47,100,126] Second, metal coordination in some octaphyrins is capable of inducing peculiar reactivity,^[267] which apparently results from the increased steric compression at the figure-eight crossing. For instance, the dinuclear complex **77a-Pd₂** undergoes an electrocyclic rearrangement to a bicyclic derivative **92a**.^[268] **77a-Pd₂** and **92a** are at equilibrium which can be controlled thermally and photochemically (Scheme 25). The nonaromatic compound **93a-H₄**, which is a dioxo derivative of **77a-H₄**, yields dinickel(II) spirodicorrole **94a** as one of the

metallation products.^[268] The formation of spirodicorrole presumably involves a conformational change that places the carbonyl groups in the vicinity of the figure-eight crossing (Scheme 25). The other isolated metalation product is the orthodox dinuclear complex **93a**-Ni₂, which could not be converted into the spirodicorrole species. Compound **94a** exhibits features in its electronic spectrum that could be ascribed to spiroconjugation.^[269] Dicopper(II) complex of octaphyrin(1.1.1.1.1.1.1.1), **81e**-(Cu^{II})₂, is thermally cleaved into two copper(II) porphyrin molecules in an apparently electrocyclic process.^[67] The outcome of this particular reaction has limited synthetic utility, but the possibility of obtaining boron(III) subporphyrin from heptaphyrin(1.1.1.1.1.1.1) in an analogous splitting process might be envisaged as a practicable preparative procedure in some cases (Section 4). The efficiency of the splitting reaction depends on the coordinated metal, disilver(I) and dizinc(II) complexes being completely unreactive.^[264,270]

Even though the *T*₂ structure is the preferred conformation for the majority of high- τ_F octaphyrins, some systems were shown to stabilize *T*₁ and *T*₀ conformations (Table 10).

Table 10: Conformers of octaphyrin(1.1.1.1.1.1.1.1).

Species	Conformer	Binary ^[a]	Decimal ^[a]	τ_F
81e -H ₄	<i>T</i> ₂	0000000100000001	(257)	0.00
95e	<i>T</i> ₂	0000011100000111	(1799)	0.00
90e -H ₄	<i>T</i> ₂	1000001110000011	(33667)	0.00
		0000011100000111 ^[b]	(1799) ^[b]	
96e	<i>T</i> ₁	0000011110000111	(1927)	n/a
[81e -H ₆] ²⁺	<i>T</i> ₁	0110010110011110	(26014)	n/a
81f -H ₄	<i>T</i> ₀ ^{5,10,25,30}	0000111100001111	(3885)	1.06
82e -H ₆	<i>T</i> ₀ ^{A,E,5,40}	0000100100000110	(2310)	1.19
82f -H ₆	<i>T</i> ₀ ^{A,E,5,25,40}	0000000100001001	(265)	0.93
[82e -H ₈] ²⁺	<i>T</i> ₀ ^{A,B,D,E,G}	0110011110011110	(26526)	1.07

[a] For explanation see Section 2.4. [b] Minimum value obtained by moving ring A to a nonfused position.

Unusual conformers were observed in the solid state for *meso*- β -perfluorinated octaphyrins **81f**-H₄ and **82f**-H₆ (Figure 16).^[238] These structures are highly nonplanar and, when projected perpendicular to the averaged plane of cyclic subunits, show numerous intersections. However, both conformations are in fact untwisted (i.e. their linking number *Lk* = 0) and can be described as *T*₀^{5,10,25,30} and *T*₀^{A,E,5,40}, respectively. The latter structure may be viewed as a highly distorted pseudoplectoneme with two crossings (cf. Section 2.3). A related conformation, *T*₀^{A,E,5,40} was also proposed for the *meso*-C₆F₅-substituted derivative **82e**-H₆ on the basis of ¹H NMR spectroscopy.^[134] Protonation of the latter macrocycle with TFAH yields a dication [**82e**-H₈]²⁺, which was characterized in the solid state (Figure 16).^[134] The unusual conformation, containing five inverted pyrrole rings, is stabilized in the solid state by an extensive network of hydrogen bonds between the NH protons of the macrocycle, counteranions and solvating molecules of acid, alcohol and water. The structure is apparently fluxional in solution but it

was nevertheless characterized as aromatic. Importantly, [36]octaphyrin forms a similar dication [**81e**-H₆]²⁺, in which two pyrrolic nitrogens remain unprotonated. The solid state conformation of [**81e**-H₆]²⁺, although similar to that of [**82e**-H₈]²⁺, actually has the Möbius *T*₁ topology, which provides aromatic stabilization for a 4*n*-electron system. The aromatic nature of this species was conformed by low-temperature ¹H NMR experiments.^[134]

Significant structural diversity can also be induced in octaphyrins(1.1.1.1.1.1.1.1) by metal coordination. **81e**-H₄ forms a dinuclear complex **81e**-(Cu^{II})₂, in which the conformation of the free base is largely retained (Figure 16).^[67] It is apparent from the solid state structure of **81e**-(Cu^{II})₂ that the geometry of the macrocycle is not optimal for square-planar coordination of two metal centers. Consequently, the coordination environment of Cu^{II} is significantly distorted from planarity. In addition, metal binding results in significant compression of the nonbonding distances at the figure-eight crossing, compared to the structure of the free base **81e**-H₄. The distortion of the macrocycle results in significant lowering of the Π parameter (from 0.64 in **81e**-H₄ to 0.06 in **81e**-(Cu^{II})₂). In a disilver analogue of **81e**-(Cu^{II})₂, the metal centers were assigned the +1 oxidation state, whereas the macrocycle was assumed to be oxidized to the level of a [34]annulene.^[264] Interestingly, upon metallation with palladium(II) acetate, **81e**-H₄ yields two dinuclear complexes **95e** and **96e** (Figure 16), none of which is structurally analogous to **81e**-(Cu^{II})₂^[103] (an additional product with broken macrocyclic conjugation was subsequently reported^[270]). In **95e**, each palladium(II) ion, is bound to three pyrrolic nitrogens and one β -carbon. That latter feature requires the corresponding pyrrole rings to be inverted relative to their original orientation in **81e**-H₄. This inversion leads to a different type of *T*₂ conformer characterized by fairly smooth π -conjugated surface (Π = 0.50). Interestingly, the conformation of **95e** is analogous to that observed in the pyrrolidine fused octaphyrin **90e**-H₄ (see above). In the other complex, **96e**, each of the Pd^{II} ions resides in a different coordinating environment. One of the coordinating pockets resembles those present in **95e**, whereas in the other one, the metal forms two M–N and two M–C bonds. Such a binding mode induces the inversion of an additional pyrrole subunit leading to a conformation with *T*₁ topology, and fairly efficient π overlap (Π = –0.49).

9. Giant Porphyrinoids

The final section of this Review deals with porphyrinoids containing more than eight cyclic subunits (Table 11, Scheme 26). Structural diversity among these expanded systems is extraordinary, even though the development of the field has apparently depended more on serendipitous discoveries than on targeted syntheses. Nevertheless, three families of expanded homologues were developed in recent years on the basis of the structural themes of porphyrin, rosarin, and rubyrin. Most of the knowledge about the conformations of giant porphyrinoids has been gathered from crystallographic analyses, and the difficulty of growing X-ray

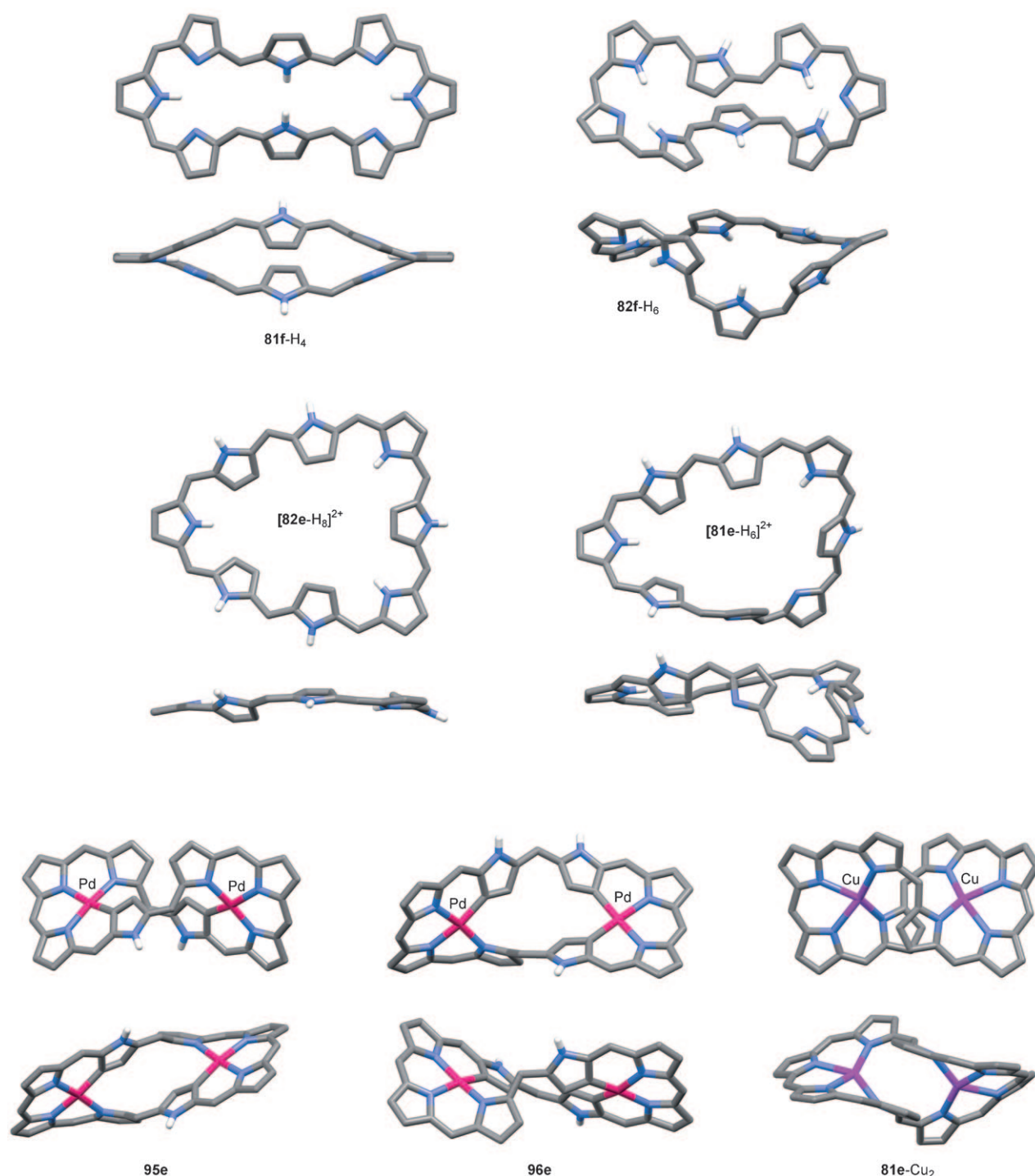


Figure 16. Three-dimensional structures of selected octaphyrins(1.1.1.1.1.1.1.1). Coordinates have been taken from X-ray structural data. Solvent molecules, counteranions, and peripheral substituents are removed for clarity.

quality crystals may be one of the factors limiting the development of the area. In most instances, ^1H NMR spectroscopy reveals some degree of conformational flexibility but frequently sharp low-symmetry spectra are obtained even at room temperature. These latter instances likely correspond to well-defined solution structures, amenable to detailed NMR structural analysis. Such analyses are rarely

attempted and, consequently, the correspondence between the solution conformation and the solid-state structure (if available) is usually unknown. Lack of definitive signal assignments also precludes reliable discussion of the aromaticity of giant porphyrinoids. It is however evident that π -conjugation in these uniquely large macrocycles is weaker than in many of their smaller congeners.

Table 11: Giant porphyrinoids discussed in the text.

Entry ^[a]	Structure ^[b]	S	$\tau_F^{[c]}$	Conformer ^[d]	$I\pi^{[e]}$	Ref.
turcasarins						
97a -H ₆	[40]{N ₁₀ } (1.0.1.0.0.1.0.1.0.0)	34	1.99	T ₂₀	$\langle 129 \rangle$	0.54 [23]
98a -H ₄	[40]{N.N.N.N.O.N.N.N.N.O} (1.0.1.0.0.1.0.1.0.0)	34	2.03	T ₂₀	$\langle 129 \rangle$	0.84 [271]
porphyrin class						
99b -H ₄	[40]{N ₉ } (1 ₉)	36	2.69	T ₂₀	$\langle 1121 \rangle$	0.61 [272]
100b -H ₆	[42]{N ₉ } (1 ₉)	36	2.69	T ₀ ^{A,B,F,5,25,30}	$\langle 4617 \rangle$	0.59 [272]
[100b -H ₇] ⁺	[42]{N ₉ } (1 ₉)	36	2.69	T ₀ ^{A,B,F,5,25,30}	$\langle 4617 \rangle$	0.56 [100]
101b -H ₄	[44]{N ₁₀ } (1 ₁₀)	40	2.99	T ₂₀	$\langle 71750 \rangle$	0.58 [273]
102c -H ₆	[46]{N ₁₀ } (1 ₁₀)	40	2.99	T ₂₀	$\langle 19475 \rangle$	0.56 [211]
103b -H ₆	[50]{N ₁₁ } (1 ₁₁)	44	3.28			[100]
104b -H ₄	[52]{N ₁₂ } (1 ₁₂)	48	3.58			[273]
105b -H ₆	[54]{N ₁₂ } (1 ₁₂)	48	3.58			[100]
106c -H ₈	[56]{N ₁₂ } (1 ₁₂)	48	3.58	T ₄₁	$\langle 2829 \rangle$	0.37 [211]
107b -H ₆	[62]{N ₁₄ } (1 ₁₄)	56	4.18			[273]
108b -H ₈	[72]{N ₁₆ } (1 ₁₆)	64	4.78			[273]
109b -H ₈	[80]{N ₁₈ } (1 ₁₈)	72	5.37			[273]
ruberin class						
110b -H ₅	[38]{N ₉ } ([1.1.0] ₃)	33	2.19	T ₂₀	$\langle 4112 \rangle$	0.75 [44]
111b -H ₈	[52]{N ₁₂ } ([1.1.0] ₄)	44	2.92	T ₀ ^{B,H,5,10,32,37}	$\langle 18450 \rangle$	0.62 [45]
112b -H ₇	[62]{N ₁₅ } ([1.1.0] ₅)	55	3.65	T ₂₂	$\langle 9234 \rangle$	0.56 [45]
rosarin class						
113d -H ₆	[48]{N ₁₂ } ([1.0] ₆)	42	2.58	T ₀ ^{A,B,G,H,5,32}	$\langle 4617 \rangle$	0.19 [42]
114d -H ₈	[64]{N ₁₆ } ([1.0] ₈)	56	3.44	T ₂₀	$\langle 299081 \rangle$	0.001 [42, 274]
115d -H ₁₀	[80]{N ₂₀ } ([1.0] ₁₀)	70	4.30			[274]
116d -H ₁₂	[96]{N ₂₄ } ([1.0] ₁₂)	84	5.17			[274]
cyclothiophenes						
117a	[40]{S ₁₀ } (0 ₁₀)	30	0.87			[275]
118a	[48]{S ₁₂ } (0 ₁₂)	36	1.05			[276]
119a	[60]{S ₁₅ } (0 ₁₅)	45	1.31			[275]
120a	[64]{S ₁₆ } (0 ₁₆)	48	1.40			[276]
121a	[72]{S ₁₈ } (0 ₁₈)	54	1.57			[276]
122a	[80]{S ₂₀ } (0 ₂₀)	60	1.75			[275]
123a	[100]{S ₂₅ } (0 ₂₅)	75	2.18			[275]
124a	[120]{S ₃₀ } (0 ₃₀)	90	2.62			[275]
125a	[140]{S ₃₅ } (0 ₃₅)	105	3.06			[275]
126a	[160]{S ₄₀ } (0 ₄₀)	120	3.49			[275]
127e -H ₂	[54]{S.N.S.N.S.S.S.N.S.N.S} (1.1.1.1.0.0.1.1.1.0.0)	44	2.56			[225]
128df -H ₃	[36]{[N.N.CC] ³ } ([1.0.0] ³)	33	1.29	T ₀	$\langle 0 \rangle$	[277]
129df -H ₄	[48]{[N.N.CC] ⁴ } ([1.0.0] ⁴)	44	1.72	T ₂₀	$\langle 129 \rangle$	[277]

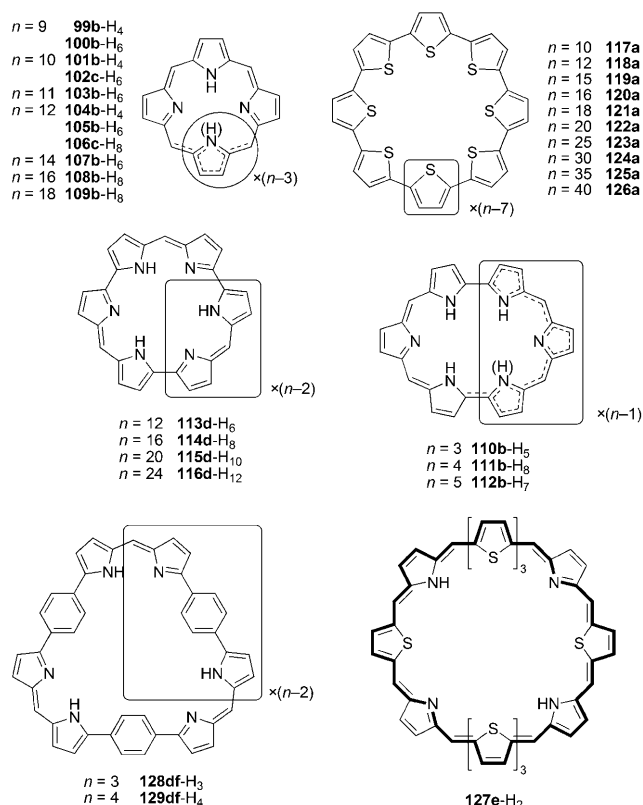
[a] Representative substitution patterns: **a** partial β -alkyl; **b** *meso*-C₆F₅; **c** *meso*-CF₃; **d** β -alkyl-*meso*-Ar; **e** *meso*-Mes-*meso*-Anis; **f** *meso*-Ph-phenylene-(OMe)₂.^[278] [b] For explanations, see footnote [b] of Table 5. [c] Free curvature without inversions (Section 2.1). [d] For explanation of conformational descriptors see Section 2.4. [e] Torsional π -conjugation index calculated for available X-ray structures (Section 3.4).

9.1. Porphyrin Homologues

The majority of compounds in the porphyrin class are accessible through direct pyrrole–aldehyde condensations. Even though this approach is truly general only in the case of tetrapyrrole systems, its scope can be extended under certain conditions to furnish larger macrocycles up to dodecaphyrin.^[100,211] Larger even-membered systems (up to octadecaphyrin) can be synthesized from dipyrromethanes under appropriate conditions.^[273] Another route, involving the use of tripyranes, preferentially yields macrocycles containing 6, 9, and 12 pyrrole rings.^[272]

Nonaphyrin(1.1.1.1.1.1.1.1.1) has two accessible oxidation levels, **99b**-H₄ and **100b**-H₆, which have respectively 40- and 42-electron CP's and are mutually interconvertible by chemical oxidation and reduction.^[100,272] In the solid state, the free base **100b**-H₆ and its salt [**100b**-H₇][TFA] are characterized by

a pseudoplectonemic conformation with two crossings (Section 2.3). This conformation, containing two inequivalent loops, can be designated as T₀^{A,B,F,5,25,30} (Figure 17). ¹H NMR spectra of **100b**-H₆ and its salt [**100b**-H₇][TFA] indicate that solution structures have low symmetry and that a conformational equilibrium may be involved for **100b**-H₆. Furthermore, chemical shift ranges of NH and β -H protons suggest that the macrocycles are diatropic in accordance with their Hückel-type conjugation.^[100,272] Compound **99b**-H₄, investigated crystallographically in the free base form, adopts an unsymmetrical figure-eight conformation with a T₂₀ topology (Figure 17).^[272] The smaller of the two pockets formed by the figure-eight structure resembles a tetrapyrrolic core, whereas the larger one is reminiscent of the biconcave T₀^{A,D} conformation of hexaphyrin(1.1.1.1.1.1) (Scheme 16). These similarities are reflected in the coordination properties of **99b**-H₄, which is capable of binding up to three divalent metal



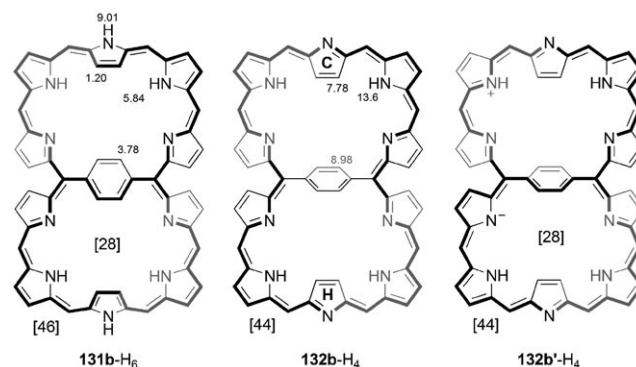
Scheme 26. Ring types of giant porphyrinoids discussed in the text.

ions without significantly changing its conformation. The smaller pocket was shown to bind Cu^{II} or Zn^{II} , whereas the larger pocket coordinates one or two Pd^{II} ions through Pd-N and Pd-C bonds.^[272] In the $\text{Cu}^{\text{II}}(\text{Pd}^{\text{II}})_2$ complex **130b**, which was characterized crystallographically, one of the palladium(II) ions is formally tricoordinate and interacts agostically with a $\beta\text{-CH}$ fragment of one of the pyrroles (Figure 17).

Two oxidation levels have also been reported for decaphyrin(1.1.1.1.1.1.1.1.1.1), however, the substitution pattern was different in each case. **102c-H₆**, which bears trifluoromethyl substituents, is a 46-electron system and was shown to adopt an unusual, C_2 -symmetric *T2* conformation in the solid state.^[211] The structure consists of two helically arranged tripyrrin units of the same handedness, whose ends are connected by meso bridges with two nearly planar dipyrin units (Figure 17). In solution, the molecule is fluxional but a sharp ^1H NMR spectrum could be recorded at 213 K. The spectrum revealed the existence of two conformations with C_2 and C_1 symmetry. The C_2 species shows no apparent ring current, whereas in the case of the C_1 conformer, chemical shift ranges are consistent with a diatropic effect. The spread of NH shifts (8.16 to 1.08 ppm) may result from conformational effects or from the influence of hydrogen bonding. The solid-state conformation of the C_6F_5 -substituted **101b-H₄** is related to the structure of **102c-H₆** as it also contains helical tripyrrin fragments and planar dipyrromethene linkers.^[273] However, the relative orientation of these fragments and the intervening meso bridges is different. In particular, each of the tripyrrin units in **101b-H₄** contains one inverted pyrrole

ring. The conformational difference between **101b-H₄** and **102c-H₆** may be caused by the difference in oxidation level but may also result from the different steric bulk of meso substituents in these two systems. As in the case of **102c-H₆**, the crescent-like conformer of **101b-H₄** is partly stabilized by intramolecular hydrogen bonding. The C_2 symmetry of **101b-H₄** observed in the solid state is apparently preserved in solution.

A very unusual case of π -conjugation topology was provided by the synthesis of two *p*-phenylene-bridged decaphyrins **131b-H₆** and **132b-H₄** (Scheme 27).^[279] These two systems can be viewed as conformationally restricted, bridged



Scheme 27. Macrocyclic conjugation in **131b-H₆** and **132b-H₄**. The helical twist of the decaphyrin ring and the relative orientations of phenylene and pyrrole rings are indicated schematically. The valence structure shown for **131b-H₆** belongs to the 46-electron CP of the large ring and to the 28-electron CP of the lower small ring. Similarly, the valence structure **132b'-H₄** belongs to the 44-electron CP of the large ring and to the 28-electron CP of the lower small ring. Relevant ^1H NMR shifts are given in ppm. *meso*- C_6F_5 groups are omitted for clarity.

variants of **102-H₆** and **101-H₄**, respectively. Such a description was used in the original report and, in fact, **131b-H₆**, which has a 46-electron CP, exhibits a fairly pronounced diatropic ring current. In contrast, the ^1H NMR shifts of **132b-H₄** indicate that the macrocycle is largely nonaromatic. The Π parameter for the decaphyrin circuit in the crystal structure of **131b-H₆** equals 0.43, whereas in the two crystallographically independent molecules of **132b-H₄** it takes the values of 0.28 and 0.15. The above picture can now be extended by noting that each macrocycle can be viewed as a union of two *p*-benzihexaphyrins sharing the unique *p*-phenylene ring and adjacent *meso* bridges. The normal of the phenylene ring in **131b-H₆** and **132b-H₄** is respectively perpendicular and parallel to the long axis of the molecule. In spite of this difference, the conformations are adjusted in such a way that in each case both hexaphyrin rings have the Möbius topology (the adjustment is largely due to rotations of pyrrolic rings C and H). Thus each of the bridged systems can be viewed as two Möbius bands glued together. The conformational switching between **131b-H₆** and **132b-H₄** is reminiscent of the topology selection process described for **44h-H₂** (Section 6.5). Möbius π -conjugation in the hexaphyrin rings is reflected in the negative values of Π calculated on the basis

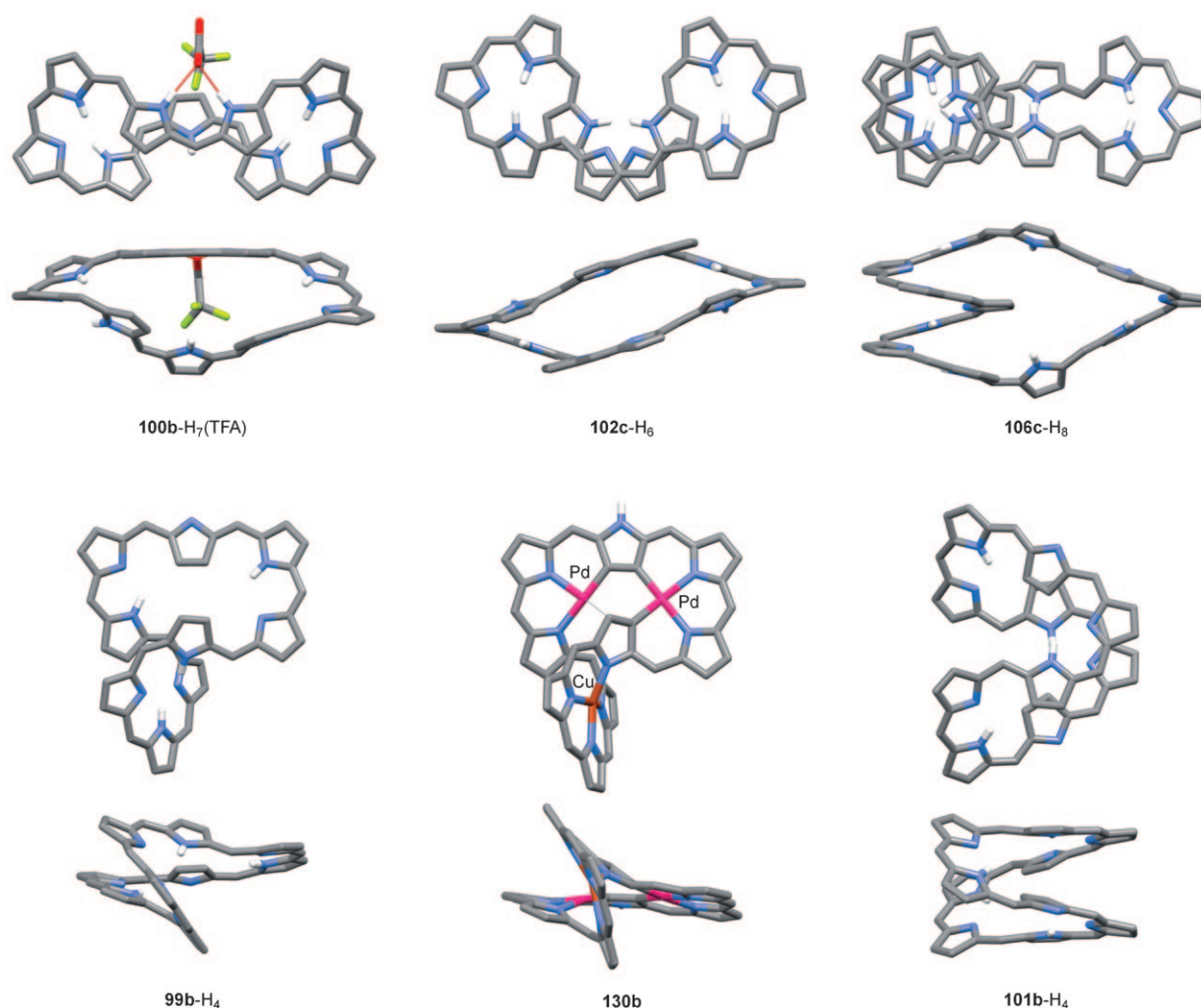


Figure 17. Three-dimensional structures of selected *n*-phyrins(1ⁿ). Coordinates have been taken from X-ray structural data. Solvent molecules and peripheral substituents are removed for clarity.

of X-ray geometries of **131b**-H₆ and **132b**-H₄. Furthermore, the figure eight twist of the two sub-rings has the same sense of chirality in each species.

The above observations provoke a question of the extent to which Möbius π -conjugation of the hexaphyrin sub-rings affects the aromaticity of bridged decaphyrins. A 28-electron π -conjugated circuit, corresponding to Möbius aromaticity, can be constructed in each of the hexaphyrin rings of **131b**-H₆ (there are three canonical structures available for **131b**-H₆, which collectively describe one 46-electron CP and two 28-electron CP's). Thus, with the exception of the phenylene bridge, the sign of the ring current effect due to the smaller CP would coincide with that resulting from the larger, 46-electron CP. However, the averaged Π parameter for the hexaphyrin rings in **131b**-H₆ is only -0.16 , suggesting that the Möbius diatropic contribution may be very small. Interestingly the average Π for the hexaphyrin rings in **132b**-H₄ is -0.39 . Here, however, the basic valence structures are cross-conjugated with respect to the Möbius rings. Interestingly, by considering charge-separated forms such as **132b'**-H₄ (Scheme 27), it is possible to construct a 28-electron CP, analogous to that in

131b-H₆. Even though the unusual topological features of **131b**-H₆ and **132b**-H₄ do not seem to have a marked influence on the aromaticity of these macrocycles, the underlying structural paradigm may be further exploited to expand the topological diversity among aromatic molecules.

The first dodecaphyrin(1.1.1.1.1.1.1.1.1.1.1.1) reported in the literature was **105b**-H₆.^[100] The compound, which was isolated in minute amounts, was only partly characterized and its 54-electron CP was deduced on the basis of mass spectrometry (traces of undecaphyrin **103b**-H₆ were isolated alongside **105b**-H₆). An analogous dodecaphyrin, **104b**-H₄, oxidized to the [52]annulenoid level, was subsequently obtained in a refined synthetic procedure.^[273] The latter compound was only characterized in solution, and it revealed a sharp ¹H NMR spectrum of C₁ symmetry at room temperature. Further details of the solution structure remain to be elucidated, however, the ring current in **104b**-H₄ appears to be rather weak. Interestingly, another dodecaphyrin, the CF₃-substituted species **106c**-H₈, was characterized crystallographically and displayed unique structural features.^[211] The solid-state conformer (Figure 17) contains an unusually long

section of a conjugated oligopyrrole helix (seven rings). The ends of this helix are interconnected through an outer chain of five pyrrolic rings, which contains a helical tripyrrin fragment. This fairly complex arrangement, which can be described as a limaçon with an additional loop, has the T_{4_1} topology. The linking number can be verified by disentangling the edges of the “rubber band” representation, as shown in Figure 18. It is

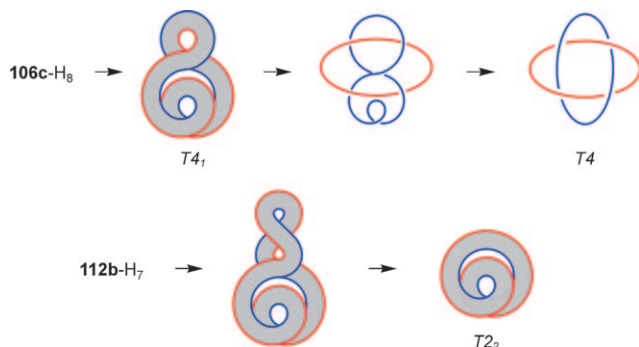


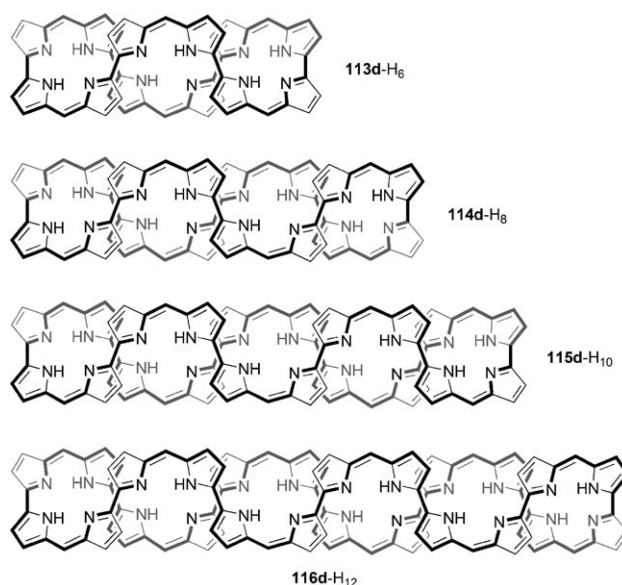
Figure 18. Schematic representations of the T_{4_1} and T_{2_2} conformers of **106c-H₈** and **112b-H₇**.

of interest that even for such a high Lk value, the macrocycle converts most of the actual twist into writhe ($Tw = 1.16$, $Wr = 2.84$). The ^1H NMR spectrum of **106c-H₈** indicates dynamic behavior at room temperature. At 183 K, the spectrum is complex and contains signals corresponding to two conformers of different symmetry.

Tetradeca-, hexadeca- and octadecaphyrin substituted with C_6F_5 groups (**107b-H₆**, **108b-H₈**, **109b-H₈**) were obtained in small amounts in dipyrromethane–aldehyde condensations.^[273] Their ^1H NMR spectra indicate the presence of relatively rigid low-symmetry conformers, even at room temperature. This observation is noteworthy, because in an n -phyrin(1^n) all pyrrole rings and meso substituents are chemically equivalent in the limit of fast NH tautomerization. The NH signals of these three species, which occupy the range of 10 to 14 ppm, become sufficiently sharp at 213 K to enable their identification. Interestingly, in each case the pattern is different: **107b-H₆** contains a mixture of low-symmetry conformers, **108b-H₈** contains one conformer with twofold symmetry, whereas the structure of **109b-H₈** has no symmetry elements. These data suggest that a systematic analysis of NMR spectra might provide detailed information on the solution structures of the largest porphyrin homologues.

9.2. Rosarin and Rubyrin Homologues

Norcorrole **3-H₂**, rosarin **34-H₃**, and octaphyrin(1.0.1.0.1.0.1.0) **76-H₄** are the three smallest members of the rosarin class. Higher homologues containing $4n$ pyrrolic rings can be prepared from appropriate bipyrrrolic precursors.^[42,274] The series includes four systems, **113d-H₆**, **114d-H₈**, **115d-H₁₀**, and **116d-H₁₂**, containing respectively 12, 16, 20, and 24 cyclic subunits (Scheme 26 and Scheme 28). The first two of these macrocycles have been characterized crystallograph-



Scheme 28. Structures of rosarin homologues. Pseudoplectonemic representations are based on those proposed in the original work.^[274]

ically (Figure 19). The structure of dodecaphyrin^[42] **113d-H₆** can be described as a pseudoplectoneme with two crossings, homologous to the figure-eight conformers observed for derivatives of **76-H₄**. It should be noted, however, that the structure is not flat and the distance between the zigzag chains of the pseudoplectoneme is ca. 5.6 Å (Figure 19). The separation is likely caused by the presence of bulky *meso*- and β -substituents, which act as spacers between the oligopyrrole chains. Consequently, π -conjugation in **113d-H₆** is rather inefficient, as indicated by the low value of $\Pi = 0.19$. Hexadecaphyrin^[274] **114d-H₈** forms an even larger diamond-shaped cavity, with edge-to-edge dimensions of 10 to 11.5 Å. The π -surface in this system is kinked in several places, yielding $\Pi = 0.001$, and the macrocyclic conjugation is effectively interrupted. Interestingly, the cumulative twist Tw of the solid-state structure of **114d-H₈** is only 0.05. This observation shows that low Tw values are not universally associated with efficient π conjugation. In spite of its kinked geometry, the solid-state conformer of **114d-H₈** can be classified as T_{2_0} , in accord with the depiction given in Scheme 28. The sharpest turns in the SMC ($|\theta|$ approaching 90°) are formed at the direct bipyrrrole linkages, indicating that higher rosarin homologues effectively comprise a cyclic array of largely nonconjugated dipyrrolic subunits. It may be argued that, because of similar steric requirements of peripheral substituents, the efficiency of macrocyclic conjugation will also be limited in the largest members of the rosarin class: eicosaphyrin **115d-H₁₀** and tetracosaphyrin **116d-H₁₂**. Thus the appealing representation of the largest members of the series adopted in the original work (Scheme 28) probably does not correspond to actual conformations of these systems. ^1H NMR spectra of **113d-H₆**, **114d-H₈**, **115d-H₁₀**, and **116d-H₁₂** recorded at room temperature suggest that the conformations are partly locked, however, no detailed spectroscopic analysis was attempted.

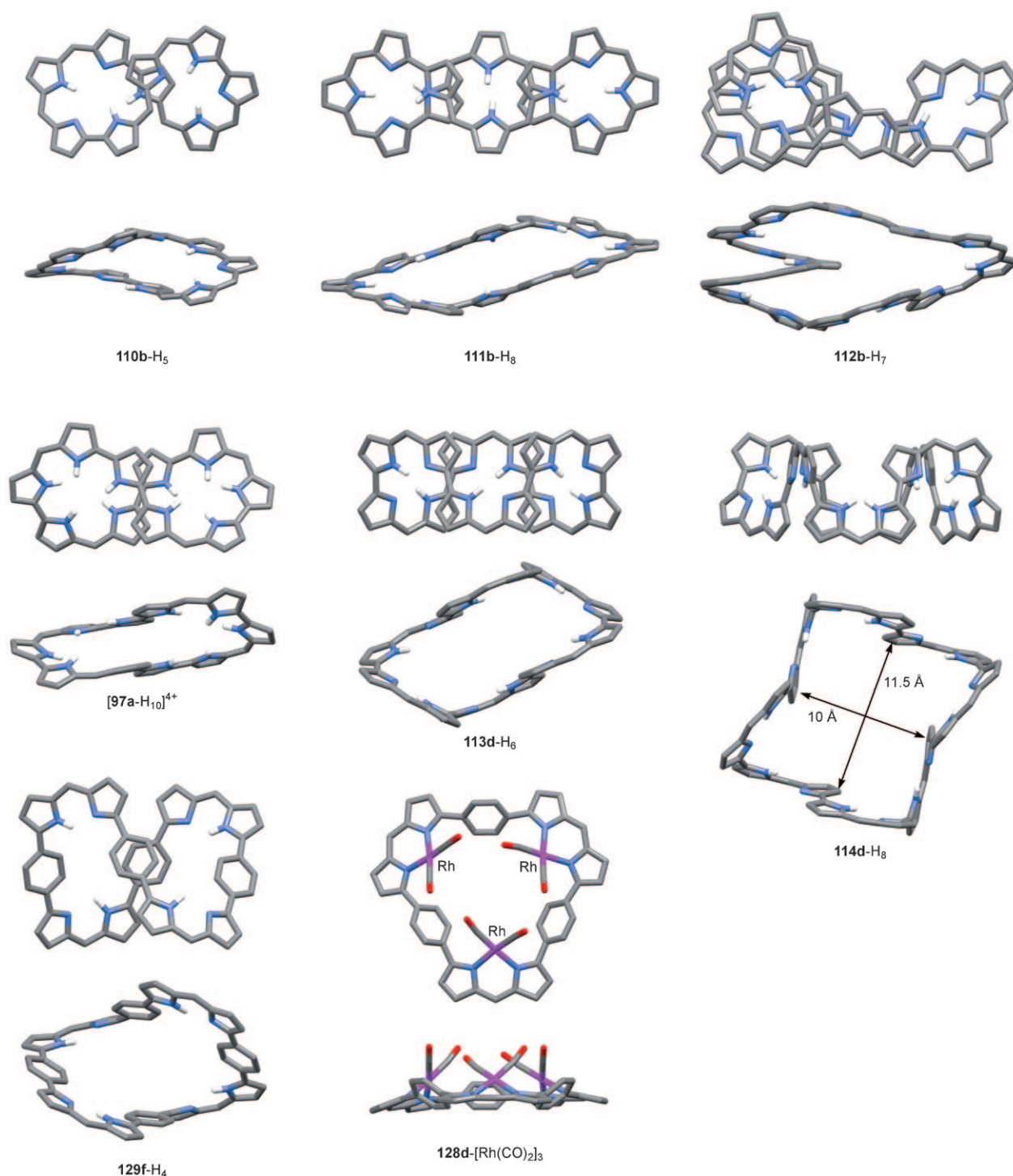


Figure 19. Three-dimensional structures of selected giant porphyrinoids. Coordinates have been taken from X-ray structural data. Solvent molecules and peripheral substituents are removed for clarity.

Nonaphyrin(1.1.0.1.1.0.1.1.0) **110b-H₅** was obtained in an oxidative coupling of tripyrranes alongside its lower homologue, rubyrin **35c-H₄** (Section 6.3).^[44] Further refinement of this procedure yielded two additional macrocycles, dodecaphyrin **111b-H₈** and pentadecaphyrin **112b-H₇**.^[45] With $\tau_F = 2.19$, the macrocycle of **110b-H₅** has an optimal free curvature for the figure-eight conformation, which is indeed observed in

the solid state ($\Pi = 0.75$, Figure 19). A low symmetry structure, likely corresponding to the solid-state conformation, is also observed in solution and it is transformed into a quadricconcave conformer upon protonation with MSAH.^[111] In the crystal, dodecaphyrin **111b-H₈** was shown to adopt a pseudoplectonemic conformation with two crossings, which was slightly distorted from the C_{2h} symmetry and had a

smooth π -conjugated surface ($\Pi=0.62$, Figure 19).^[45] The ^1H NMR spectroscopic pattern was consistent with the retention of the solid-state structure in solution. In contrast, pentadecaphyrin **112b**-H₇ appears to be conformationally fluxional in solution, displaying significantly broadened ^1H NMR spectra at 253 K. The crystal structure of **112b**-H₇ reveals a distorted limaçon conformation T_2 (Figure 19), which contains a helical oligopyrrole section similar to that in the T_4 conformer of **106c**-H₈. It is of interest that the τ_F values calculated for these two systems are very similar (3.65 and 3.58, respectively), showing that the optimum free curvature for feasible T_2 conformers is larger than that required by T_0 structures. This observation is not surprising because the outer loop in the limaçon structures has to be large enough to hold the smaller loop. The π -conjugated surface is even smoother in **112b**-H₇ ($\Pi=0.56$) than in **106c**-H₈ ($\Pi=0.37$), corresponding to a fairly large writhe value in the former system ($Tw=0.50$, $Wr=1.50$).^[45]

9.3. Cyclo[n]thiophenes

Even though the family of cyclo[n]thiophenes (**74b**, **117a**–**126a**)^[255,275,276,280] is seldom discussed in the context of porphyrinoid chemistry, these unusual macrocycles can be regarded as heteroanalogues of cyclo[n]pyrroles. Unlike the latter class of compounds, of which only three representatives have been reported (**29**-H₄, **56**-H₅, **72**-H₆ with $n=6, 7, 8$), cyclo[n]thiophenes, synthesized using carefully designed metal-mediated coupling reactions, can be obtained in a spectacular variety of molecular sizes ranging from octa- to tetracontamers (Scheme 26). While X-ray diffraction structures of cyclothiophenes have not yet been reported, STM data^[276] and computational work^[281] indicate that the conformations of the lower members of the series should be convex. As the ring size increases, the macrocycles are predicted to adopt saddle-type conformations. Additionally, in-plane conjugated anti-type structures were predicted to become energetically preferred for cyclo[n]thiophenes with $n \geq 20$.^[281]

9.4. Other Systems

Apart from the above families of porphyrinoids, few other macrocycles have been reported containing more than eight cyclic subunits. Turcasarin **97a**-H₆, mentioned in the introduction was the first reported example of a “giant” porphyrinoid and the first documented instance of a figure-eight conformation (Scheme 1, Figure 19).^[23] A structurally similar analogue **98a**-H₄, containing two furan rings was subsequently reported.^[271] Both systems have 40-electron CP's and their ^1H NMR spectra are indicative of very weak paratropicity. Octathiadodecaphyrin **127e**-H₂ (Scheme 26) was formed as a higher homologue of trithiahexaphyrin(1.1.1.1.0.0) (Section 6.3).^[225] **127e**-H₂ and its hexathiadiselenane analogue show fluxional behavior in solution, and low-temperature ^1H NMR spectra indicate that several conformations may be accessible. However, in the absence of detailed spectroscopic analyses or

crystal structures, the conformational behavior of **127e**-H₂ remains to be elucidated.

Two macrocycles containing directly linked pyrrole and *p*-phenylene subunits, **128df**-H₃ and **129df**-H₄, have recently been reported (Scheme 26).^[277,278] Even though these systems contain respectively 36- and 48-electron CP's, their ^1H NMR spectra indicated the absence of macrocyclic ring currents. Nonaphyrin **128d**-H₃ can be considered a derivative of rosarin **34b**-H₃, modified by insertion of phenylene rings between directly linked pyrrole units. **128d**-H₃ and **129d**-H₄ have been shown to form multinuclear complexes with rhodium(I), **128d**-[Rh(CO)₂]₃ and **129d**-[Rh(CO)₂]₄. The first of these two species adopts a relatively planar conformation in the solid state with all three Rh(CO)₂ fragments tilted away from the core and located on the same side of the macrocyclic plane. In solution, this C_{3v} -symmetric structure is subject to fast pseudoinversion occurring through intermediate structures of C_s symmetry in which one of the Rh(CO)₂ groups is tilted on the opposite side of the ring. A relatively rigid saddle-shaped conformation was proposed to account for the observed spectroscopic behavior of **129d**-[Rh(CO)₂]₄. In contrast, the free base **129d**-H₄ is conformationally fluxional, revealing a spectral pattern similar to that of **128d**-H₃. Compounds **128f**-H₃ and **129f**-H₄, in which β -pyrrolic positions are unsubstituted whereas each phenylene ring bears two methoxy substituents, have been characterized crystallographically.^[278] **128f**-H₃ adopts a relatively planar conformation with slightly tilted phenylene rings ($\Pi=0.52$). In contrast, the tetrameric structure **129f**-H₄ assumes a saddle shaped conformation that is flattened on one side to yield a C_2 -symmetric T_0 conformer ($\Pi=0.54$, Figure 19).

10. Concluding Remarks

Three-dimensional structure plays a pivotal role in controlling many properties of porphyrinoids, such as optical absorption, redox behavior, or supramolecular interactions, all of which are related to typically targeted applications. In spite of the enormous recent progress in the field, it is still difficult to predict the three-dimensional structure “encoded” in a particular array of building blocks and even more so to envisage its dynamic behavior. We hope that a systematic analysis of porphyrinoid conformation undertaken in this Review will be helpful in correlating the three-dimensional structures of these fascinating macrocycles with their constitution and provide hints for selection of interesting synthetic targets. In particular, the concept of “free curvature” and the new conformational descriptor may potentially become useful tools in the conformational analysis of porphyrin analogues.

The stereochemical problems encountered in porphyrinoid chemistry are often inherent to this particular class of macrocycles, which combine partial structural rigidity with considerable conformational freedom. Conformational dynamics of porphyrin analogues are often coupled to other chemical phenomena, such as prototropic tautomerism, acid–base equilibria, anion binding, and metal ion coordination, making such processes difficult to investigate in solution. In

those cases in which such investigations were attempted, the behavior revealed by NMR spectroscopy often proved more complex than could have been inferred from solid-state structural data. At a computational level, the problem of predicting the three dimensional structure becomes particularly severe in the largest members of the porphyrinoid family, in which the increased number of degrees of freedom translates into exceedingly complex conformational spaces, often containing numerous closely spaced energy minima. It is therefore noteworthy that many giant porphyrinoids are capable of achieving a high degree of conformational ordering not only in the solid state but also in solution. Systematic exploration of the synthetic limits of macrocycle expansion may be viewed as one of significant challenges in porphyrinoid chemistry, especially when combined with in-depth conformational analysis. Achieving precise control of the three-dimensional structure of large-ring porphyrinoids is a prerequisite for constructing supramolecular devices such as receptors or molecular switches. In particular, the availability of Möbius π -conjugation enables translating a mechanical stimulus, such as binding of a sterically demanding guest molecule, into a significant change of electronic structure.

The design of new porphyrin analogues relies on a building block approach that is effective and conceptually simple, even though it often becomes synthetically demanding. The effectiveness of this approach is manifested in the ease of creating structurally nontrivial macrocycles, often imparted with unique physical and chemical characteristics. As we have tried to show in this Review, the cornucopia of macrocyclic motifs that can be derived from the porphyrin “Leitstruktur” creates diverse research opportunities, extending beyond the pure synthetic approach, many of which may reveal substantial application potential. The belated identification of Möbius aromaticity among porphyrin analogues shows that exciting discoveries can be made even in a seemingly well-explored field of research.

Abbreviations

acac	acetylacetonate
Anis	anisyl (4-methoxyphenyl)
Bn	benzyl
CP	conjugation pathway
DCA	dichloroacetate
DCFM	dichlorofluoromethane
DDQ	2,3-dichloro-5,6-dicyano-1,4-benzoquinone
Lk	linking number
Mes	mesityl (2,4,6-trimethylphenyl)
MO	molecular orbital (theory)
MSA	methanesulfonate
N	length of the conjugation pathway
S	size of the smallest macrocyclic circuit
SMC	smallest macrocyclic circuit
TFA	trifluoroacetate
Tn	(T0, T1, etc.) topology with Lk = n
Tol	p-tolyl
Tw	twist
Wr	writhe

θ	torsion angle (between consecutive p orbitals in a π -conjugated system)
Π	torsional π -conjugation index
τ	turning number
τ_F	free curvature (without inversions)
τ_{FI}	free curvature with inversions
τ_{subunit}	subunit curvature

The work was supported by the Ministry of Science and Higher Education (Grant N N204 013536). Quantum chemical calculations were performed in the Wrocław Center for Networking and Supercomputing. We thank one of the referees for helpful comments.

Received: June 2, 2010

Published online: April 14, 2011

- [1] M. Faraday, *Philos. Trans. R. Soc. London* **1825**, 115, 440–446.
- [2] V. I. Minkin, M. N. Glukhovtsev, B. Y. Simkin, *Aromaticity and Antiaromaticity. Electronic and Structural Aspects*, Wiley-Interscience, New York, **1994**.
- [3] P. v. R. Schleyer, *Chem. Rev.* **2001**, 101, 1115–1117.
- [4] P. v. R. Schleyer, *Chem. Rev.* **2005**, 105, 3433–3435.
- [5] R. M. Willstätter, W. von Schmaedel, *Ber. Dtsch. Chem. Ges.* **1905**, 38, 1992–1999.
- [6] R. M. Willstätter, E. Waser, *Ber. Dtsch. Chem. Ges.* **1911**, 44, 3423–3445.
- [7] L. T. Scott, H. E. Bronstein, D. V. Preda, R. B. Ansems, M. S. Bratcher, S. Hagen, *Pure Appl. Chem.* **1999**, 71, 209–219.
- [8] A. Bühl, A. Hirsch, *Chem. Rev.* **2001**, 101, 1153–1183.
- [9] X. Lu, Z. Chen, *Chem. Rev.* **2005**, 105, 3643–3696.
- [10] R. Herges in *Modern Cyclophane Chemistry* (Eds.: R. Gleiter, R. Herges), Wiley-VCH, Weinheim, **2004**, pp. 337–358.
- [11] R. Herges, *Chem. Rev.* **2006**, 106, 4820–4842.
- [12] J. L. Sessler, S. J. Weghorn, *Expanded, Contracted, and Isomeric Porphyrins*, Elsevier, Amsterdam, **1997**.
- [13] L. Latos-Grażyński in *The Porphyrin Handbook*, Vol. 2 (Eds.: K. M. Kadish, K. M. Smith, R. Guilard), Academic Press, San Diego, **2000**, pp. 361–416.
- [14] T. D. Lash in *The Porphyrin Handbook*, Vol. 2 (Eds.: K. M. Kadish, K. M. Smith, R. Guilard), Academic Press, San Diego, **2000**, pp. 125–199.
- [15] J. L. Sessler, A. Gebauer, E. Vogel in *The Porphyrin Handbook*, Vol. 2 (Eds.: K. M. Kadish, K. M. Smith, R. Guilard), Academic Press, San Diego, **2000**, pp. 1–54.
- [16] J. L. Sessler, D. Seidel, *Angew. Chem.* **2003**, 115, 5292–5333; *Angew. Chem. Int. Ed.* **2003**, 42, 5134–5175.
- [17] M. Stępień, L. Latos-Grażyński in *Topics in Heterocyclic Chemistry*, Vol. 19 (Eds.: T. M. Krygowski, M. K. Cyrański), **2009**, pp. 83–153.
- [18] M. Pawlicki, L. Latos-Grażyński in *Handbook of Porphyrin Science*, Vol. 2, World Scientific, Singapore, **2010**, pp. 104–192.
- [19] A. Gossauer, R. Charrière, T. A. Jenny, H. Rexhausen, *Heterocycles* **1993**, 36, 1561–1575.
- [20] H. Furuta, T. Asano, T. Ogawa, *J. Am. Chem. Soc.* **1994**, 116, 767–768.
- [21] P. J. Chmielewski, L. Latos-Grażyński, K. Rachlewicz, T. Głowiak, *Angew. Chem.* **1994**, 106, 805–808; *Angew. Chem. Int. Ed. Engl.* **1994**, 33, 779–781.
- [22] H. Furuta, T. Ishizuka, A. Osuka, T. Ogawa, *J. Am. Chem. Soc.* **1999**, 121, 2945–2946.
- [23] J. L. Sessler, S. J. Weghorn, V. Lynch, M. R. Johnson, *Angew. Chem.* **1994**, 106, 1572–1575; *Angew. Chem. Int. Ed. Engl.* **1994**, 33, 1509–1512.

- [24] M. Stępień, L. Latos-Grażyński, N. Sprutta, P. Chwalisz, L. Sztrenberg, *Angew. Chem.* **2007**, *119*, 8015–8019; *Angew. Chem. Int. Ed.* **2007**, *46*, 7869–7873.
- [25] M. Stępień, B. Szyszko, L. Latos-Grażyński, *J. Am. Chem. Soc.* **2010**, *132*, 3140–3152.
- [26] a) Z. S. Yoon, A. Osuka, D. Kim, *Nat. Chem.* **2009**, *1*, 113–122; b) J.-Y. Shin, K. S. Kim, M.-C. Yoon, J. M. Lim, Z. S. Yoon, A. Osuka, D. Kim, *Chem. Soc. Rev.* **2010**, *39*, 2751–2767.
- [27] P. A. Gale, J. L. Sessler, V. Kral, *Chem. Commun.* **1998**, 1–8.
- [28] P. A. Gale, P. Anzenbacher Jr., J. L. Sessler, *Coord. Chem. Rev.* **2001**, *222*, 57–102.
- [29] J. L. Sessler, R. S. Zimmerman, C. Bucher, V. Král, B. Andrioletti, *Pure Appl. Chem.* **2001**, *73*, 1041–1057.
- [30] A. Jasat, D. Dolphin, *Chem. Rev.* **1997**, *97*, 2267–2340.
- [31] B. Franck, A. Nonn, *Angew. Chem.* **1995**, *107*, 1941–1957; *Angew. Chem. Int. Ed. Engl.* **1995**, *34*, 1795–1811.
- [32] J. L. Sessler, A. Gebauer, S. J. Weghorn, in *The Porphyrin Handbook*, Vol. 2 (Eds.: K. M. Kadish, K. M. Smith, R. Guilard), Academic Press, San Diego, **2000**, pp. 55–124.
- [33] T. K. Chandrashekar, S. Venkatraman, *Acc. Chem. Res.* **2003**, *36*, 676–691.
- [34] R. Misra, T. K. Chandrashekar, *Acc. Chem. Res.* **2008**, *41*, 265–279.
- [35] G. P. Moss, *Pure Appl. Chem.* **1987**, *59*, 779–832.
- [36] N. Kobayashi, Y. Takeuchi, A. Matsuda, *Angew. Chem.* **2007**, *119*, 772–774; *Angew. Chem. Int. Ed.* **2007**, *46*, 758–760.
- [37] H. Rexhausen, A. Gossauer, *J. Chem. Soc. Chem. Commun.* **1983**, 275.
- [38] T. Kohler, D. Seidel, V. Lynch, F. O. Arp, Z. P. Ou, K. M. Kadish, J. L. Sessler, *J. Am. Chem. Soc.* **2003**, *125*, 6872–6873.
- [39] D. Seidel, V. Lynch, J. L. Sessler, *Angew. Chem.* **2002**, *114*, 1480–1483; *Angew. Chem. Int. Ed.* **2002**, *41*, 1422–1425.
- [40] J. L. Sessler, S. J. Weghorn, T. Morishima, M. Rosingana, V. Lynch, V. Lee, *J. Am. Chem. Soc.* **1992**, *114*, 8306–8307.
- [41] M. Bröring, J. Jendry, L. Zander, H. Schmickler, J. Lex, Y.-D. Wu, M. Nendel, J. Chen, D. A. Plattner, K. N. Houk, E. Vogel, *Angew. Chem.* **1995**, *107*, 2709–2711; *Angew. Chem. Int. Ed. Engl.* **1995**, *34*, 2515–2517.
- [42] J.-i. Setsune, Y. Katakami, N. Iizuna, *J. Am. Chem. Soc.* **1999**, *121*, 8957–8958.
- [43] J. L. Sessler, T. Morishima, V. Lynch, *Angew. Chem.* **1991**, *103*, 1018–1020; *Angew. Chem. Int. Ed. Engl.* **1991**, *30*, 977–980.
- [44] S. Shimizu, R. Taniguchi, A. Osuka, *Angew. Chem.* **2005**, *117*, 2265–2269; *Angew. Chem. Int. Ed.* **2005**, *44*, 2225–2229.
- [45] S. Shimizu, W. S. Cho, J. L. Sessler, H. Shinokubo, A. Osuka, *Chem. Eur. J.* **2008**, *14*, 2668–2678.
- [46] A. W. Johnson, I. T. Kay, *J. Chem. Soc.* **1965**, 1620–1629.
- [47] E. Vogel, M. Bröring, J. Fink, D. Rosen, H. Schmickler, J. Lex, K. W. Chan, Y.-D. Wu, D. A. Plattner, M. Nendel, K. N. Houk, *Angew. Chem.* **1995**, *107*, 2705–2709; *Angew. Chem. Int. Ed. Engl.* **1995**, *34*, 2511–2514.
- [48] R. B. Woodward, Aromaticity Conference, Sheffield, UK, **1966**.
- [49] J. L. Sessler, J. M. Davis, V. Lynch, *J. Org. Chem.* **1998**, *63*, 7062–7065.
- [50] J. L. Sessler, D. Seidel, C. Bucher, V. Lynch, *Chem. Commun.* **2000**, 1473–1474.
- [51] S. Hiroto, H. Shinokubo, A. Osuka, *J. Am. Chem. Soc.* **2006**, *128*, 6568–6569.
- [52] C. Bucher, D. Seidel, V. Lynch, J. L. Sessler, *Chem. Commun.* **2002**, 328–329.
- [53] S. Gokulnath, V. Prabhuraja, T. K. Chandrashekar, *Org. Lett.* **2007**, *9*, 3355–3357.
- [54] R. Kumar, R. Misra, T. K. Chandrashekar, A. Nag, D. Goswami, E. Suresh, C. H. Suresh, *Eur. J. Org. Chem.* **2007**, 4552–4562.
- [55] J. L. Sessler, S. J. Weghorn, Y. Hisaeda, V. Lynch, *Chem. Eur. J.* **1995**, *1*, 56–67.
- [56] M. J. Broadhurst, R. Grigg, A. W. Johnson, *J. Chem. Soc. Perkin Trans. I* **1972**, 2111–2116.
- [57] J. L. Sessler, D. Seidel, A. E. Vivian, V. Lynch, B. L. Scott, D. W. Keogh, *Angew. Chem.* **2001**, *113*, 611–614; *Angew. Chem. Int. Ed.* **2001**, *40*, 591–594.
- [58] J. L. Sessler, D. Seidel, V. Lynch, *J. Am. Chem. Soc.* **1999**, *121*, 11257–11258.
- [59] S. K. Pushpan, V. R. Anand, S. Venkatraman, A. Srinivasan, A. K. Gupta, T. K. Chandrashekar, *Tetrahedron Lett.* **2001**, *42*, 3391–3394.
- [60] V. G. Anand, S. K. Pushpan, S. Venkatraman, S. J. Narayanan, A. Dey, T. K. Chandrashekar, R. Roy, B. S. Joshi, S. Deepa, G. N. Sastry, *J. Org. Chem.* **2002**, *67*, 6309–6319.
- [61] R. Kumar, R. Misra, T. K. Chandrashekar, E. Suresh, *Chem. Commun.* **2007**, 43–45.
- [62] J. S. Lindsey in *The Porphyrin Handbook*, Vol. 1 (Eds.: K. M. Kadish, K. M. Smith, R. Guilard), Academic Press, San Diego, **2000**, pp. 45–118.
- [63] G. P. Arsenault, E. Bullock, S. F. MacDonald, *J. Am. Chem. Soc.* **1960**, *82*, 4384–4389.
- [64] J. L. Sessler, M. J. Johnson, V. Lynch, *J. Org. Chem.* **1987**, *52*, 4394–4397.
- [65] D. Sánchez-García, J. L. Sessler, *Chem. Soc. Rev.* **2008**, *37*, 215–232.
- [66] J. L. Sessler, A. Aguilar, D. Sánchez-García, D. Seidel, T. Kohler, F. Arp, V. M. Lynch, *Org. Lett.* **2005**, *7*, 1887–1890.
- [67] Y. Tanaka, W. Hoshino, S. Shimizu, K. Youfu, N. Aratani, N. Maruyama, S. Fujita, A. Osuka, *J. Am. Chem. Soc.* **2004**, *126*, 3046–3047.
- [68] E. Pacholska, L. Latos-Grażyński, Z. Ciunik, *Chem. Eur. J.* **2002**, *8*, 5403–5406.
- [69] A. Baeyer, *Ber. Dtsch. Chem. Ges.* **1885**, *18*, 2269–2281.
- [70] L. Ružicka in *Nobel Lectures, Chemistry 1922–1941*, Elsevier, Amsterdam, **1966**.
- [71] H. Fischer in *Nobel Lectures, Chemistry 1922–1941*, Elsevier, Amsterdam, **1966**, p. 165.
- [72] A. Baeyer, *Ber. Dtsch. Chem. Ges.* **1886**, *19*, 2184–2185.
- [73] P. A. Gale, J. L. Sessler, V. Kral, V. Lynch, *J. Am. Chem. Soc.* **1996**, *118*, 5140–5141.
- [74] M. Berger, A Panoramic View of Riemannian Geometry, Springer, **2003**.
- [75] W. Fenchel, *Math. Ann.* **1929**, *101*, 238–252.
- [76] M. O. Senge in *The Porphyrin Handbook*, Vol. 1 (Eds.: K. M. Kadish, K. M. Smith, R. Guilard), Academic Press, San Diego, **2000**, pp. 239–347.
- [77] M. O. Senge, *Chem. Commun.* **2006**, 243–256.
- [78] H. Furuta, H. Maeda, A. Osuka, *Chem. Commun.* **2002**, 1795–1804.
- [79] P. G. Mezey, *Shape in Chemistry: An Introduction to Molecular Shape and Topology*, Wiley-VCH, New York, **1993**.
- [80] H. Dodziuk, *Modern Conformational Analysis: Elucidating Novel Exciting Molecular Structures*, Wiley-VCH, Weinheim, **1996**.
- [81] E. Flapan, *When Topology Meets Chemistry: A Topological Look at Molecular Chirality*, Cambridge University Press, **2000**.
- [82] J. W. Rutter, *Geometry of Curves*, Chapman & Hall/CRC, **2000**.
- [83] E. Heilbronner, *Tetrahedron Lett.* **1964**, *5*, 1923–1928.
- [84] F. B. Fuller, *Proc. Natl. Acad. Sci. USA* **1971**, *68*, 815–819.
- [85] S. M. Rappaport, H. S. Rzepa, *J. Am. Chem. Soc.* **2008**, *130*, 7613–7619.
- [86] A. D. Bates, A. Maxwell, *DNA Topology*, Oxford University Press, **2005**.
- [87] D. Ajami, O. Oeckler, A. Simon, R. Herges, *Nature* **2003**, *426*, 819–821.
- [88] J. F. Oth, *Pure Appl. Chem.* **1971**, *25*, 573–622.
- [89] M. Toganoh, H. Furuta, *J. Phys. Chem. A* **2009**, *113*, 13953–13963.

- [90] H. S. Rzepa, *Chem. Rev.* **2005**, *105*, 3697–3715.
- [91] E. Flapan, *THEOCHEM* **1995**, *336*, 157–164.
- [92] D. Ajami, K. Hess, F. Köhler, C. Näther, O. Oeckler, A. Simon, C. Yamamoto, Y. Okamoto, R. Herges, *Chem. Eur. J.* **2006**, *12*, 5434–5445.
- [93] A. Werner, M. Michels, L. Zander, J. Lex, E. Vogel, *Angew. Chem.* **1999**, *111*, 3866–3870; *Angew. Chem. Int. Ed.* **1999**, *38*, 3650–3653.
- [94] F. Sondheimer, R. Wolovsky, Y. Amiel, *J. Am. Chem. Soc.* **1962**, *84*, 274–284.
- [95] E. Vogel, *Pure Appl. Chem.* **1993**, *65*, 143–152.
- [96] A. R. Katritzky, M. Karelson, S. Sild, T. M. Krygowski, K. Jug, *J. Org. Chem.* **1998**, *63*, 5228–5231.
- [97] A. R. Katritzky, K. Jug, D. C. Oniciu, *Chem. Rev.* **2001**, *101*, 1421–1449.
- [98] P. George, *Chem. Rev.* **1975**, *75*, 85–111.
- [99] K. B. Wiberg, *Chem. Rev.* **2001**, *101*, 1317–1331.
- [100] J.-Y. Shin, H. Furuta, K. Yoza, S. Igarashi, A. Osuka, *J. Am. Chem. Soc.* **2001**, *123*, 7190–7191.
- [101] Z. S. Yoon, J. H. Kwon, M. C. Yoon, M. K. Koh, S. B. Noh, J. L. Sessler, J. T. Lee, D. Seidel, A. Aguilar, S. Shimizu, M. Suzuki, A. Osuka, D. Kim, *J. Am. Chem. Soc.* **2006**, *128*, 14128–14134.
- [102] Z. S. Yoon, D. G. Cho, K. S. Kim, J. L. Sessler, D. Kim, Z. S. AF Yoon, D.-G. Cho, K. S. Kim, J. L. Sessler, D. Kim, *J. Am. Chem. Soc.* **2008**, *130*, 6930–6931.
- [103] Y. Tanaka, S. Saito, S. Mori, N. Aratani, H. Shinokubo, N. Shibata, Y. Higuchi, Z. S. Yoon, K. S. Kim, S. B. Noh, J. K. Park, D. Kim, A. Osuka, *Angew. Chem.* **2008**, *120*, 693–696; *Angew. Chem. Int. Ed.* **2008**, *47*, 681–684.
- [104] E. D. Becker, R. B. Bradley, *J. Chem. Phys.* **1959**, *31*, 1413–1414.
- [105] C. J. Medforth in *The Porphyrin Handbook*, Vol. 5 (Eds.: K. M. Kadish, K. M. Smith, R. Guilard), Academic Press, San Diego, **2000**, pp. 1–80.
- [106] P. v. R. Schleyer, C. Meaerker, A. Dransfeld, H. Jiao, N. J. Hommes, *J. Am. Chem. Soc.* **1996**, *118*, 6317–6318.
- [107] Z. Chen, C. S. Wannere, C. Corminboeuf, R. Puchta, P. v. R. Schleyer, *Chem. Rev.* **2005**, *105*, 3842–3888.
- [108] M. K. Cyrański, T. M. Krygowski, M. Wisiorowski, N. J. Hommes, P. v. R. Schleyer, *Angew. Chem.* **1998**, *110*, 187–190; *Angew. Chem. Int. Ed.* **1998**, *37*, 177–180.
- [109] C. S. Wannere, K. W. Sattelmeyer, H. F. Schaefer, P. v. R. Schleyer, *Angew. Chem.* **2004**, *116*, 4296–4302; *Angew. Chem. Int. Ed.* **2004**, *43*, 4200–4206.
- [110] E. Pacholska-Dudziak, J. Skonieczny, M. Pawlicki, L. Sztrenberg, Z. Ciunik, L. Latos-Grażyński, *J. Am. Chem. Soc.* **2008**, *130*, 6182–6195.
- [111] J. Y. Shin, J. M. Lim, Z. S. Yoon, K. S. Kim, M. C. Yoon, S. Hiroto, H. Shinokubo, S. Shimizu, A. Osuka, D. Kim, *J. Phys. Chem. B* **2009**, *113*, 5794–5802.
- [112] a) E. Steiner, P. W. Fowler, *ChemPhysChem* **2002**, *3*, 114–116; b) E. Steiner, P. W. Fowler, *Org. Biomol. Chem.* **2003**, *1*, 1785–1789; c) E. Steiner, P. W. Fowler, *Org. Biomol. Chem.* **2004**, *2*, 34–37; d) E. Steiner, P. W. Fowler, *Org. Biomol. Chem.* **2006**, *4*, 2473–2476.
- [113] D. Geuenich, K. Hess, F. Köhler, R. Herges, *Chem. Rev.* **2005**, *105*, 3758–3772.
- [114] J. S. Lee, J. M. Lim, M. Toganoh, H. Furuta, D. Kim, *Chem. Commun.* **2010**, *46*, 285–287.
- [115] T. Higashino, J. M. Lim, T. Miura, S. Saito, J.-Y. Shin, D. Kim, A. Osuka, *Angew. Chem. Int. Ed.* **2010**, *49*, 4950–4954.
- [116] S. Shaik, A. Shurki, D. Danovich, P. C. Hiberty, *Chem. Rev.* **2001**, *101*, 1501–1539.
- [117] T. M. Krygowski, M. K. Cyrański, *Chem. Rev.* **2001**, *101*, 1385–1419.
- [118] J. L. Sessler, D.-G. Cho, M. Stępień, V. Lynch, J. Waluk, Z. S. Yoon, D. Kim, *J. Am. Chem. Soc.* **2006**, *128*, 12640–12641.
- [119] M. Stępień, L. Latos-Grażyński, L. Sztrenberg, *J. Org. Chem.* **2007**, *72*, 2259–2270.
- [120] J. K. Park, Z. S. Yoon, M.-C. Yoon, K. S. Kim, S. Mori, J.-Y. Shin, A. Osuka, D. Kim, *J. Am. Chem. Soc.* **2008**, *130*, 1824–1825.
- [121] J. Sankar, S. Mori, S. Saito, H. Rath, M. Suzuki, Y. Inokuma, H. Shinokubo, K. Suk Kim, Z. S. Yoon, J.-Y. Shin, J. M. Lim, Y. Matsuzaki, O. Matsushita, A. Muranaka, N. Kobayashi, D. H. Kim, A. Osuka, *J. Am. Chem. Soc.* **2008**, *130*, 13568–13579.
- [122] S. Tokui, J.-Y. Shin, K. S. Kim, J. M. Lim, K. Youfu, S. Saito, D. Kim, A. Osuka, *J. Am. Chem. Soc.* **2009**, *131*, 7240–7241.
- [123] K. S. Kim, Z. S. Yoon, A. B. Ricks, J.-Y. Shin, S. Mori, J. Sankar, S. Saito, Y. M. Jung, M. R. Wasielewski, A. Osuka, D. Kim, *J. Phys. Chem. A* **2009**, *113*, 4498–4506.
- [124] J. Kruszewski, T. M. Krygowski, *Tetrahedron Lett.* **1972**, *13*, 3839–3842.
- [125] T. M. Krygowski, R. Anulewicz, J. Kruszewski, *Acta Crystallogr. Sect. B* **1983**, *39*, 732–739.
- [126] N. Sprutta, L. Latos-Grażyński, *Chem. Eur. J.* **2001**, *7*, 5099–5112.
- [127] P. J. Chmielewski, L. Latos-Grażyński, K. Rachlewicz, *Chem. Eur. J.* **1995**, *1*, 68–73.
- [128] H. E. Zimmerman, *J. Am. Chem. Soc.* **1966**, *88*, 1564–1565.
- [129] C. Castro, W. L. Karney, M. A. Valencia, C. M. Vu, R. P. Pemberton, *J. Am. Chem. Soc.* **2005**, *127*, 9704–9705.
- [130] J. F. Moll, R. P. Pemberton, M. G. Gutierrez, C. Castro, W. L. Karney, *J. Am. Chem. Soc.* **2007**, *129*, 274–275.
- [131] a) M. Mauksch, V. Gogonea, H. Jiao, P. v. R. Schleyer, *Angew. Chem.* **1998**, *110*, 2515–2517; *Angew. Chem. Int. Ed.* **1998**, *37*, 2395–2398. For a reinvestigation see: b) G. Bucher, S. Grimme, R. Huenerbein, A. Auer, E. Mucke, F. Köhler, J. Siegwirth, R. Herges *Angew. Chem.* **2009**, *121*, 10156; *Angew. Chem. Int. Ed.* **2009**, *48*, 9971; *Angew. Chem. Int. Ed.* **2009**, *48*, 9971.
- [132] S. Saito, J.-Y. Shin, J. M. Lim, K. S. Kim, D. Kim, A. Osuka, *Angew. Chem.* **2008**, *120*, 9803–9806; *Angew. Chem. Int. Ed.* **2008**, *47*, 9657–9660.
- [133] T. Koide, K. Youfu, S. Saito, A. Osuka, *Chem. Commun.* **2009**, 6047–6049.
- [134] J. M. Lim, J.-Y. Shin, Y. Tanaka, S. Saito, A. Osuka, D. Kim, *J. Am. Chem. Soc.* **2010**, *132*, 3105–3114.
- [135] N. Trinajstić in *Chemical Graph Theory. Introduction and Fundamentals* (Eds.: D. Bonchev, D. H. Rouvray), Abacus, **1991**, p. 235.
- [136] R. Paolesse in *The Porphyrin Handbook*, Vol. 2 (Eds.: K. M. Kadish, K. M. Smith, R. Guilard), Academic Press, San Diego, **2000**, pp. 201–232.
- [137] Y. Inokuma, A. Osuka, *Dalton Trans.* **2008**, 2517–2526.
- [138] A. W. Johnson, I. T. Kay, *Proc. Chem. Soc. London* **1964**, 89–90.
- [139] M. Bröring, S. Köhler, C. Kleeberg, *Angew. Chem.* **2008**, *120*, 5740–5743; *Angew. Chem. Int. Ed.* **2008**, *47*, 5658–5660.
- [140] R. Myśliborski, L. Latos-Grażyński, L. Sztrenberg, T. Lis, *Angew. Chem.* **2006**, *118*, 3752–3756; *Angew. Chem. Int. Ed.* **2006**, *45*, 3670–3674.
- [141] H. Furuta, H. Maeda, A. Osuka, *J. Am. Chem. Soc.* **2001**, *123*, 6435–6436.
- [142] A. Młodzianowska, L. Latos-Grażyński, L. Sztrenberg, *Inorg. Chem.* **2008**, *47*, 6364–6374.
- [143] M. Toganoh, T. Kimura, H. Uno, H. Furuta, *Angew. Chem.* **2008**, *120*, 9045–9048; *Angew. Chem. Int. Ed.* **2008**, *47*, 8913–8916.
- [144] M. Stępień, L. Latos-Grażyński, *J. Am. Chem. Soc.* **2002**, *124*, 3838–3839.
- [145] L. Latos-Grażyński, E. Pacholska, P. J. Chmielewski, M. M. Olmstead, A. L. Balch, *Angew. Chem.* **1995**, *107*, 2467–2469; *Angew. Chem. Int. Ed. Engl.* **1995**, *34*, 2252–2255.

- [146] E. Pacholska-Dudziak, F. Ulatowski, Z. Ciunik, L. Latos-Grażyński, *Chem. Eur. J.* **2009**, *15*, 10924–10929.
- [147] E. Pacholska, L. Latos-Grażyński, Z. Ciunik, *Angew. Chem.* **2001**, *113*, 4598–4601; *Angew. Chem. Int. Ed.* **2001**, *40*, 4466–4469.
- [148] M. Pawlicki, L. Latos-Grażyński, L. Szterenberg, *J. Org. Chem.* **2002**, *67*, 5644–5653.
- [149] J. Skonieczny, L. Latos-Grażyński, L. Szterenberg, *Chem. Eur. J.* **2008**, *14*, 4861–4874.
- [150] A. Ghosh, I. H. Wasbotten, A. Davis, J. C. Swarts, *Eur. J. Inorg. Chem.* **2005**, 4479–4485.
- [151] Calculations in this work have been performed with Gaussian09. The full reference to the program can be found in the Supporting Information.
- [152] C. Claessens, D. González-Rodríguez, T. Torres, *Chem. Rev.* **2002**, *102*, 835–854.
- [153] Y. Inokuma, Z. S. Yoon, D. Kim, A. Osuka, *J. Am. Chem. Soc.* **2007**, *129*, 4747–4761.
- [154] S. Saito, K. S. Kim, Z. S. Yoon, D. Kim, A. Osuka, *Angew. Chem.* **2007**, *119*, 5687–5689; *Angew. Chem. Int. Ed.* **2007**, *46*, 5591–5593.
- [155] M. Stępień, J. L. Sessler, *Org. Lett.* **2007**, *9*, 4785–4787.
- [156] D. Cremer, H. Günther, *Justus Liebigs Ann. Chem.* **1972**, 763, 87–108.
- [157] R. H. Mitchell, *Chem. Rev.* **2001**, *101*, 1301–1315.
- [158] P. J. Chmielewski, L. Latos-Grażyński, *Coord. Chem. Rev.* **2005**, *249*, 2510–2533.
- [159] H. Maeda, H. Furuta, *Pure Appl. Chem.* **2006**, *78*, 29–44.
- [160] M. Pawlicki, L. Latos-Grażyński, *Chem. Rec.* **2006**, *6*, 64–78.
- [161] H. Furuta, T. Ishizuka, A. Osuka, T. Ogawa, *J. Am. Chem. Soc.* **2000**, *122*, 5748–5757.
- [162] J.-Y. Shin, H. Furuta, A. Osuka, *Angew. Chem.* **2001**, *113*, 639–641; *Angew. Chem. Int. Ed.* **2001**, *40*, 619–621.
- [163] C.-H. Hung, J.-P. Jong, M.-Y. Ho, G.-H. Lee, S.-M. Peng, *Chem. Eur. J.* **2002**, *8*, 4542–4548.
- [164] A. Srinivasan, T. Ishizuka, H. Furuta, *Angew. Chem.* **2004**, *116*, 894–897; *Angew. Chem. Int. Ed.* **2004**, *43*, 876–879.
- [165] M. Suzuki, R. Taniguchi, A. Osuka, *Chem. Commun.* **2004**, 2682–2683.
- [166] I. Gupta, A. Srinivasan, T. Morimoto, M. Toganoh, H. Furuta, *Angew. Chem.* **2008**, *120*, 4639–4643; *Angew. Chem. Int. Ed.* **2008**, *47*, 4563–4567.
- [167] M. Toganoh, T. Ishizuka, H. Furuta, *Chem. Commun.* **2004**, 2464–2465.
- [168] M. Toganoh, S. Ikeda, H. Furuta, *Chem. Commun.* **2005**, 4589–4591.
- [169] A. Młodzianowska, L. Latos-Grażyński, L. Szterenberg, M. Stępień, *Inorg. Chem.* **2007**, *46*, 6950–6957.
- [170] J. Skonieczny, L. Latos-Grażyński, L. Szterenberg, *Inorg. Chem.* **2009**, *48*, 7394–7407.
- [171] L. Szterenberg, L. Latos-Grażyński, *J. Porphyrins Phthalocyanines* **2001**, *5*, 474–480.
- [172] M. Toganoh, J. Konagawa, H. Furuta, *Inorg. Chem.* **2006**, *45*, 3852–3854.
- [173] M. Stępień, L. Latos-Grażyński, *Acc. Chem. Res.* **2005**, *38*, 88–98.
- [174] K. Berlin, E. Breitmaier, *Angew. Chem.* **1994**, *106*, 1356–1357; *Angew. Chem. Int. Ed. Engl.* **1994**, *33*, 1246–1247.
- [175] M. Stępień, L. Latos-Grażyński, *Chem. Eur. J.* **2001**, *7*, 5113–5117.
- [176] M. Stępień, L. Latos-Grażyński, L. Szterenberg, J. Panek, Z. Latajka, *J. Am. Chem. Soc.* **2004**, *126*, 4566–4580.
- [177] M. Stępień, L. Latos-Grażyński, L. Szterenberg, *Inorg. Chem.* **2004**, *43*, 6654–6662.
- [178] C.-H. Hung, C.-Y. Lin, P.-Y. Lin, Y.-J. Chen, *Tetrahedron Lett.* **2004**, *45*, 129–132.
- [179] J. Reddy, V. G. Anand, *Chem. Commun.* **2008**, 1326–1328.
- [180] E. Pacholska-Dudziak, L. Latos-Grażyński, *Coord. Chem. Rev.* **2009**, *253*, 2036–2048.
- [181] E. Pacholska-Dudziak, J. Skonieczny, M. Pawlicki, L. Latos-Grażyński, L. Szterenberg, *Inorg. Chem.* **2005**, *44*, 8794–8803.
- [182] V. J. Bauer, D. L. J. Clive, D. Dolphin, J. B. Paine, F. L. Harris, M. M. King, J. Loder, S. W. C. Wang, R. B. Woodward, *J. Am. Chem. Soc.* **1983**, *105*, 6429–6436.
- [183] B. Sridevi, S. J. Narayanan, R. Rao, T. K. Chandrashekar, U. English, K. Ruhlandt-Senge, *Inorg. Chem.* **2000**, *39*, 3669–3677.
- [184] S. Venkatraman, R. Kumar, J. Sankar, T. K. Chandrashekar, K. Sendhil, C. Vijayan, A. Kelling, M. O. Senge, *Chem. Eur. J.* **2004**, *10*, 1423–1432.
- [185] R. Misra, R. Kumar, T. K. Chandrashekar, A. Nag, D. Goswami, *Org. Lett.* **2006**, *8*, 629–631.
- [186] R. Misra, R. Kumar, T. K. Chandrashekar, C. H. Suresh, *Chem. Commun.* **2006**, 4584–4586.
- [187] R. Misra, R. Kumar, T. K. Chandrashekar, C. H. Suresh, A. Nag, D. Goswami, *J. Am. Chem. Soc.* **2006**, *128*, 16083–16091.
- [188] S. Gokulnath, V. Prabhuraja, J. Sankar, T. K. Chandrashekar, *Eur. J. Org. Chem.* **2007**, 191–200.
- [189] J. L. Sessler, M. Cyr, A. K. Burrell, *Tetrahedron* **1992**, *48*, 9661–9672.
- [190] J. Lisowski, J. L. Sessler, V. Lynch, *Inorg. Chem.* **1995**, *34*, 3567–3572.
- [191] N. Sprutta, L. Latos-Grażyński, *Org. Lett.* **2001**, *3*, 1933–1936.
- [192] A. Srinivasan, V. G. Anand, S. J. Narayanan, S. K. Pushpan, M. Ravi Kumar, T. K. Chandrashekar, *J. Org. Chem.* **1999**, *64*, 8693–8697.
- [193] S. J. Narayanan, B. Sridevi, T. K. Chandrashekar, A. Vij, R. Roy, *Angew. Chem.* **1998**, *110*, 3582–3585; *Angew. Chem. Int. Ed.* **1998**, *37*, 3394–3397.
- [194] J. L. Sessler, J. M. Davis, *Acc. Chem. Res.* **2001**, *34*, 989–997.
- [195] J. L. Sessler, P. A. Gale, W.-S. Cho, *Anion Receptor Chemistry*, RSC Publishing, Cambridge, **2006**.
- [196] K. Rachlewicz, N. Sprutta, L. Latos-Grażyński, P. J. Chmielewski, L. Szterenberg, *J. Chem. Soc. Perkin Trans. 2* **1998**, 959–967.
- [197] K. Rachlewicz, N. Sprutta, P. J. Chmielewski, L. Latos-Grażyński, *J. Chem. Soc. Perkin Trans. 2* **1998**, 969–975.
- [198] L. Szterenberg, L. Latos-Grażyński, *THEOCHEM* **1999**, *490*, 33–46.
- [199] G. I. Cardenas-Jiron, C. Venegas, R. Lopez, M. I. Menendez, *J. Phys. Chem. A* **2008**, *112*, 8100–8106.
- [200] J. L. Sessler, M. J. Cyr, V. Lynch, E. McGhee, J. A. Ibers, *J. Am. Chem. Soc.* **1990**, *112*, 2810–2813.
- [201] M. Shionoya, H. Furuta, V. Lynch, A. Harriman, J. L. Sessler, *J. Am. Chem. Soc.* **1992**, *114*, 5714–5722.
- [202] J. L. Sessler, M. C. Hoehner, A. Gebauer, A. Andrievsky, V. Lynch, *J. Org. Chem.* **1997**, *62*, 9251–9260.
- [203] A. Srinivasan, V. R. Anand, S. K. Pushpan, T. K. Chandrashekar, K.-i. Sugiura, Y. Sakata, *J. Chem. Soc. Perkin Trans. 2* **2000**, 1788–1793.
- [204] J. L. Sessler, A. Gebauer, M. C. Hoehner, V. Lynch, *Chem. Commun.* **1998**, 1835–1836.
- [205] A. K. Burrell, G. Hemmi, V. Lynch, J. L. Sessler, *J. Am. Chem. Soc.* **1991**, *113*, 4690–4692.
- [206] J. L. Sessler, A. K. Burrell, J. Lisowski, A. Gebauer, M. J. Cyr, V. Lynch, *Bull. Soc. Chim. Fr.* **1996**, *133*, 725–734.
- [207] A. Krivokapic, A. R. Cowley, H. L. Anderson, *J. Org. Chem.* **2003**, *68*, 1089–1096.
- [208] C. Comuzzi, S. Cogoi, M. Overhand, G. A. Van der Marel, H. S. Overkleeft, L. E. Xodo, *J. Med. Chem.* **2006**, *49*, 196–204.
- [209] C. Comuzzi, S. Cogoi, L. E. Xodo, *Tetrahedron* **2006**, *62*, 8147–8151.
- [210] S. Mori, J.-Y. Shin, S. Shimizu, F. Ishikawa, H. Furuta, A. Osuka, *Chem. Eur. J.* **2005**, *11*, 2417–2425.

- [211] S. Shimizu, N. Aratani, A. Osuka, *Chem. Eur. J.* **2006**, *12*, 4909–4918.
- [212] A. Srinivasan, T. Ishizuka, H. Maeda, H. Furuta, *Angew. Chem.* **2004**, *116*, 3011–3015; *Angew. Chem. Int. Ed.* **2004**, *43*, 2951–2955.
- [213] P. J. Melfi, S. K. Kim, J. T. Lee, F. Bolze, D. Seidel, V. M. Lynch, J. M. Veauthier, A. J. Gaunt, M. P. Neu, Z. Ou, K. M. Kadish, S. Fukuzumi, K. Ohkubo, J. L. Sessler, *Inorg. Chem.* **2007**, *46*, 5143–5145.
- [214] S. J. Weghorn, J. L. Sessler, V. Lynch, T. F. Baumann, J. W. Sibert, *Inorg. Chem.* **1996**, *35*, 1089–1090.
- [215] J. L. Sessler, A. Gebauer, A. Guba, M. Scherer, V. Lynch, *Inorg. Chem.* **1998**, *37*, 2073–2076.
- [216] S. Hannah, D. Seidel, J. L. Sessler, V. Lynch, *Inorg. Chim. Acta* **2001**, *317*, 211–217.
- [217] T. Kohler, M. C. Hodgson, D. Seidel, J. M. Veauthier, S. Meyer, V. Lynch, P. Boyd, P. J. Brothers, J. L. Sessler, *Chem. Commun.* **2004**, 1060–1061.
- [218] J. Sessler, P. Melfi, V. M. Lynch, *J. Porphyrins Phthalocyanines* **2007**, *11*, 287–293.
- [219] P. J. Melfi, S. Camiolo, J. T. Lee, M. F. Ali, J. T. McDevitt, V. M. Lynch, J. L. Sessler, *Dalton Trans.* **2008**, 1538–1540.
- [220] S. J. Narayanan, B. Sridevi, T. K. Chandrashekar, A. Vij, R. Roy, *J. Am. Chem. Soc.* **1999**, *121*, 9053–9068.
- [221] A. Gossauer, *Bull. Soc. Chim. Belg.* **1983**, *92*, 793–795.
- [222] Y.-S. Xie, K. Yamaguchi, M. Toganoh, H. Uno, M. Suzuki, S. Mori, S. Saito, A. Osuka, H. Furuta, *Angew. Chem.* **2009**, *121*, 5604–5607; *Angew. Chem. Int. Ed.* **2009**, *48*, 5496–5499.
- [223] B. Lament, J. Dobkowski, J. L. Sessler, S. J. Weghorn, J. Waluk, *Chem. Eur. J.* **1999**, *5*, 3039–3045.
- [224] J. L. Sessler, D. Seidel, C. Bucher, V. Lynch, *Tetrahedron* **2001**, *57*, 3743–3752.
- [225] R. Kumar, R. Misra, T. K. Chandrashekar, *Org. Lett.* **2006**, *8*, 4847–4850.
- [226] M. R. Johnson, D. C. Miller, K. Bush, J. J. Becker, J. A. Ibers, *J. Org. Chem.* **1992**, *57*, 4414–4417.
- [227] Z. Hu, J. L. Atwood, M. P. Cava, *J. Org. Chem.* **1994**, *59*, 8071–8075.
- [228] M. Kozaki, J. P. Parakka, M. P. Cava, *J. Org. Chem.* **1996**, *61*, 3657–3661.
- [229] A. Gebauer, Diplomarbeit thesis, University of Cologne (Germany), **1993**.
- [230] S. J. Narayanan, B. Sridevi, T. K. Chandrashekar, U. Englich, K. Ruhlandt-Senge, *Inorg. Chem.* **2001**, *40*, 1637–1645.
- [231] S. J. Narayanan, A. Srinivasan, B. Sridevi, T. K. Chandrashekar, M. O. Senge, K.-i. Sugiura, Y. Sakata, *Eur. J. Org. Chem.* **2000**, 2357–2360.
- [232] D. Wu, A. Descalzo, F. Weik, F. Emmerling, Z. Shen, X.-Z. You, K. Rurack, *Angew. Chem.* **2008**, *120*, 199–203; *Angew. Chem. Int. Ed.* **2008**, *47*, 193–197.
- [233] A. Srinivasan, T. Ishizuka, A. Osuka, H. Furuta, *J. Am. Chem. Soc.* **2003**, *125*, 878–879.
- [234] M. Suzuki, M. C. Yoon, D. Y. Kim, J. H. Kwon, H. Furuta, D. Kim, A. Osuka, *Chem. Eur. J.* **2006**, *12*, 1754–1759.
- [235] A. Gossauer, *Chimia* **1983**, *37*, 341–342.
- [236] M. G. P. M. S. Neves, R. M. Martins, A. C. Tomé, A. J. D. Silvestre, A. M. S. Silva, V. Félix, M. G. B. Drew, J. A. Cavaleiro, *Chem. Commun.* **1999**, 385–386.
- [237] C. Brückner, E. D. Sternberg, R. W. Boyle, D. Dolphin, *Chem. Commun.* **1997**, 1689–1690.
- [238] S. Shimizu, J. Y. Shin, H. Furuta, R. Ismael, A. Osuka, *Angew. Chem.* **2003**, *115*, 82–86; *Angew. Chem. Int. Ed.* **2003**, *42*, 78–82.
- [239] K. Youfu, A. Osuka, *Org. Lett.* **2005**, *7*, 4381–4384.
- [240] M. Suzuki, A. Osuka, *Chem. Commun.* **2005**, 3685–3687.
- [241] H. Hata, H. Shinokubo, A. Osuka, *Angew. Chem.* **2005**, *117*, 954–957; *Angew. Chem. Int. Ed.* **2005**, *44*, 932–935.
- [242] T. K. Ahn, J. H. Kwon, D. Y. Kim, D. W. Cho, D. H. Jeong, S. K. Kim, M. Suzuki, S. Shimizu, A. Osuka, D. Kim, *J. Am. Chem. Soc.* **2005**, *127*, 12856–12861.
- [243] M. Suzuki, A. Osuka, *Chem. Eur. J.* **2007**, *13*, 196–202.
- [244] S. Mori, S. Shimizu, R. Taniguchi, A. Osuka, *Inorg. Chem.* **2005**, *44*, 4127–4129.
- [245] M. Suzuki, A. Osuka, *J. Am. Chem. Soc.* **2007**, *129*, 464–465.
- [246] R. Misra, R. Kumar, T. K. Chandrashekar, B. S. Joshi, *J. Org. Chem.* **2007**, *72*, 1153–1160.
- [247] H. Rath, V. G. Anand, J. Sankar, S. Venkatraman, T. K. Chandrashekar, B. S. Joshi, C. L. Khetrapal, U. Schilde, M. O. Senge, *Org. Lett.* **2003**, *5*, 3531–3533.
- [248] M. Stępień, B. Szyszko, L. Latos-Grażyński, *Org. Lett.* **2009**, *11*, 3930–3933.
- [249] M. Stępień, B. Szyszko, L. Latos-Grażyński, *Unpublished data*.
- [250] H. Rath, J. Sankar, V. PrabhuRaja, T. K. Chandrashekar, B. S. Joshi, *Org. Lett.* **2005**, *7*, 5445–5448.
- [251] S. Saito, A. Osuka, *Chem. Eur. J.* **2006**, *12*, 9095–9102.
- [252] S. Saito, K. Furakawa, A. Osuka, *Angew. Chem.* **2009**, *121*, 8230–8233; *Angew. Chem. Int. Ed.* **2009**, *48*, 8086–8089.
- [253] P. J. Chmielewski, *Angew. Chem.* **2010**, *122*, 1399–1401; *Angew. Chem. Int. Ed.* **2010**, *49*, 1359–1361.
- [254] T. Kohler, Z. P. Ou, J. T. Lee, D. Seidel, V. Lynch, K. M. Kadish, J. L. Sessler, *Angew. Chem.* **2005**, *117*, 85–89; *Angew. Chem. Int. Ed.* **2005**, *44*, 83–87.
- [255] G. Fuhrmann, T. Debaerdemaeker, P. Bäuerle, *Chem. Commun.* **2003**, 948–949.
- [256] V. G. Anand, S. Venkatraman, H. Rath, T. K. Chandrashekar, W. Teng, K. Ruhlandt-Senge, *Chem. Eur. J.* **2003**, *9*, 2282–2290.
- [257] H. Rath, J. Sankar, H. PrabhuRaja, T. K. Chandrashekar, B. S. Joshi, R. Roy, *Chem. Commun.* **2005**, 3343–3345.
- [258] H. Xu, G. Yu, W. Xu, Y. Xu, G. Cui, D. Zhang, Y. Liu, D. Zhu, *Langmuir* **2005**, *21*, 5391–5395.
- [259] M. Stępień, B. Donnio, J. L. Sessler, *Angew. Chem.* **2007**, *119*, 1453–1457; *Angew. Chem. Int. Ed.* **2007**, *46*, 1431–1435.
- [260] L. R. Eller, M. Stępień, C. J. Fowler, J. T. Lee, J. L. Sessler, B. A. Moyer, *J. Am. Chem. Soc.* **2007**, *129*, 11020–11021.
- [261] J. M. Lintuluoto, K. Nakayama, J.-i. Setsune, *Chem. Commun.* **2006**, 3492–3494.
- [262] M. Mori, J.-i. Setsune, *Chem. Lett.* **2007**, *36*, 244–245.
- [263] J.-i. Setsune, M. Mori, T. Okawa, S. Maeda, J. M. Lintuluoto, *J. Organomet. Chem.* **2007**, *692*, 166–174.
- [264] S. Shimizu, Y. Tanaka, K. Youfu, A. Osuka, *Angew. Chem.* **2005**, *117*, 3792–3795; *Angew. Chem. Int. Ed.* **2005**, *44*, 3726–3729.
- [265] H. Hata, Y. Kamimura, H. Shinokubo, A. Osuka, *Org. Lett.* **2006**, *8*, 1169–1172.
- [266] M. Mori, T. Okawa, N. Iizuna, K. Nakayama, J. M. Lintuluoto, J.-i. Setsune, *J. Org. Chem.* **2009**, *74*, 3579–3582.
- [267] L. Latos-Grażyński, *Angew. Chem.* **2004**, *116*, 5234–5238; *Angew. Chem. Int. Ed.* **2004**, *43*, 5124–5128.
- [268] E. Vogel, M. Michels, L. Zander, J. Lex, N. S. Tuzun, K. N. Houk, *Angew. Chem.* **2003**, *115*, 2964–2969; *Angew. Chem. Int. Ed.* **2003**, *42*, 2857–2862.
- [269] G. Hohlneicher, D. Bremm, J. Wytke, J. Bley-Eschrich, J.-P. Gisselbrecht, M. Gross, M. Michels, J. Lex, E. Vogel, *Chem. Eur. J.* **2003**, *9*, 5636–5642.
- [270] Y. Tanaka, H. Shinokubo, Y. Yoshimura, A. Osuka, *Chem. Eur. J.* **2009**, *15*, 5674–5685.
- [271] J. L. Sessler, D. Seidel, A. Gebauer, V. Lynch, K. A. Abboud, *J. Heterocycl. Chem.* **2001**, *38*, 1419–1424.
- [272] Y. Kamimura, S. Shimizu, A. Osuka, *Chem. Eur. J.* **2007**, *13*, 1620–1628.
- [273] Y. Tanaka, J. Y. Shin, A. Osuka, *Eur. J. Org. Chem.* **2008**, 1341–1349.
- [274] J.-i. Setsune, S. Maeda, *J. Am. Chem. Soc.* **2000**, *122*, 12405–12406.

- [275] F. Zhang, G. Götz, H. D. Winkler, C. Schalley, P. Bäuerle, *Angew. Chem.* **2009**, *121*, 6758–6762; *Angew. Chem. Int. Ed.* **2009**, *48*, 6632–6635.
- [276] J. Krömer, I. Rios-Carreras, G. Fuhrmann, C. Musch, M. Wunderlin, T. Debaerdemaeker, E. Mena-Osteritz, P. Bäuerle, *Angew. Chem.* **2000**, *112*, 3623–3628; *Angew. Chem. Int. Ed.* **2000**, *39*, 3481–4386.
- [277] J.-i. Setsune, M. Toda, T. Yoshida, *Chem. Commun.* **2008**, 1425–1427.
- [278] C. Ikeda, N. Sakamoto, T. Nabeshima, *Org. Lett.* **2008**, *10*, 4601–4604.
- [279] V. G. Anand, S. Saito, S. Shimizu, A. Osuka, *Angew. Chem.* **2005**, *117*, 7410–7414; *Angew. Chem. Int. Ed.* **2005**, *44*, 7244–7248.
- [280] A. Mishra, C.-Q. Ma, P. Bäuerle, *Chem. Rev.* **2009**, *109*, 1141–1276.
- [281] S. S. Zade, M. Bendikov, *J. Org. Chem.* **2006**, *71*, 2972–2981.
-